GNGTS 2024

DISASTER RISK ANALYSIS AND REDUCTION

Session 2.2

Science and technology to support earthquake prevention and preparedness

Convenors of the session:
Mauro Dolce (UniNA) – mauro.dolce@unina.it
Francesca Pacor (INGV) – francesca.pacor@ingv.it
Maria Polese (UniNA) – mapolese@unina.it

Contributions recommended for this session:

- Monitoring networks for the knowledge of seismic hazard and for rapid response
- Shaking scenarios at different territorial scales for seismic risk evaluations: methodological approaches, uncertainty management and input data
- Assessment of seismic risk and its engineering components (vulnerability and exposure) at different territorial scales and with different methodologies, and development of the necessary tools and databases
- Methodologies and examples of multi-risk analysis associated to seismic risk (e.g. earthquakes and tsunamis)
- Civil protection planning and urban planning tools for seismic risk mitigation
- Techniques and examples of seismic strengthening or retrofit interventions of rapid execution and having low impact on the service continuity of the building, also integrated with energy efficiency interventions and considering circular economy principles
- Tools for the safety assessment of individual buildings, including on-site and remote monitoring and related analysis methodologies
- Contributions for the improvement of seismic standards for different structural types (buildings, bridges, warehouses, large structures, etc.) and for different structural materials (masonry, reinforced concrete, steel, wood, etc.) for the design of new buildings or interventions on existing buildings, including the evaluation of seismic design actions

Seismic risk mitigation is a rapidly evolving field, as scientific, engineering and technological developments are providing new elements for the prevention, preparedness, response and recovery of the system and population to the effects of

earthquakes. Moreover, the need to combine the seismic risk reduction with the reduction of other risks, coupled with the requirement to consider present and future climate change issues, foster the adoption of a more articulated and complete approach, where the risk scenarios encompass also compound and induced events (e.g. tsunamis), and where the prevention actions on constructions take into account the needs for energy efficiency. This session has the scope to collect those contributions that could represent an advancement in seismic reduction strategies, also in a broader perspective to other risks.

A systematic analysis at stations of the Italian seismic network to test the role of local topographic effect.

M. Ariano[1], P.L. Fantozzi[1], D. Albarello[1]

[1]Department of Physics Sciences, Earth and Environment, University of Siena, Siena, Italy

The Italian seismic code (NTC18) provides indications about the expected effects of some morphological configurations on the expected ground motion during earthquakes. In particular, two main 2D morphologies are identified as reference: cliffs and crests. Based on numerical simulations, the value of St is assumed to depend on the steepness of the cliffs and aspect ratio of the crest. A critical aspect of these estimates is that the considered configurations are defined in terms of steepness angles and aspect ratios, without any scale indication. Moreover, the considered morphologies are very schematic, and this prevents their simple application in the natural context: in most cases an expert judgement is necessary, and this makes the final estimates potentially controversial and difficult to validate on the basis of empirical observations. To face this problem, in the frame of the PRIN project "SERENA", a procedure has been developed for the automatic identification of areas prone to morphological amplification effects by following NTC18 prescriptions, based on the Digital Terrain Model. The proposed approach allows the full exploitation of topographical data at the maximum resolution available. After a first application to restricted areas, the proposed procedure has been applied at National scale at the seismometric and accelerometric sites managed by INGV. The aim is twofold: first comparing outcomes of the new approach with the ones proposed by other Authors at the same sites, second to provide a sound basis of a coherent and reproducible estimate of St values to be compared with possible empirical evidence. In the presentation, the results obtained about the first aim will be presented and discussed.

Seismic vulnerability of masonry buildings in Montenegro: a heuristic model

F. Aloschi[1], M. Polese[1], J. Pejovic[2], N. Serdar[2]

[1] Department of Structures for Engineering and Architecture (DiSt), University of Naples Federico II, Naples, Italy
[2] Faculty of Civil Engineering, University of Montenegro UCG, Podgorica, Montenegro

Background, motivation, and scope

The first step to perform a vulnerability assessment is to classify buildings, recognizing the typological characteristics that define the seismic behavior of a *class*. The typological characteristics are discernible when conducting analyses at the territorial scale (Polese *et al.* 2019). After selecting the damage scale, vulnerability functions are assessed as a measure of the likelihood for building classes to experience damage due to earthquakes of given intensity. Main approaches for estimating the vulnerability of buildings may be distinguished as: i) empirical, where models are based on statistical processing of damage data collected from past earthquake events, ii) analytical, where fragility is computed according to an analytical-based estimation of the buildings' response, iii) hybrid, where features of i) and ii) are combined, and iv) heuristic, expert based methods with subsequent empirical calibration by observational data. Heuristic approaches were largely adopted in the last two decades as they ensure physically consistent results and fairly accurate fittings with actual damage (Lagomarsino *et al.* 2021). In this paper, we propose a heuristic approach, hereafter referred to as EXPLORA, to evaluate the vulnerability model (VM) for masonry residential buildings in Montenegro. In particular, building classification is based on the SERA model (Crowley *et al.* 2020) suitably enriched to account for building features that influence the vulnerability. The SERA model is based on the Global Earthquake Model (GEM) (Silva *et al.* 2020) and was developed to work jointly with GEM's analytical fragility curves. However, these curves were developed for global applications and were not calibrated with observed damage data. Thus, they cannot adequately capture the behaviour of buildings in specific geographic areas.

In this work, masonry buildings in Montenegro are initially subdivided in 3 building classes, namely: 1) unconfined stone masonry buildings (URM-St), 2) unconfined brick masonry buildings (URM-Br), and 3) confined masonry (CFM). In the context of Montenegro, specific VMs have not been developed as yet. To address this gap, we firstly compare Montenegrin building typologies with the SERA typologies, based on the GEM taxonomy (Scawthorn *et al.* 2013), and with those of Serbia (Blagojević *et al.* 2023), Slovenia (Babič *et al.* 2021; Polese *et al.* 2023), and Italy (Rosti *et al.* 2021; Polese *et al.* 2023). This allows a re-classification of the Montenegrin typologies according to

different VMs and a preliminary vulnerability evaluation. However, the capability of existing VMs to represent effective susceptibility to damage must be tested with real damage data. To this end, data pertaining to the April 15, 1979, Montenegro Earthquake, referred to as the Seismic Event (SE), are considered. Ultimately, damage data extracted and revised from historical reports are used to calibrate a heuristic VM that suitably combines existing VMs for similar typologies.

Damage data analysis

In Montenegro, the data on historical earthquakes and relevant damages are not collected in systematic way and there is a lack of structural database which can provide information on events and direct effects of earthquakes. However, the SE left an indelible mark on the collective memory of Montenegrins, and a few initiatives were taken to assess the extensive damage caused by this catastrophic event. We rely on two of them: the historical Report IZIIS (Petrovski *et al.* 1984) and the work by Pavićević (Pavićević Božidar S 2004). In both reports, the classification of damage differs from the European Macroseismic Scale 1998 (EMS98) (Grünthal & European Seismological Commission 1998) notation. Therefore, following an approach similar to Rota et al. (Rota *et al.* 2008), we have developed the conversion scheme reported in Tab. 1.

Usability	**Report IZIIS 84-085** (Petrovski *et al.* 1984)	**EMS 98** (Grünthal 1998)
Usable	**11** - no damage	DS0
	12 - no damage of LBS	DS1
	13 - damages of LBS	DS1
Temporary unusable	**21** - damaged LBS	DS2
	22 - heavy damages of LBS	DS2
Unusable	**31** - severely damaged	DS3
	32 - partially collapsed	DS4
	33 - collapsed	DS5

Tab. 1 – Conversion scheme for damage levels into EMS98 damage states (DSs). Note: LBS stands for load-bearing system.

The earthquake's hypocenter was located offshore, and the coastal municipalities suffered the most severe impact of the devastation. A shake map for this event is available from United States Geological Survey (USGS) (U.S. Department of the Interior 2023). In the present study, Peak Ground Acceleration (PGA) is selected as the Intensity Measure (IM). For the coastal cities a Modified Mercalli intensity (MMI) between VIII and IX was reported in (Blagojević *et al.* 2023); by adopting the I-PGA conversion law proposed in Trifunac et al. (Trifunac MD *et al.* 1991), a reasonable agreement of the corresponding PGA with the values from the USGS shake map can be observed. These shake map values are reported in Tab. 2.

	Ulcinj	Bar	Budva	Tivat	Kotor	Herceg Novi	Cetinje
Modified Mercalli Intensity (MMI)	VII	VIII	IX	VIII	IX	VI	VII
Peak Ground Acceleration (PGA) [g]	0.4	0.5	0.65	0.45	0.37	0.3	0.32

Tab. 2 – Seismic event (SE) intensities identified in 7 municipalities.

(Petrovski *et al.* 1984) classifies buildings based on their construction materials, namely: i) unconfined stone masonry buildings (URM-St), ii) unconfined brick masonry buildings (URM-Br), and iii) confined masonry (CFM). For each one of these building classes, the respective DS associated with all surveyed buildings is recorded. These results are reported in Fig. 1 (a) - (c). Conversely, in (Pavićević Božidar S 2004) the DSs are indicated for the 7 municipalities reported in Tab. 2. Being characterized by MMI ≥ VI, it is assumed that all the municipalities were completely inspected, consistently with what was observed in (Dolce & Goretti 2015) after the L'Aquila earthquake. This assumption ensures the availability of unbiased data for damage characterization. The damage data encompassed all types of construction materials, including masonry, reinforced concrete (RC), and steel. Acknowledging that masonry buildings constituted approximately 90% of the entire building dataset across all municipalities, we hypothesized that all damage pertained to masonry structures. The resulting damage data extracted from (Pavićević Božidar S 2004) is summarized in the histograms in Fig. 1 (d) - (l). One can note that the report (Pavićević Božidar S 2004) does not indicate specific building classes, such as URM-St, URM-Br, or CFM.

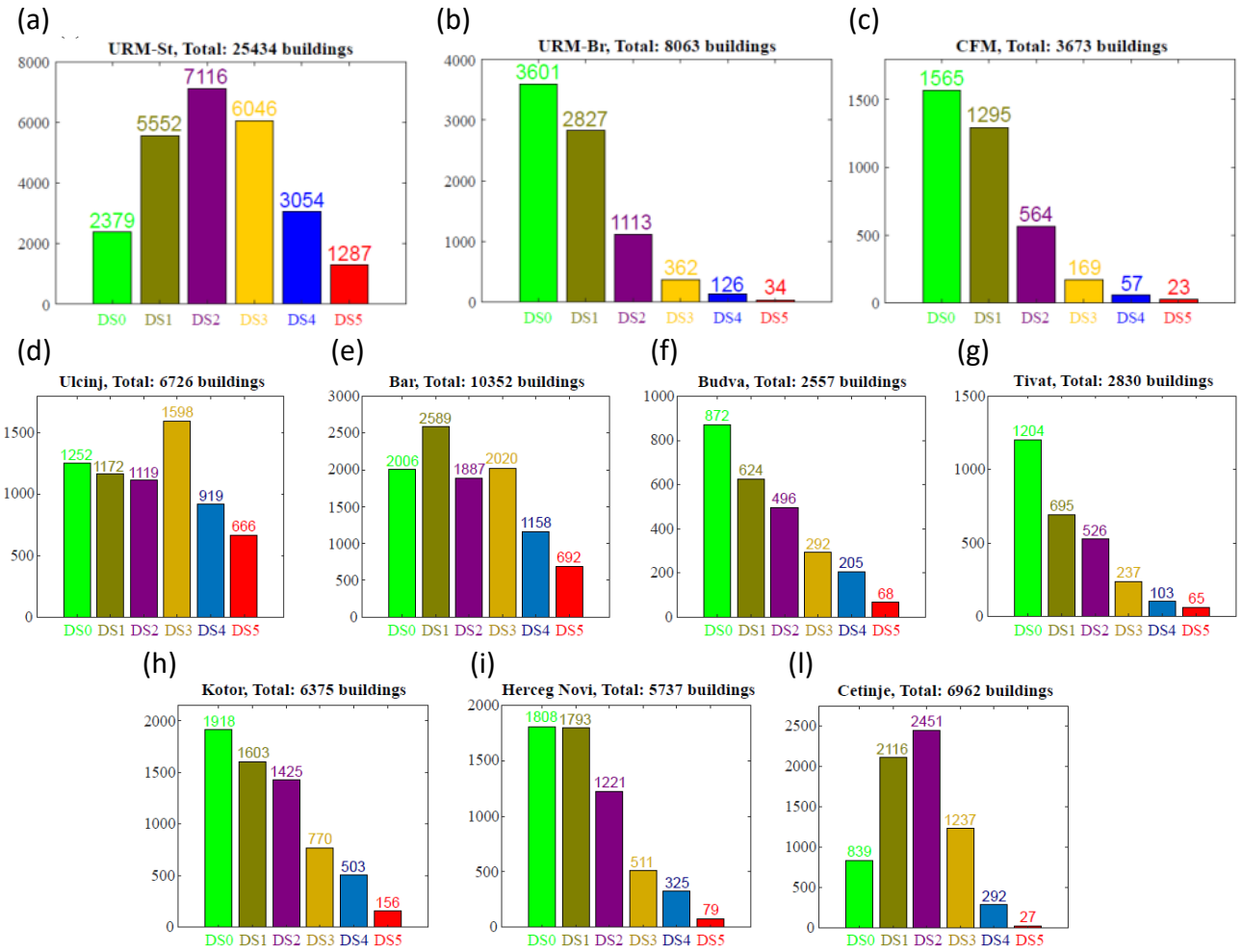

Fig. 1 – Damage data extracted from (Petrovski *et al.* 1984): a) unconfined stone masonry buildings (URM-St), b) unconfined brick masonry buildings (URM-Br), and (c) confined masonry (CFM). From (d) to (l): damage data extracted from (Pavićević Božidar S 2004) for 7 municipalities.

Given that both reports (Petrovski *et al.* 1984) and (Pavićević Božidar S 2004) are derived from surveys related to the same SE, we conducted data manipulation to extract pertinent information for establishing anchor points in fragility functions. Specifically, we initially computed, based on Fig. 1 (a) - (c), the percentage of URM-St, URM-Br, and CFM buildings within each DS. This information has been compiled and is presented in Tab. 3.

Damage State	URM-St	URM-Br	CFM
DS0	32%	48%	21%
DS1	57%	29%	13%
DS2	81%	13%	6%
DS3	92%	6%	3%
DS4	94%	4%	2%
DS5	96%	3%	2%

Tab. 3 – Distribution of building classes across damage states: derived from Fig. 1 (a) - (c).

Then, by applying the percentages of Tab. 3 to the data in Fig. 1 (d)-(l), we determine the number of buildings corresponding to each class falling in each DS. For the sake of conciseness, we do not

report this info in this paper; however, the outcomes of this manipulation will be clearly displayed in the forthcoming subsection.

The proposed heuristic model (EXPLORA)

In Montenegro, data on building structures is obtained from the 2011 census, which provides info on dwellings and their construction dates. There is no specific information detailing the typological characteristics of buildings, which is crucial for creating comprehensive building classes. Hence, the SERA exposure model (Crowley *et al.* 2020) for Montenegro is used as a reference. It defines common building classes in Montenegro based on the year of construction and location (urban or rural). With the aim of comparing the typologies with those considered in (Blagojević *et al.* 2023)-(Rosti *et al.* 2021; Polese *et al.* 2023), additional features are considered. Firstly, the SERA model (Crowley *et al.* 2020) is enriched according to the GEM building taxonomy (Scawthorn *et al.* 2013), and buildings are subdivided according to height classes Low (**L**: 1-2 stories) or Medium (**MH**: ≥ 3 stories). The percentage distribution in height classes is derived from the SERA model for Montenegro (Crowley *et al.* 2020). Next, the presence of flexible or rigid slab floors is considered, assigning equal probability. The resulting building classes are outlined on the left side of Tab. 4.

Montenegro building classes	**Lateral load resisting system (LLRS)**	**Design Code and Age of Construction**	**Floor type**	**Height**		**SERA typologies** (Scawthorn *et al.* 2013; Crowley *et al.* 2020)	**VM Serbia** (Blagojević *et al.* 2023)	**VM Italy** (Rosti *et al.* 2021)	**VM Slovenia** (Babič *et al.* 2021)
URM-St	Stone walls in both directions without tie-rods	**CDN** pre-code **1919-1964**	50% Flexible (wooden slab) 50% Rigid (RC slab)	90% Low (**L**) 1 - 2 stories 10% Medium (**MH**) ≥ 3 stories	→	**MUR-STDRE_LWAL-H1** (λ_{S1}=0.45) **MUR-STDRE_LWAL-H2** (λ_{S2}=0.45) **MUR-STDRE_LWAL-H3** (λ_{S3}=0.10)	**M1**, **M2** (λ_{Sr1}=0.5) **M3** (λ_{Sr2}=0.5)	**B-L** (λ_{It1}=0.45) **B-MH** (λ_{It2}=0.05) **C1-L** (λ_{It3}=0.45) **C1-MH** (λ_{It4}=0.05)	**1** (λ_{SI1}=0.9) **2** (λ_{SI2}=0.1)
URM-Br	Brick walls in both directions without tie-rods	**CDL** low code **1964-1980**	50% Flexible (wooden slab) 50% Rigid (RC slab)	90% Low (**L**) 1 – 2 stories 10% Medium (**MH**) ≥ 3 stories	→	**MUR-CL99_LWAL-H1** (λ_{S1}=0.45) **MUR- CL99_LWAL-H2** (λ_{S2}=0.45) **MUR- CL99_LWAL-H3** (λ_{S3}=0.10)	**M1**, **M2** (λ_{Sr1}=0.5) **M3** (λ_{Sr2}=0.5)	**B-L** (λ_{It1}=0.45) **B-MH** (λ_{It2}=0.05) **C1-L** (λ_{It3}=0.45) **C1-MH** (λ_{It4}=0.05)	**3** (λ_{SI1}=0.9) **4** (λ_{SI2}=0.1)
CFM	Brick or stone walls with vertical and horizontal RC elements without tie-rods	**CDM** moderate code **1981-2011**	50% Flexible (wooden slab) 50% Rigid (RC slab)	71% Low (**L**) 1 - 2 stories 29% Medium (**MH**) ≥ 3 stories	→	**MCF/LWAL+DUL/H:1** (λ_{S1}=0.42) **MCF/LWAL+DUL/H:2** (λ_{S2}=0.29) **MCF/LWAL+DUL/H:3** (λ_{S3}=0.29)	**M3** (λ_{Sr}=1)	**C1-L** (λ_{It1}=0.71) **C1-MH** (λ_{It2}=0.29)	**5** (λ_{SI1}=0.71) **6** (λ_{SI2}=0.29)

Tab. 4 – Association of renowned vulnerability models (VMs) to the Montenegro building classes.

Adding to the details of the SERA model and Tab. 4, it's worth mentioning that we assumed all buildings under CDN were constructed with stone masonry, while those under CDL were built with

brick masonry. In Tab. 4, the building classes identified for Montenegro are associated with the VMs of Serbia (Blagojević *et al.* 2023), Slovenia (Babič *et al.* 2021) and Italy (Rosti *et al.* 2021). Slovenia and Italy VMs were chosen because they are well-recognized in the seismic community and have undergone validation over the years. On the other hand, the Serbia VM is relatively recent, but is the result of a comprehensive effort involving also structural engineers from the Balkans with extensive experience in the local built environment. Thus, to exploit the common features of these three VMs, we created a heuristic VM called EXPLORA. Specifically, the fragility curves of EXPLORA are represented as cumulative distribution functions (CDFs) of lognormal distributions. These distributions show the probability of exceeding a certain DS at various IMs. The EXPLORA VM is designed in a way that its fragility curves are a linear combination of the VMs from (Blagojević *et al.* 2023), (Babič *et al.* 2021) and (Rosti *et al.* 2021), in terms of mean and standard deviation, as follows:

$$\Theta = w_S \vartheta_S + w_{Sr} \vartheta_{Sr} + w_{It} \vartheta_{It} + w_{Sl} \vartheta_{Sl} , \quad (1)$$

$$B = w_S \beta_S + w_{Sr} \beta_{Sr} + w_{It} \beta_{It} + w_{Sl} \beta_{Sl} , \quad (2)$$

where Θ and B are the heuristic mean and standard deviation of the EXPLORA VM, while ϑ and β are the mean and standard deviation of the employed VMs: SERA (S), Serbia (Sr), Italy (It) and Slovenia (Sl). The weights w are calculated such that:

$$w_S + w_{Sr} + w_{It} + w_{Sl} = 1. \quad (3)$$

In Eqs. (1) and (2), the means ϑ and standard deviations β are derived by weighting the various VMs' fragility curves with predetermined weights λ. These weights are indicated in Tab. 4 and are applied similarly to Eqs. (1) and (2) for each building class and VM. This step is taken to consider the potential influence of flexible and rigid diaphragms, as well as the variability in building heights (**L** or **MH**), which are unfortunately missing in the damage data. Next, to leverage the damage information, the weights w in Eqs. (1) and (2) are fine-tuned by minimizing the error between the final weighted solution and a linear regression from the damage data pertaining DS2. Currently, this error minimization is done by means of a trial-and-error process, but a more advanced procedure is planned for future stages of this research. The weights w computed for the EXPLORA VM, which characterizes the seismic vulnerability of Montenegro, are detailed in Tab. 5.

Building class	w_S	w_{Sr}	w_{It}	w_{Sl}
URM-St	0.30	0.15	0.10	0.45
URM-Br	0.20	0.05	0.70	0.05
CFM	0.35	0.03	0.55	0.07

Tab. 5 – Weights w of each building class for the EXPLORA VM defined in Eqs. (1) and (2).

The ultimate fragility curves for each building class of Tab. 4, derived from the EXPLORA approach outlined in Eqs. (1) and (2), are depicted in Fig. 2 and offer a visual comparison with the aforementioned damage data.

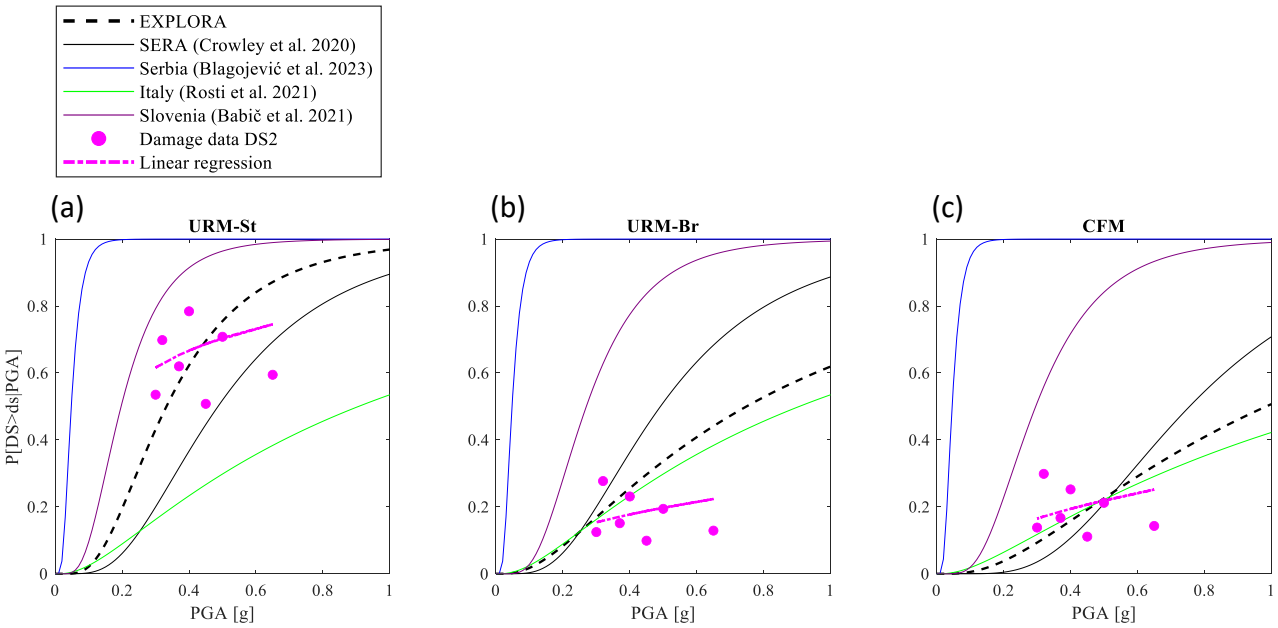

Fig. 2 – Visual comparison between the weighted DS2 EXPLORA VM and the SERA (Crowley et al. 2020), Serbia (Blagojević et al. 2023), Slovenia (Babič et al. 2021) and Italy (Rosti et al. 2021) VMs.

The weights calibrated in correspondence of the DS2 are then applied to all the DSs of each building class. The complete EXPLORA VM is depicted in Fig. 3 in comparison with the relevant damage data.

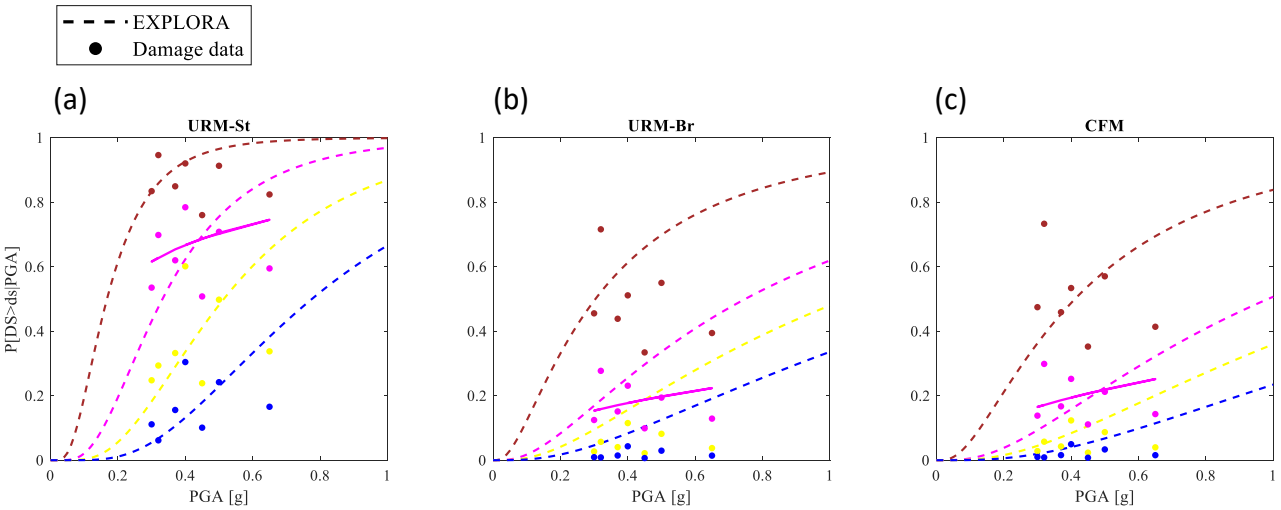

Fig. 3 – Visual comparison between the EXPLORA VM and the damage data for all the damage states (DSs): DS1 (brown), DS2 (magenta), DS3 (yellow), and DS4 (blue).

As shown in Fig. 3, the proposed EXPLORA VM reasonably captures the empirical behavior of the building classes identified for Montenegro, particularly for the URM-St and CFM. However, a slightly worse comparison is observed for the URM-Br building class. This discrepancy arises because the various VMs chosen for comparison do not accurately represent the damage data for this specific building class in DS2, as can be observed in Fig. 2 (b).

Acknowledgements

This study was performed within EXPLORA project, co-financed by Ministero degli Affari Esteri e della Cooperazione Internazionale in Italy and by the Ministarstvo nauke i tehnološkog razvoja in Montenegro.

Furthermore, we thank the authors of (Blagojević *et al.*, 2023) for sharing the fragility curve parameters from their vulnerability model for Serbia.

References

Babič, A., Dolšek, M. & Žižmond, J. 2021. Simulating Historical Earthquakes in Existing Cities for Fostering Design of Resilient and Sustainable Communities: The Ljubljana Case. *Sustainability 13(14),* 7624. DOI 10.3390/su13147624

Blagojević, N., Brzev, S., Petrović, M., Borozan, J., Bulajić, B., Marinković, M., Hadzima-Nyarko, M., Koković, V. & Stojadinović, B. 2023. Residential building stock in Serbia: classification and vulnerability for seismic risk studies. *Bulletin of Earthquake Engineering 21(9),* 4315–4383. DOI 10.1007/s10518-023-01676-0

Crowley, H., Despotaki, V., Rodrigues, D., Silva, V., Toma-Danila, D., Riga, E., Karatzetzou, A., Fotopoulou, S., Zugic, Z., Sousa, L., Ozcebe, S. & Gamba, P. 2020. Exposure model for European seismic risk assessment. *Earthquake Spectra 36(1_suppl),* 252–273. DOI 10.1177/8755293020919429

Dolce, M. & Goretti, A. 2015. Building damage assessment after the 2009 Abruzzi earthquake. *Bulletin of Earthquake Engineering 13(8),* 2241–2264. DOI 10.1007/s10518-015-9723-4

Grünthal, Gottfried. & European Seismological Commission. Working Group 'Macroseismic Scales.' 1998. *European Macroseismic Scale 1998 : EMS-98*. 99 pp. European Seismological Commission, Subcommission on Engineering Seismology, Working Group Macroseismic scales.

Lagomarsino, S., Cattari, S. & Ottonelli, D. 2021. The heuristic vulnerability model: fragility curves for masonry buildings. *Bulletin of Earthquake Engineering 19(8),* 3129–3163. DOI 10.1007/s10518-021-01063-7

Pavićević Božidar S. 2004. *An Integrated Approach to Seismic Risk Reduction through the Experience after Montenegro Earthquake 1979, Tehnika-Naše Građevinarstvo 58.2 (2004): 1-9.*

Petrovski, J., NOCEVSKI, N., RISTIC, D., MILUTINOVIC, Z., STANKOVIC, V. & PAVICEVIC BOZIDAR S. 1984. Report IZIIS 84-085 (1984) in Montenegrin.

Polese, M., Gaetani d'Aragona, M. & Prota, A. 2019. Simplified approach for building inventory and seismic damage assessment at the territorial scale: An application for a town in southern Italy. *Soil Dynamics and Earthquake Engineering 121,* 405–420. DOI 10.1016/j.soildyn.2019.03.028

Polese, M., Tocchi, G., Dolsek, M., Babič, A., Faravelli, M., Quaroni, D., Borzi, B. & Prota, A. 2023. Seismic risk assessment in transboundary areas: the case study on the border between Italy and Slovenia. In: *Procedia Structural Integrity*. 123–130. DOI 10.1016/j.prostr.2023.01.017

Rosti, A., Rota, M. & Penna, A. 2021. Empirical fragility curves for Italian URM buildings. *Bulletin of Earthquake Engineering 19(8),* 3057–3076. DOI 10.1007/s10518-020-00845-9

Rota, M., Penna, A. & Strobbia, C.L. 2008. Processing Italian damage data to derive typological fragility curves. *Soil Dynamics and Earthquake Engineering 28(10–11),* 933–947. DOI 10.1016/j.soildyn.2007.10.010

Scawthorn, C., Charleson, A., Allen, L., Greene, M., Jaiswal, K. & Silva, V. 2013. *GEM Global Earthquake Model GEM Building Taxonomy Version 2.0 Exposure Modelling*.

Silva, V., Amo-Oduro, D., Calderon, A., Costa, C., Dabbeek, J., Despotaki, V., Martins, L., Pagani, M., Rao, A., Simionato, M., Viganò, D., Yepes-Estrada, C., Acevedo, A., Crowley, H., Horspool, N., Jaiswal, K., Journeay, M. & Pittore, M. 2020. Development of a global seismic risk model. *Earthquake Spectra 36(1_suppl),* 372–394. DOI 10.1177/8755293019899953

Trifunac MD, Lee VW, Zivcic M & Manic MI. 1991. On the correlation of Mercalli-Cancani-Sieberg intensity scale in Yugoslavia with the peaks of recorded strong earthquake ground motion. *European Earthquake Engineering (1)(5),* 27–33.

U.S. Department of the Interior. 2023. https://www.usgs.gov/programs/earthquake-hazards.

Corresponding author: fabrizio.aloschi@unina.it

Correlation between site effects proxies: the case of Argostoli basin (Greece)

D. Attolico[1,2], G. Cultrera[1], V. De Rubeis[1], N. Theodoulidis[1]

[1] Istituto Nazionale di Geofisica e Vulcanologia (INGV, Italy)
[2] Asset - Agenzia regionale Strategica per lo Sviluppo Ecosostenibile del Territorio (Regione Puglia, Italy)

The purpose of this work is to explore the potential of multivariate statistical analysis method to define possible correlations between site response properties. The considered data are seismological instrumental observations and geological-geophysical parameters that could be used as proxy for the characterization of local site effect wherever seismological observations are not available.
The study area is the Argostoli basin (Greece), chosen for both the amount of earthquake and seismic noise recordings, and the geological and geophysical available information (Figure 1).
We follow the approach of Attolico et al. (2022) where multivariate statistical analysis was used to evaluate the most important site effect indicators and to deduce how the geological context influences their behaviours.
The statistical Factor Analysis technique has been applied to the different available or computed parameters including Horizontal-to-Vertical spectral ratios on earthquakes (HVSR) and noise (HVNSR), averaged over 4 frequency intervals (see Cultrera et al., 2014, for further details), the predominant frequency of HVSR and corresponding amplitude, maximum duration lengthening value (calculated from the frequency dependent mean group delay of the Fourier spectrum phases, as proposed by Sawada, 1998) and the corresponding frequency; thicknesses of the 3 lithological contrasts identified inside the basin; Vs average within the 3 aforementioned thicknesses (from Cushing et al., 2020); PGA normalized to magnitude and hypocentral distance; depth of seismic events.
The findings of this study suggest that the statistical variation of ground motion is influenced by the location of the seismic stations around and inside the basin, and by the type of lithology present underneath the site. Additionally, duration lengthening parameter is strictly correlated with the basin morphology and it is a useful tool to describe the seismic motion prolongation estimation for the site effects studies.

Towards an earthquake-induced landslide triggering map for Italy

S. Azhideh, S. Barani, G. Ferretti, D. Scafidi, G. Pepe

[1] *Università degli Studi di Genova, Genova, Italy*

Landslides are one of the most frequent geohazards that have caused devasting damage throughout history. Landslides often occur as a consequence of other natural hazards among which earthquakes can be considered as one of the main triggering factors. When an earthquake occurs, the effects of the induced ground shaking are often sufficient to cause failure of slopes that were marginally to moderately stable before the earthquake.

In the present study, we present a first attempt to define a screening map for all of Italy that classifies sites in terms of their potentiality of triggering earthquake-induced landslides based on seismic hazard. To this end, we analyze seismic hazard disaggregation results on a national scale (Barani et al., 2009) and compare magnitude-distance (*M*-*R*) scenarios with the upper-bound *M*-*R* curves defined by Keefer (1984) for different types of landslides: disrupted slides and falls, coherent slides, and lateral spreads and flows. For a given magnitude value, these curves define the critical distance below which earthquake-induced failures may occur and, as a consequence, the possibility of triggering a landslide can not be discounted.

First, for all computation nodes considered in the hazard assessment of Italy (MPS Working Group, 2004; Stucchi et al., 2011), joint distributions (i.e., probability mass functions, PMFs) of *M* and *R* are analyzed to identify all modal scenarios (i.e., local maxima). To this end, we treat each PMF as an image and apply morphological image processing techniques to find local maxima. Specifically, we apply the maximum (dilation) filter operation (e.g., Gonzales and Woods, 2018). Each *M*-*R* scenario in the PMF matrix is treated as a pixel. Each pixel is updated based on comparing it against the surrounding pixels in a running window process (a 3-by-3 square window around the target pixel is used). Specifically, the maximum filter replaces the value of the PMF associated with the central pixel with the greatest one in the running window. Finally, local maxima in the distribution are obtained by checking for element-wise equality within the original and filtered matrices, creating an array of Boolean values (Boolean matrix) within which True values indicate the modes. Figure 1 shows an example *M*-*R* distribution with indication of the modal scenarios resulting from maximum filtering and Boolean mask.

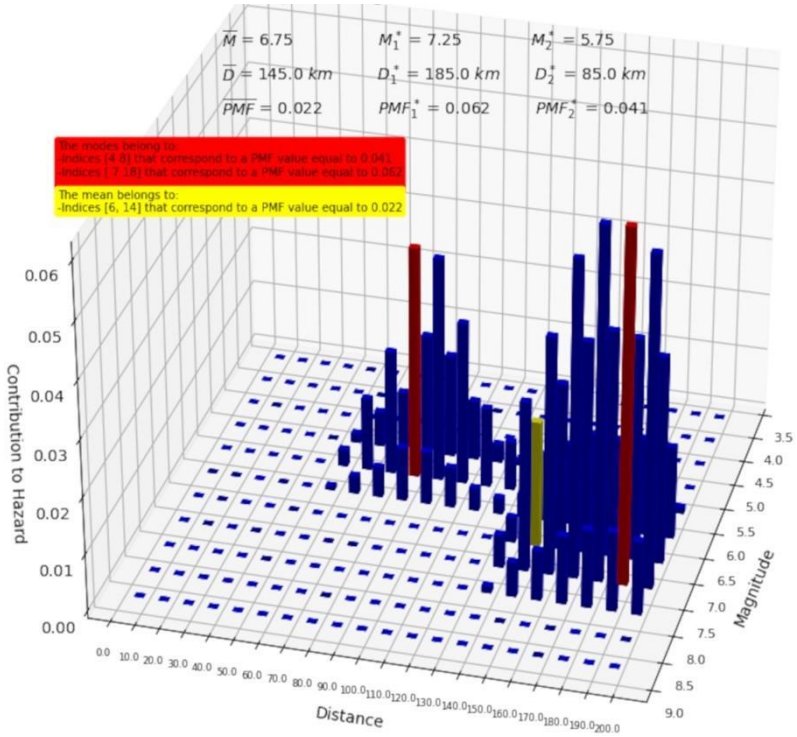

Fig. 1 Example distribution of *M* and *R* with indication of the mean and modal scenarios.

For each distribution, mean and modal scenarios of *M*-*R* are then compared to the upper-bound curves defined by Keefer (1984) and the preferred magnitude is selected as follows:

- if all *M*-*R* pairs stand above the reference upper-bound curve, then the triggering of earthquake-induced landslides can be neglected.
- if at least one *M*-*R* pair is below the reference upper-bound curve, then the triggering of earthquake-induced landslides can not be discounted.
- if more than one *M*-*R* pair lies below the reference upper-bound curve, then the triggering of earthquake-induced landslides can not be excluded and the *M*-*R* scenario that contributes the most to hazard (i.e., the *M*-*R* pair with the largest PMF value) is selected as the preferred magnitude.

Figure 2 shows an application of the criteria above to the case displayed in Figure 1.

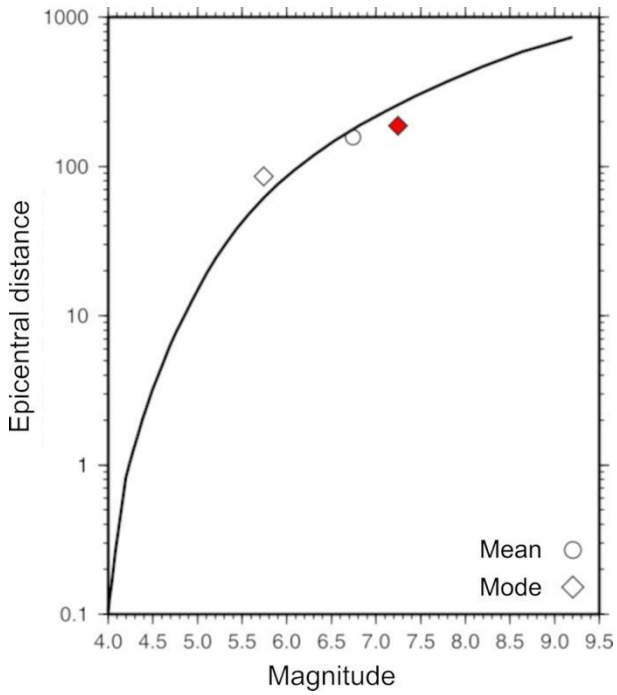

Fig. 2 Comparison of the mean and modal *M*-*R* scenarios shown in Figure 1 with the upper-bound curve for disrupted slides and falls proposed by Keefer (1984). The preferred *M*-*R* pair is displayed in red.

Figure 3 shows the geographic distribution of the preferred values of *M* and *R* resulting from the application of the methodology described above to the *M*-*R* distributions obtained from the disaggregation of the PGA hazard for a 475-yr return period together with the relevant triggering map.

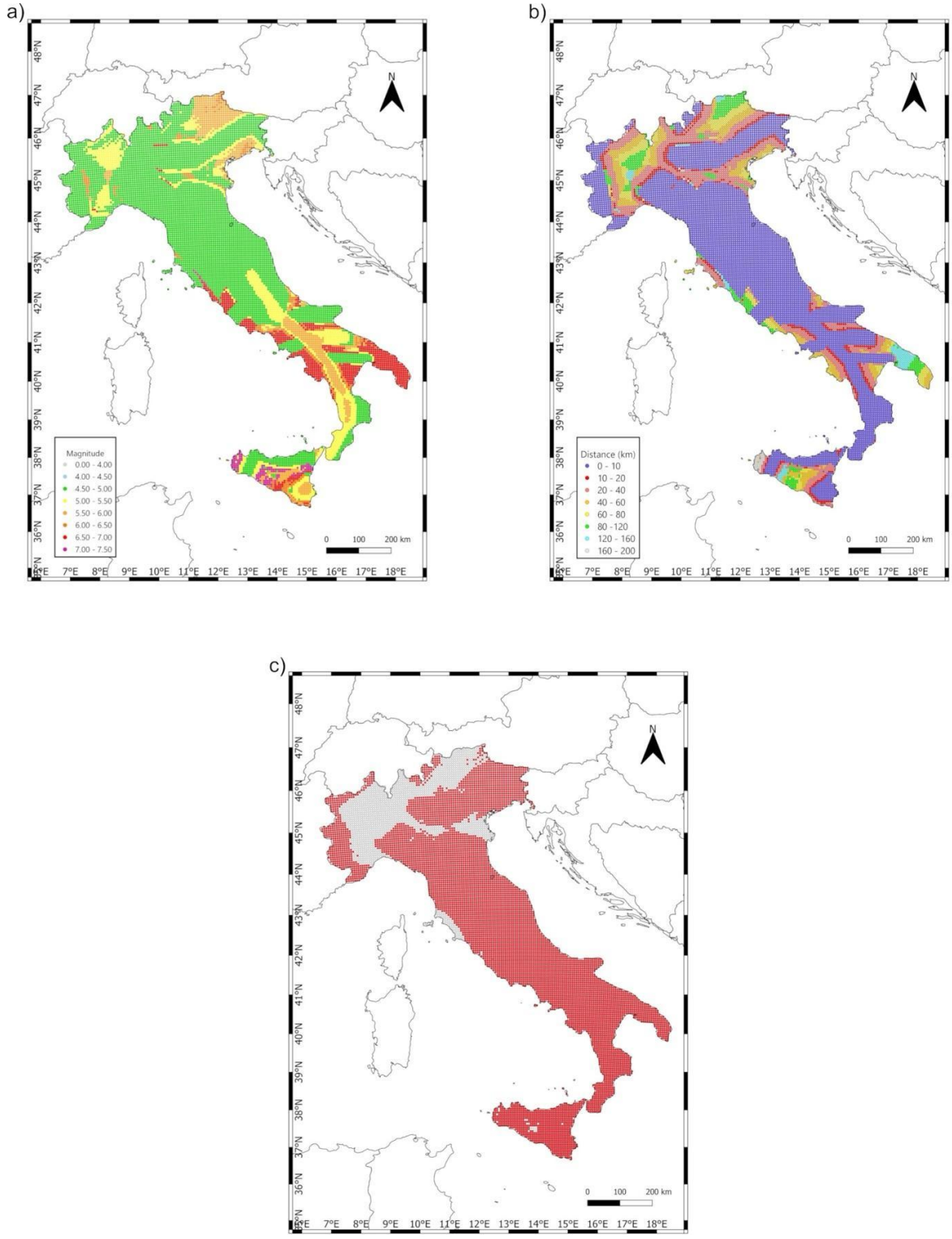

Fig. 3 Map of preferred magnitude (a) and distance (b) associated with the PGA hazard for a 475-yr return period and corresponding earthquake-induced landslide triggering map (c). In the latter, red points are nodes for which the triggering of earthquake-induced landslides can not be excluded.

Analyzing the triggering map in Figure 3c clearly shows an over-conservative scenario as the triggering of earthquake-induced slope failures can not be excluded in most of the Italian territory. It is worth noting, however, that the effect of other parameters related to the triggering of landslides deserve future consideration, particularly slope angle and stratigraphic

conditions. Moreover, can the selected *M-R* pairs produce acceleration levels above a certain critical value, thus inducing permanent slope displacement? It follows that some condition on critical acceleration (i.e., minimum acceleration to produce slope instability) should be incorporated in our methodology. Moreover, following Barani et al. (2023), future development of the work should include disaggregation results for different spectral periods as a function of soil classification. It is known, indeed, that soils resonate at different periods depending on local stratigraphic conditions (e.g., Kramer, 1996) and that disaggregation results are sensitive to the response period considered (i.e., the larger the spectral period, the greater the contribution from distant, higher magnitude events).

References

Barani S., Ferretti G., and Scafidi D.; 2023: *Evaluation of liquefaction triggering potential in Italy: a seismic hazard-based approach*. Nat. Hazards Earth Syst. Sci., 23, 1685-1698.

Barani S., Spallarossa D. and Bazzurro P.; 2009: *Disaggregation of probabilistic ground-motion hazard in Italy*. Bull. Seismol. Soc. Am., 99, 2638-2661.

Gonzales R. C. & Woods R. E.; 2018: *Digital image processing*. Pearson, New York, 1019 pp.

Keefer D. K.; 1984: *Landslides caused by earthquakes*. Bull. Geol. Soc. Am., 95, 406-421.

Kramer, S. L.; 1996: *Geotechnical Earthquake Engineering*. Prentice-Hall, Upper Saddle River, New Jersey, 653 pp.

MPS Working Group; 2004: *Redazione della mappa di pericolosità sismica prevista dall'Ordinanza PCM 3274 del 20 marzo 200*3, Final Report. INGV, Milano-Roma 2004, 65 pp + 5 appendixes.

Stucchi M., Meletti C., Montaldo V., Crowley H., Calvi G. M. and Boschi E.; 2011: *Seismic hazard assessment (2003-2009) for the Italian building code*. Bull. Seismol. Soc. Am., 101, 1885-1911.

Corresponding author: Azhideh_sina@yahoo.com

One-dimensional numerical approach VERSUS experimental quantifications of site effect parameters: the Ferrara test area

C. Barnaba (1), L. Minarelli (2), G. Di Giulio (2), G. Laurenzano (1), A. Affatato (1), P. Taverna (1), M. Vassallo (2), R. Caputo (3), G. Cultrera (2)

[1] National Institute of Oceanography and Applied Geophysics –OGS, Italy
[2] National Institute of Geophysics and Volcanology –INGV, Italy
[3] University of Ferrara - Italy

Within the work package WP06 - Empirical Testing and Calibration of the ongoing project PRIN-SERENA (Mapping Seismic Site Effects at REGional and NAtional Scale), we test the predicted estimates of ground motion parameters with the experimental values in an area with high-density geophysical investigations. The study area belongs to the lower alluvial Po plain, near Ferrara, and corresponds to an external buried portion of the Apennines foredeep basin, involved into active thrust-fold compressive structures (Martelli et al. 2017), of late Neogene-Quaternary age (Ghielmi et al., 2013). The active faults induce an important earthquake activity, documented by many historic events (Guidoboni et al., 2018, 2019), including the most recent ones in May 2012. The subsurface thick unlithified terrigenous Quaternary successions record an evolution from deep marine to alluvial plain environments. The successions are characterized by low seismic velocities (Minarelli et al. 2016; Petronio et al. 2023), and reduced seismic impedance contrasts (Mascandola et al., 2021).

Shortly after the event of May 20, 2012, the Istituto Nazionale di Geofisica e Vulcanologia (INGV) and the Istituto Nazionale di Oceanografia e di Geofisica Sperimentale (OGS) set up a dense temporary network of 18 stations (see Moretti et al., 2012; Priolo et al.,2012; Bordoni et al., 2012; Milana et al., 2014), equipped with short period and strong motion sensors. In addition, geophysical data were collected from microzonations studies and research projects performed by the city of Ferrara as well as by INGV and OGS. Around 200 single-station ambient noise measurements, 300 Vs profiles derived by seismic cone (SCPT) and 6 deep seismic boreholes (DH) were carried out.

The large amount of geophysical data (Vp, Vs, DH, noise measurements) and the availability of earthquake records, combined with the flat topography, make the Ferrara area the perfect site to test the resolving power of the one-dimensional numerical approaches (e.g. Falcone et al., 2021) to determine the amplification factors.

We collected and organized all available information in a dedicated geographic information system (GIS, Fig. 1) and reprocessed the earthquake records of all temporary seismological stations in the area.

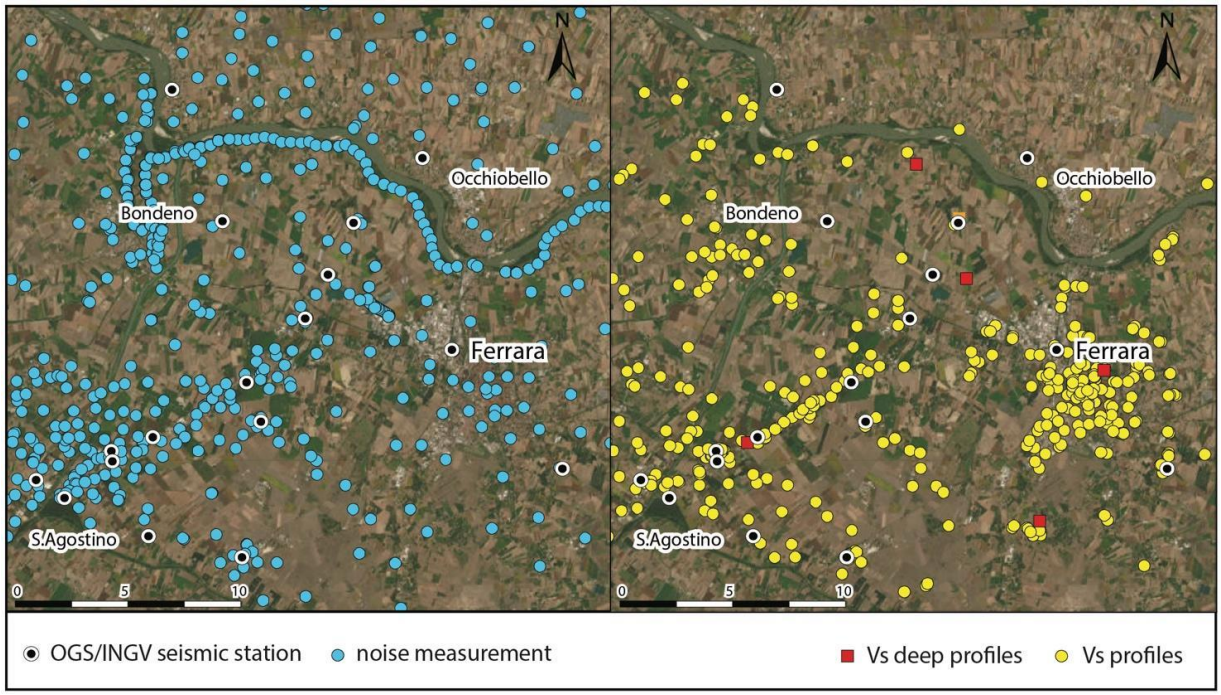

Fig. 1: The study area in the Po plain, near the city of Ferrara: on the left, noise measurements and seismic station position; on the right, Vs profiles available.

Since the Ferrara area is located in the alluvial deposits, far from rocks on the surface, the standard approach of spectral ratio to the reference site is not applicable for the assessment of FAs. To circumvent this, we computed the amplification function using the generalized inversion technique (GIT), using as reference site a virtual site (as proposed by Laurenzano et al., 2017) that mimics the conditions of the reference site considered by the building code (class A soil, with Vs=800 m/s). Due to the large amount of Vs profiles and data available at the Casaglia well, we constrained the virtual site at the surface and calculated the seismic ground motion parameters (PGA, PGV, FA, etc.). We plan to extend the pointwise results at the seismic network sites by a cluster analysis applied to the denser network of noise measurements and the Vs profiles, and compare the results with the numerical predictions of the one-dimensional approach.

References

Bordoni P., Azzara R. M., Cara F., Cogliano R., Cultrera G., Di Giulio G., Fodarella A., Milana G., Pucillo S., Riccio G., Rovelli A., Augliera P., Luzi L., Lovati S., Massa M., Pacor F., Puglia R., Ameri G.; 2012: Preliminary results from EMERSITO, the rapid response network for site effect studies. Annals of Geophysics, 55, 4, 599-607; DOI: 10.4401/ag-6153

Falcone G., Acunzo G., Mendicelli A., Mori F., Naso G., Peronace E., Porchia A., Romagnoli G., Tarquini E., Moscatelli M., 2021. Seismic amplification maps of Italy based on site-specific

microzonation dataset and one-dimensional numerical approach. Engineering Geology, 289, 106170. https://doi.org/10.1016/j.enggeo.2021.106170

Guidoboni E., Ferrari G., Mariotti D., Comastri A., Tarabusi G., Sgattoni G., Valensise G.; 2018: CFTI5Med, Catalogo dei Forti Terremoti in Italia (461 a.C.-1997) e nell'area Mediterranea (760 a.C.-1500). Istituto Nazionale di Geofisica e Vulcanologia (INGV).

Guidoboni E., Ferrari G., Tarabusi G., Sgattoni G., Comastri A., Mariotti D., Ciuccarelli C., Bianchi M.G., Valensise G.; 2019: CFTI5Med, the new release of the catalogue of strong earthquakes in Italy and in the Mediterranean area. Scientific Data 6, Article Number: 80 (2019).

Laurenzano, G., Priolo, E., Mucciarelli, M., Martelli, L., Romanelli, M., 2017. Site response estimation at Mirandola by virtual reference station. Bull. Earthquake Eng., 15:2393-2409, https://doi.org/10.1007/s10518-016-0037-y

Mascandola, C., Barani, S., Massa, M., & Albarello, D. (2021). New insights into long-period (> 1 s) seismic amplification effects in deep sedimentary basins: A case of the Po Plain basin of northern Italy. Bulletin of the Seismological Society of America, 111(4), pp.2071-2086.

Milana, G., Bordoni, P., Cara, F., Di Giulio, G., Hailemikael, S. and Rovelli, A., 2014. 1D velocity structure of the Po River plain (Northern Italy) assessed by combining strong motion and ambient noise data. Bull Earthquake Eng 12, 2195–2209 (2014). https://doi.org/10.1007/s10518-013-9483-y.

Minarelli, L., Amoroso, S., Tarabusi, G., Stefani, M., & Pulelli, G. (2016). Down-hole geophysical characterization of middle-upper Quaternary sequences in the Apennine Foredeep, Mirabello, Italy. Annals of Geophysics, 59(5), p. S0543, https://doi.org/10.4401/ag-7114.

Moretti, M., et al. (2012). Rapid response to the earthquake emergency of May 2012 in the Po Plain, northern Italy, Annals of Geophysics, 55 (4); doi:10.4401/ag-6152

Petronio, L., Baradello, L., Poggi, V., Minarelli, L., Böhm, G., Affatato, A., Barbagallo, A., Cristofano, G., Sorgo, D., Martelli, L., & Lai, C.G. (2023). Combining SH-and P-wave seismic reflection survey to support seismic response analysis. A case study from Cavezzo (Italy) after the 2012 Emilia earthquake. Engineering Geology, 313, p.106916. https://doi.org/10.1016/j.enggeo.2022.106916

Priolo, E., Romanelli, M., Barnaba, C., Mucciarelli, M., Laurenzano, G., Dall'Olio, L., Abu Zeid, N., Caputo, R., Santarato, G., Vignola, L., Lizza, C., Di Bartolomeo, P., 2012. The Ferrara thrust earthquakes of May-June 2012: Preliminary site response analysis at the sites of the OGS temporary network. Annals of geophysics, 55. 10.4401/ag-6172.

Corresponding author: cbarnaba@ogs.it

A dense accelerometric network supporting rapid damage estimation in Veneto

P.L. Bragato[1], J. Boaga[2], G. Capotosti[1], P. Comelli[1], S. Parolai[1,3], G. Rossi[1], H. Siracusa[1], P. Ziani[1], D. Zuliani[1]

[1] National Institute of Oceanography and Applied Geophysics – OGS, Italy
[2] University of Padova, Italy
[3] University of Trieste, Italy

On 20 April 2020 Regione del Veneto and the Italian National Institute of Oceanography and Applied Geophysics – OGS signed an agreement for the deployment of a dense accelerometric network covering over 50% of the municipalities in Veneto. The project continued similar initiatives undertaken by OGS in recent years (Bragato et al., 2021): its main objective was to give reliable shaking scenarios after severe earthquakes, allowing rapid damage estimations for civil protection purposes (Poggi et al., 2021). The network was built in less than nine months between February and October 2022 and currently comprises 312 three-component MEMS accelerometers each one installed in the basement of a building (Fig. 1). Twenty-two edifices were also equipped with an accelerometer at the top for studying their dynamical response. In order to reduce the administrative work and the number of formal agreements, the edifices were chosen among the headquarters of organizations of volunteers coordinated by the Civil Protection of Regione del Veneto, telephone exchange buildings of TIM s.p.a., and post offices of Poste Italiane s.p.a. (129, 120 and 42 structures, respectively). Another 21 buildings were made available by municipalities (mainly town halls). Seismic noise characterization has been performed for 100 sites and will be continued for the other ones. The network is based on the accelerometer ADEL ASX2000, developed and tested in close collaboration between OGS and the manufacturer, highlighting the interconnection between research and the private sector. It is a cost-effective instrument that guarantees mechanical robustness, quality of the recordings and sufficient sensitivity to give usable signals in the near field roughly from ML=2.5. The seismic recordings are transmitted in real-time by means of LTE internal modems using the “seedlink” protocol. The data are acquired on a virtual machine in the cloud hosted by TIM s.p.a. All the adopted solutions aim to allow the technical and economical sustainability of the network in the long term, so that similar monitoring systems can be proposed for other regions in Italy. The network proved its validity for two earthquakes that occurred in southern Veneto on 25 and 28 October 2023 (magnitude ML 4.4 and 4.3, respectively).

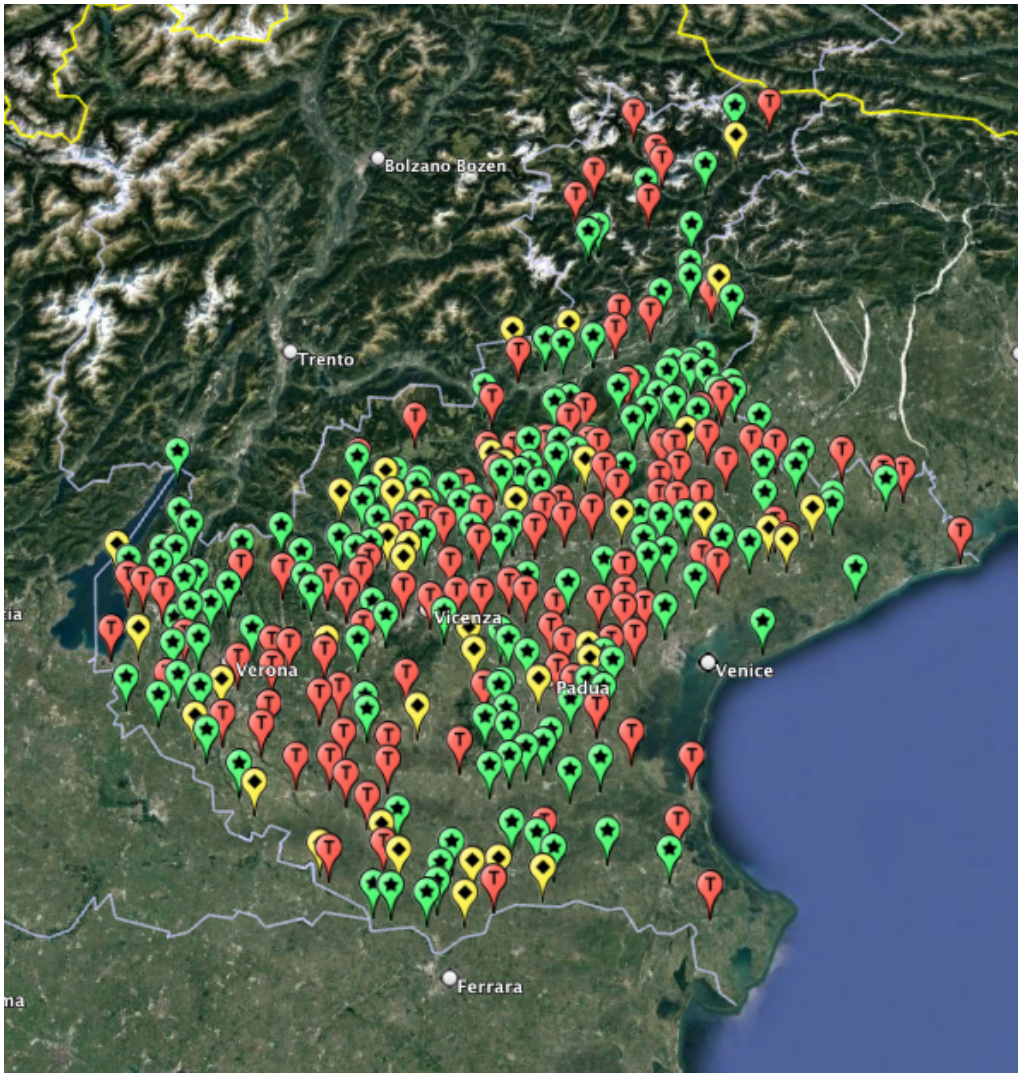

Fig. 1 – Stations composing the dense accelerometric network in Veneto: green, organizations of volunteers and other public edifices; red, telephone exchange buildings of TIM s.p.a.; yellow, post offices of Poste Italiane s.p.a.

Acknowledgements

This project was financed by the programme POR-FESR Regione Veneto 2014–2020, Action 5.3.1.

References

Bragato P.L., Comelli P., Saraò A., Zuliani D., Moratto L., et al.; 2021: The OGS–northeastern Italy seismic and deformation network: current status and outlook. Seismol. Res. Lett. 92, 1704–1716.

Poggi V., Scaini C., Moratto L., Peressi G., Comelli P., Bragato P.L., Parolai S.; 2021: Rapid damage scenario assessment for earthquake emergency management. Seismol. Res. Lett. 92, 2513–2530.

Corresponding author: pbragato@ogs.it

A GEOLOGICAL GEOPHYSICAL APPROACH FOR THE LARGE-SCALE EVALUATION OF SEISMIC AMPLIFICATION IN THE PLAIN AREA: EXAMPLE OF THE BRESCIA BASIN (PIANURA PADANA)

G. Caielli[1], R. de Franco[1], I. Gaudiosi[2], A. Mendicelli[2], M. Moscatelli[2], G. Norini[1], D. Rusconi[1], M. Simionato[2].

[1] ISTITUTO DI GEOLOGIA AMBIENTALE E GEOINGEGNERIA – CNR - Milano - Italy
[2] ISTITUTO DI GEOLOGIA AMBIENTALE E GEOINGEGNERIA – CNR - Montelibretti - Italy

This presentation aims to answer the scientific question: how to model the expected effects of site seismic amplification at different scales in a plain environment where the informative contribution of the geological-morphological survey is almost nil but widespread spatial information deriving from well geo-stratigraphy and few direct geophysical measurements in the well and indirect from surface are available.

We present the result of the analyses of the data available from surface geophysical studies with the aim of creating a database of the physical parameters characterizing the lithotypes outcropping to the depth of the “seismic” bedrock that is hypothesized coinciding with the top of the early Pleistocene, named “red discontinuity)”, in the area of the Brescia basin (CARG-ISPRA).

Quaternary deposits will be analyzed in order to associate geological units with engineering-geological units (UGT) and attribute the Vs and Vp values. For the reconstruction of the surface part, it has been decided to use seismic microzonation studies (MS). The data and information retrieved and analyzed have been collected in a data-base, each survey contains the identification code, the geographical coordinates, layer thickness and velocity values.

The fundamental objective of the work is the association of UGT to each layer identified and inserted in the tables of geophysical measurements. Then using well for the hydrogeological data, we try to assign to each layer the UGT. The results of 246 geophysical surveys and 623 hydrogeological data, mainly water wells, were analyzed. These were the starting point for the statistical analyses carried out with ArcGis and ArcGis Pro. The statistical analyses carried out relate above all to the velocities Vs and available Vp subset. Using the information derived from the analysis, it has been possible the attribution of the velocity range Vs to each UGT recognized within the Brescia basin.

This allow us to obtain a big set of seismostratigraphies for which we can calculate the site amplification and then study statistically the seismic response for the Brescia basin.

Fig. 1 – Map of the studied area.

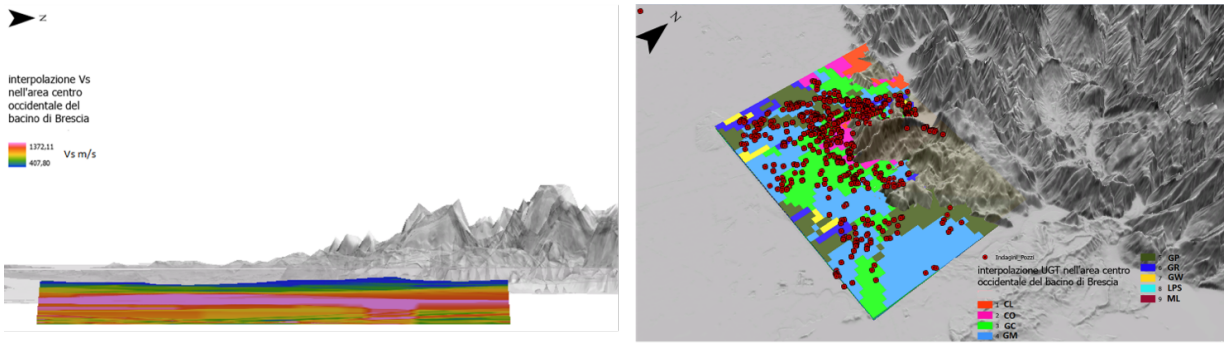

Fig. 2 – Left panel: Vp section of the 3D geological-geophysical model. Right panel: Interpolation of outcropping UGT in the western part of the Brescia basin.

References

Gino Romagnoli, Emanuele Tarquini, Attilio Porchia, Stefano Catalano, Dario Albarello, Massimiliano Moscatelli, 2022 - Constraints for the Vs profiles from engineering-geological qualitative characterization of shallow subsoil in seismic microzonation studies, Soil Dynamics and Earthquake Engineering, 161, 107347, https://doi.org/10.1016/j.soildyn.2022.107347.

Geoportale Regione Lombardia https://www.cartografia.servizirl.it/viewer32/index.jsp?config=config_caspita.json.

Acknowledgments

This work was carried out as part of the projects:
DTA.AD004.330 - CARG-BS - Realizzazione della Carta Geologica e Geotematica d'Italia Foglio 121 Brescia.
DTA.AD003.757 - PRIN-SERENA MUR-2020MMCPER - Mapping seismic site effects at regional and national scale.

Corresponding author: davide.rusconi@igag.cnr.it

Mapping seismostratigraphical amplification effects at regional scale from geological data

N. Carfagna[1], P. Pieruccini[2], P. Fantozzi[1], D. Albarello[2,3]

[1] Department of Physical Science, Earth and Environment, University of Siena, Siena, Italy
[2] Department of Earth Science, University of Turin, Turin, Italy
[3] Consiglio Nazionale delle Ricerche, Istituto di Geologia Ambientale e Geoingegneria, Rome, Italy

It is widely recognized that the amplification of ground motion during earthquakes is attributed to the interference of seismic waves trapped between the free surface and impedance contrasts in the shallow subsoil. Seismic Microzonation (SM) studies are devoted to evaluating these site effects, but their application in wider contexts is a hard and expensive task. To estimate seismic site effects at regional scale, the most viable approach is to utilize detailed geological and geomorphological data (1:10.000-1:50.000), which are available for a large part of Italy.

In the frame of the national research project “SERENA”, in this study a procedure is proposed and tested to constrain the entity of 1D seismostratigraphical ground motion amplification based on geological information at the most detailed scale available. In particular, amplification factors are estimated for Seismically Homogeneous Microzones (SHM) defined on the basis of geological information. Each SHM is represented as a stack flat homogeneous layer, each characterized in terms of engineering-geological units by following the seismic microzonation standards (*Commissione Tecnica, 2018; SM Working Group, 2015*). Seismic properties of each layer (shear waves velocity, density, damping and G/G0 curves) and respective range of variability are determined on the basis of the most recent literature (*Romagnoli et al., 2022*; *Gaudiosi et al., 2023*).

This information feeds a linear equivalent numerical approach and the Inverse Random Vibration Theory (*Kottke and Rathje, 2008*) to compute the expected seismic response at each SHM. To account for the relevant uncertainty, 100 random profiles were generated for each SHM, which were compatible with available data. Outcomes of the relevant numerical simulations were considered to assess uncertainty affecting amplification estimates at each SHM.

Through this procedure, approximately 4000 Seismically Homogeneous Microzones were identified, distributed across over 80,000 formation outcrops mapped on Geological map of Tuscany Region, selected by dedicated ArcgisPro ™/Arcpy ™ scripts elaborated for this aim. The 50th percentile of the amplification factor (AF) distribution for each SHM was taken into consideration. This process aimed to create a new map of amplification factors for the entire territory of Tuscany, achieving an optimal spatial resolution of 1:10,000.

To assess the reliability of the results obtained from numerical simulations, and evaluate the possible presence of biases, outcomes of the numerical procedure here considered were

compared with those from second and third levels of Seismic Microzonation studies available in Tuscany. Approximately 1500 benchmark samples were identified, revealing distinct trends among various SHM, particularly between those with outcropping sedimentary covers and those with exposed geological bedrock.
In general, amplification estimates provided by the approach here proposed provide a slight overestimate of the ones provided by the detailed seismic microzonation studies (less than 10% on average). However, this overestimate is largely within the range of uncertainty affecting regional estimates and mostly concerns SHMs where bedrock outcrops.
It is worth to note that by no way the proposed approach should be considered as a substitute for detailed local studies. Anyway it could be considered to provide ex-ante evaluations to be used as a preliminary reference for large scale risk analysis and for a preliminary assessment of expected ground motion effects where more detailed studies are not available so far.

References

Commissione Tecnica MS; 2018: Standard di rappresentazione e archiviazione informatica degli studi di MS vers.4.1.

Gaudiosi I., Romagnoli G., Albarello D., Fortunato C., Imprescia P., Stigliano F. Moscatelli M.; 2023: G/G 0 (γ) and D(γ) curves joined with engineering geological units in Italy. In press on Sci.Data,

Romagnoli G., Tarquini E., Porchia A., Catalano S., Albarello D., Moscatelli M.; 2022: The possible use of engineering-geological qualitative characterization of shallow subsoil for a preliminary estimate of the Vs profile in seismic microzonation studies. Soil Dyn. Earthq. Eng., 161, 107347,

SM Working Group; 2015: Guidelines for Seismic Microzonation, Conference of Regions and Autonomous Provinces of Italy – Civil Protection Department, Rome.

Corresponding author: nicolo.carfagna@student.unisi.it

Seismic isolation for Glass Curtain Walls

N. Cella, C. Bedon

University of Trieste, Department of Engineering and Architecture, Trieste, Italy

Introduction

Glass curtain walls (GCWs) are a typical component of modern buildings, providing them a sleek and modern aesthetic. However, glass façades are also a criticality for buildings, and require special design strategies under extreme design loads like earthquakes. The main reason is the brittle behaviour of glass, which makes these composite systems a potential hazard for life.

Several surveys conducted after natural earthquakes, as well as extensive laboratory experimental campaigns, highlighted the high vulnerability and susceptibility of GCWs to major damage following inter-story drifts, even in those buildings that have suffered for minimal damage in structural members (Bedon et al., 2017). This damage is generally due to an incompatibility between the deformation of the primary structure and the façade components. As such, there is a major need to develop technological solutions to optimise the capability of GCWs to satisfy these displacement demands caused by seismic actions. Possible approaches – like the device fabricated by Heonseok et al. (2021) – should be able to offer energy dissipation and flexibility to accommodate the seismic shock and demand.

In this paper, the in-plane lateral performance of a full-scale case-study glass façade (Aiello et al., 2018) is numerically investigated to explore its criticalities and to assess the potential and feasibility of a possible isolation system inspired by the well-known rubber seismic isolators for structures. The discussion of numerical comparative results poses attention on the different behaviour of the reference “fixed” façade and the “isolated” façade configurations, highlighting the potential benefits in terms of seismic demand reduction.

Case study

As a reference for the numerical modelling, the GCW presented in Aiello et al. (2018) was taken in account.

The tested façade is a typical stick system with five mullions and twenty transoms in extruded aluminium (alloy EN-AW 6060, supply type T5). The GCW is 7.80 m high and 5.38 m wide with a constant inter-story height of 3.4 m. The transom to mullion connection is made through a U-shaped steel joint fixed to the mullion with two stainless steel screws.

Glass panels (1300x1900h mm) consist of insulated glass units (IGUs) where two laminated elements (4+4 mm thick annealed glass panels with two PVB interlayers) are spaced by a 16 mm cavity. Each panel is supported by two setting blocks made of aluminium alloy with a layer of plastic material (rubber pad) on top, located at about L/10 from the end of the transom, where L is the length of the transom. Glass panels are then fixed in position by means of pressure plates, which are screwed to the aluminium frame. The clearance between glass panels and frame is about 6 mm.

Finite Element model

A geometrically simplified and computationally efficient numerical model - inspired by the strategic modelling steps discussed by Caterino et al. (2017) - was implemented in SAP2000 (Fig. 1(a)).

The model consists of 1D beam elements to accurately represent the mechanical properties of the aluminium frame mullions and transoms. The latter are assumed to be hinged at both ends. 2D shell elements are employed to describe the insulated glazing units (IGUs), with their total thickness corresponding to the sum of the glass layers (thus excluding cavity and PVB layers). A linear constitutive law is adopted for both glass and aluminium, with input material properties summarized in Tab. 1. Two different link types available in SAP2000 are employed to reproduce the mechanical interactions between the different components of the façade:

- "Gap" links are used to represent potential contact between IGUs and frame members following clearance closure. To account for the role of setting blocks, the gap value for the respective links is set to zero.
- "Wen" links are used to characterize the mechanical behaviour of the gaskets.

The typical simulation consisted of nonlinear Direct-Integration time-history analysis in displacement control. For the validation of the numerical model, the experimental displacement time-history was applied to the intermediate constrained joints, while the displacement obtained from a natural earthquake record (Newhall - Los Angeles County Fire Station) was used to evaluate the effectiveness of the isolation system (Fig. 1(b)). The chosen mesh size results in approximately 450 frame elements, 1200 shell elements, and 1600 joints.

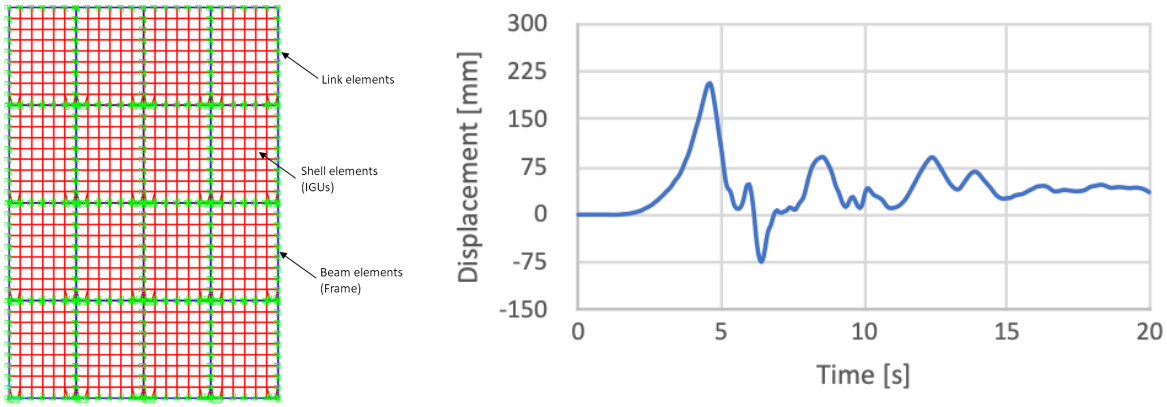

(a) (b)

Fig. 1– (a) Numerical model in SAP2000 and (b) Displacement Time-History from a natural earthquake.

Material	Density [kg/m³]	Modulus of elasticity [MPa]	Poisson' coefficient [-]
Aluminium (6060 T5)	2700	70,000	0.3
Annealed glass	2500	70,000	0.23

Tab. 1 – Input material properties.

To assess the effect and potential of the seismic isolation system, the "fixed" model was modified by introducing a set of linear links with specific stiffness components. In addition, the position of the lower constraints was changed by assuming that the façade is supported at the base.

The linear links in use for the isolation system are characterized by two different stiffness values in the three translational directions. For the present investigation, the isolator is assumed to be rigid along the direction of the link (i.e., the Fixed option of SAP2000 is used). The stiffness in the other two directions is calculated following the design approach for rubber seismic isolators. Specifically, given the period of the isolated system, T_{isol}, the stiffness of the isolation system is given by:

(1)

$$k_{isol} = \left(\frac{2 \bullet \pi}{T_{isol}}\right)^2 \bullet M$$

Where $M = 1880kg$ is the total mass of the GCW. The stiffness of the isolator is thus calculated as follows:

(2)

$$k_{isol,i} = \frac{k_{isol}}{n}$$

where $n = 15$ is the number of isolators.

The input features of isolating system were chosen to result in a vibration period of the isolated system of 2.0 seconds. For comparison, the "fixed" configuration has an in-plane vibration period of 0.0053 seconds. An equivalent viscous damping coefficient of 10% was also considered for the isolated system. It is worth noting that, assuming a dynamic shear modulus of 0.4 MPa for the rubber layers and a cylindrical shape for the isolator, the stiffness corresponds to a ratio $\frac{r^2}{h} = 0.98$ (e.g., a 30 mm high rubber cylinder with a radius of 5.4 mm).

The above link parameters have been calibrated as shown in Tab. 2.

Parameter	Gap	Wen	Linear
Stiffness [N/mm]	75	500	1.24
Damping [N·s/m]	-	-	78.75
open [mm]	6	-	-
ratio [-]	-	0	-
yield [kN]	-	50	-
exp [-]	-	1	-

Tab. 2 – Link parameters.

It is important to note that the parameters for Wen and Gap links were chosen with the aim of achieving the best agreement between the numerical results and the experimental data.

Discussion of numerical results

Fig. 2(a) shows the numerical response of the façade subjected to in-plane lateral displacement as a function of the corresponding reaction force, compared to the reference literature experiment (Aiello et al., 2018). The numerical results have good agreement with the test, confirming the goodness of the modelling strategy proposed by Caterino et al. (2017) and further elaborated in Aiello et al. (2018) for predicting the global seismic behaviour of a stick curtain wall.

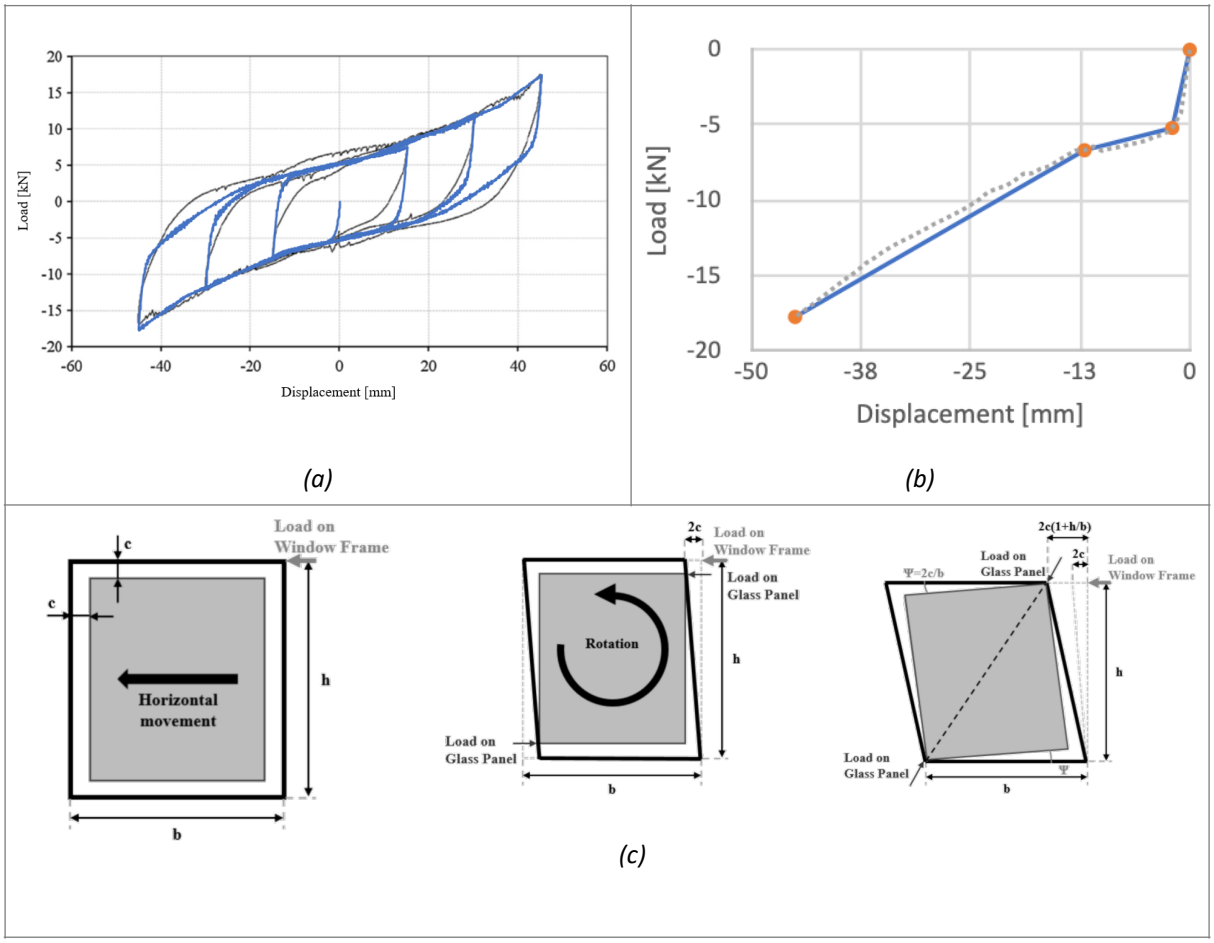

Fig. 2 – (a) Load-displacement response compared to the reference experiment (Aiello et al., 2018) for the "fixed" model; (b) Schematization of the load-displacement response; (c) Movement of a glass panel under in-plane seismic action (Sucuoğlu & Vallabhan, 1997).

The load-displacement response of the façade can be schematize as shown in Fig. 2(b), where it is possible to subdivide it into three branches:

1. The first branch, AB, is governed by friction between glass panels and gaskets.
2. The second one, BC, is governed by the lateral stiffness of the bare aluminium frame.
3. In the point C the glass panels make contact with the aluminium frame; in the last branch, CD, glass panels start to contribute to the global stiffness of the façade.

The movement of a glass panel within the frame can be summarized as in Fig. 2(c) (Sucuoğlu & Vallabhan, 1997):

1. Rigid horizontal movement of the panel until the contact with the frame.
2. The contact happens in two opposite glass corners and the panel start to rotate.
3. When the two opposite glass panel corners make contact with those of the surrounding frame, the panel acts like a diagonal strut.

The final configuration may result in either a compressive crushing failure or the practically intact glass panel falling out due to the loss of support on the contour.

Fig. 3(a) and (b) show the deformed shape of the “fixed” and “isolated” models at the maximum imposed displacement. The effect of the adopted isolation system is evident and corresponds to a major reduction in the frame deformation, as well as a decrease in its absolute in-plane lateral displacement. The latter is also highlighted by Fig. 3(c), where the displacement of the same control point is reported for the two configurations. The reduction corresponding to the maximum imposed displacement is - 67%. Such a major decrease in the in-plane bending frame deformation naturally leads to a reduction of stress peaks in both metal and glass components, as Fig. 3(d) shows. In this case, the stress reduction corresponding to the maximum imposed displacement is quantified in - 99%.

As shown in Fig. 2(c), breaking of the glass or its fall-out depends to the contact with the frame. Fig. 3(e) shows the relative distance between two joints, one from a glass panel and one from the frame, connected with a link. Fig. 3(e) shows a constant relative distance for the “isolated” model, equal to the initial clearance of 6 mm. This confirms the possibility of avoiding glass failure adopting the seismic isolation system presented. Additionally, Fig. 3(e) highlights an intrinsic limitation of the modelling strategy adopted for the “fixed” model in the local performance assessment as the relative distance becomes negative.

Conclusions

Due to brittle behaviour of glass, façades are vulnerable building components, especially under extreme actions, such as earthquakes. In this paper, preliminary considerations and numerical results about the effects of a seismic isolation system inspired by rubber seismic isolators are presented. The attention was given primarily to reduction in displacement and stress peaks through a comparison between the numerical results of an experimental tested glass façade and the same GCW equipped with the isolation system. In this regard, a - 67% reduction in maximum frame displacement and a - 99% reduction in peak frame stress was recorded. In addition, the absence of relative displacement between glass and frame was noted for the “isolated” façade. In this sense, the analysis of present results confirms the positive effects of such a system in reducing damage of GCWs subjected to in-plane lateral displacement.

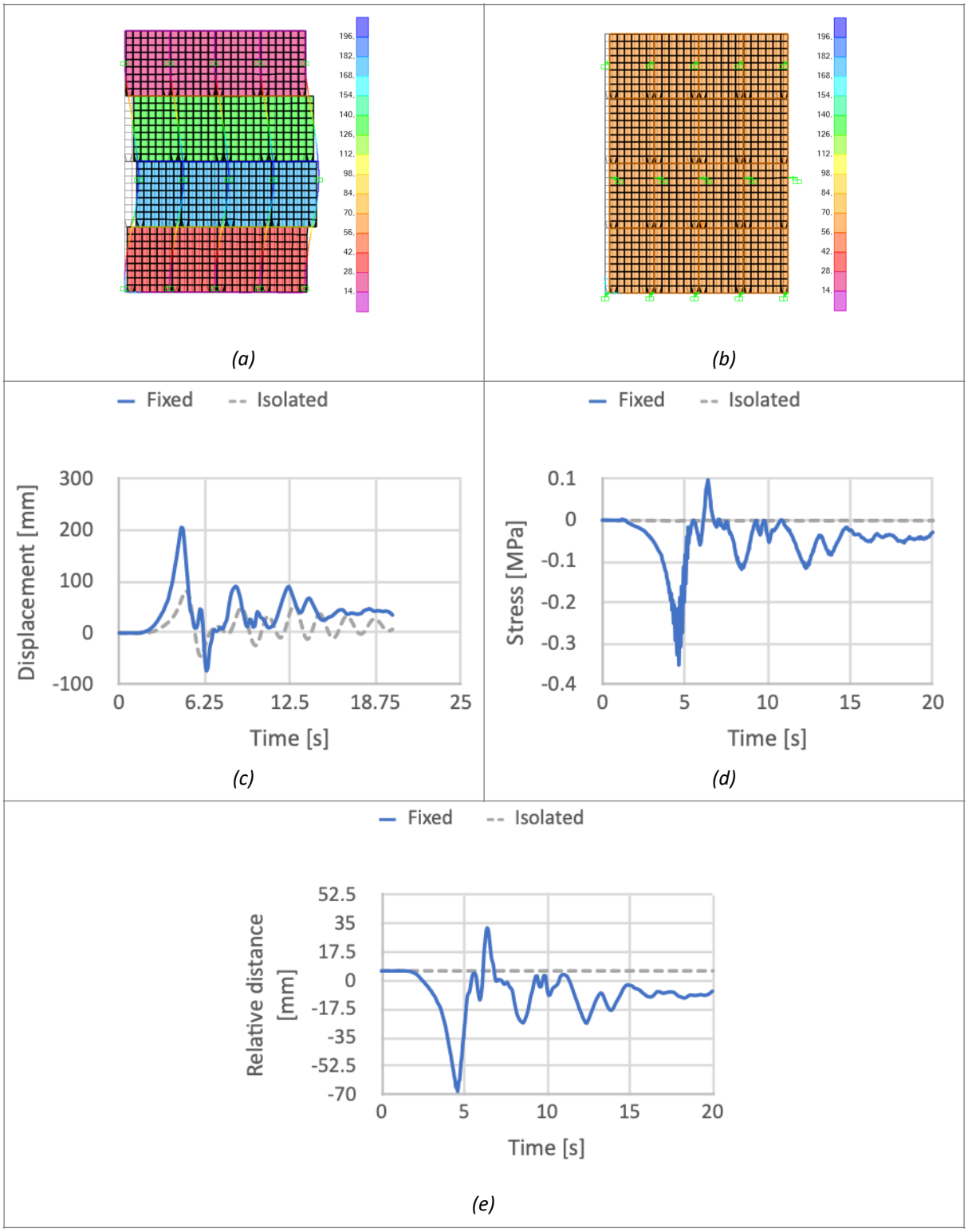

Fig. 3 – Deformed shape for (a) "fixed" and (b) "isolated" model and comparison for (c) frame absolute displacement, (d) frame stress and (e) glass-frame relative distance.

References

Aiello C., Caterino N., Maddaloni G., Bonati A., Franco A., Occhiuzzi A.; 2018: Experimental and numerical investigation of cyclic response of a glass curtain wall for seismic performance assessment. Construction and Building Materials.

Bedon C., Zhang X., Santos F., Honfi D., Kozłowski M., Arrigoni M., Lange D.; 2017: Performance of structural glass façades under extreme loads - Design methods, existing research, current issues and trends. Construction and Building Materials.

Caterino N., Del Zoppo M., Maddaloni G., Bonati A., Cavanna G., Occhiuzzi A.; 2017: Seismic assessment and finite element modelling of glazed curtain walls. Structural Engineering and Mechanics.

Heonseok L., Myunghwan O., Junwon S., Woosuk K.; 2021: Seismic and Energy Performance Evaluation of Large-Scale Curtain Walls Subjected to Displacement Control Fasteners. Applied Sciences.

SAP2000 Static and Dynamic Finite Element Analysis of Structures; 2014: Berkeley, USA. Computers and Structures Inc.

Sucuoğlu, H., Vallabhan, C.; 1997: Behaviour of window glass panels during earthquakes. Engineering Structures.

Corresponding author: chiara.bedon@dia.units.it

The state of art of the Italian National Seismic Network

L. Chiaraluce, A. Mandiello, M. Massa, D. Piccinini and RSNM-BOARD[1]

[1] *Istituto Nazionale di Geofisica e Vulcanologia (INGV, Italy)*

The National Seismic Network (RSN) is a research infrastructure that must allow the scientific community to practise and develop cutting-edge seismological research topics. To do this, the RSN must have a configuration able to guarantee the continuous production in real time of high-quality data, in standard formats, correctly described and easily and freely accessible to all users. It is our opinion that if the RSN allows the development of front-line scientific research, it will easily be able to allow a detailed monitoring service of seismic activity throughout the whole national territory.

In this context, network configuration and technology play a fundamental role. For this reason, we have established a series of analyses aimed at evaluating the quality of the data produced by both the velocity and accelerometer stations of the IV and MN Networks managed by the INGV. Thus, through a complex analysis of the signal's characteristic and continuity and instruments association from which the data are produced, we have therefore generated a sort of quality ranking of the stations managed by INGV.

The result of this study will serve not only to carry out interventions aimed at improving the qualitatively less performing stations and to decide on a maintenance policy based on the importance of the specific station, but also to allow us to propose a new project for the true modernization of the National Network. Modernization that will pass not only through a simple densification, but also through an implementation of instrumentation, acquisition technology and installation methods.

Corresponding author: lauro.chiaraluce@ingv.it

Regional scale geological/geotechnical parametrization for seismic amplification abacuses – a global approach in the Piedmont Region.

C. Comina [1], G.M. Adinolfi[1], A. Bertea[2], C. Bertok[1], V. Giraud[2], P. Pieruccini[1]

[1] Università degli studi di Torino, Department of Earth Sciences; Torino, Italy.
[2] Seismic Sector, Piedmont Region; Pinerolo, Italy.

Introduction

Amplification abacuses are widely diffused simplified tools for the quantification of local stratigraphic amplifications of the seismic ground motion over large areas, i.e. Regions. To be effective, the abacuses should be representative of a geological/geotechnical model including all possible seismo-stratigraphical settings of the study area (Pieruccini et al., 2022). Thus, abacuses must be the result of a compromise between generalization and specialization (Peruzzi et al., 2016) and several approaches have been adopted in the past for their formulation (e.g. Pagani et al., 2006). Most of these approaches include as fundamental steps: 1) geological/geotechnical modelling, 2) parameterization, 3) numerical simulations, 4) statistical analysis and the final compilation of representative abacuses. The first two phases are undoubtedly the most important and troublesome. An extensive characterization of the study area is required, preferably based on geological, geotechnical and geophysical databases from Regional Authority's repositories. The statistical significance of the collected data should be resumed in a proper parameterization of the geological/geotechnical model of the area of study, in terms of potential seismo-stratigraphical settings. We present in this study the preliminary work done for the assessment of the Piedmont Region (Northern Italy) amplification abacuses focussing on the shear wave velocity (Vs) distribution of the Geological Domains (GD) within the Region that will be adopted as a driving tool for the following numerical simulations and statistical analysis.

Methodology

The first step was the assessment of the Engineering Geological Model for the Piedmont Region by the identification and mapping of the different Geological Domains (GD), each one characterised by an homogeneous Geological and Geomorphological setting, including a number of litho-stratigraphical logs. The original regional database was 1:250.000 scale Geological Map that allowed the identification of 13 different GDs (Figure 1).

Each GD is characterized by different bedrock typologies and potentially different litho-stratigraphic settings, including Cover Terrains. The GDs are related to: a) the Alpine mountain chain with different bedrocks (GD 1 to 4) including the main Alpine valleys (GD 5); b) the foreland hilly landscape both with different bedrock and cover terrains typologies and thicknesses (GD 6 and 7); c) the Po river plain, fed by alpine rivers, with thick mostly coarse-grained Quaternary deposits overlying at depth different bedrocks (GD 8); d) minor alluvial plains fed by rivers coming from the Apennines and the foreland hills with thick mostly fine-grained Quaternary deposits overlying at depth different bedrocks (GD 9 and 10); e) the morain amphitheatres and the associated fluvio-glacial and lacustrine deposits (GD 11 and 12); f) the complex successions belonging to the Ligurian Units (GD 13).

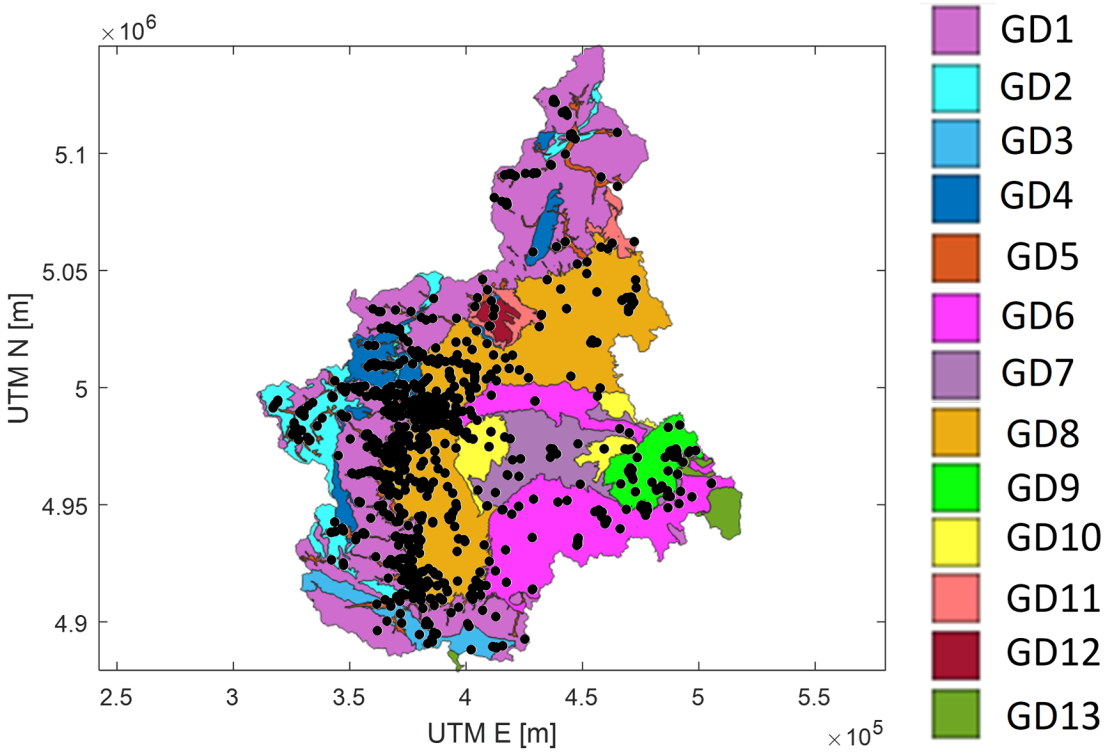

Figure 1 – Map of the Geological Domains within the Piedmont Region, black dots represent the available geophysical information in terms of shear wave velocity profiles from Regional repository database, on purpose implemented information and specific field tests executed.

Once the GDs were identified the available geotechnical and geophysical databases from Regional authority's repositories were used for the geological/geotechnical characterization and for parameterization within each GD. One of the main parameters to be considered in the study of stratigraphic amplifications is the seismic bedrock depth and the shear wave velocity (Vs) of the different units overlaying the seismic bedrock. With this respect the analysis of the Regional geophysical database allowed the assessment of about 1200 Vs profiles. In order to fill the gap in the geographic data distribution we added more Vs profiles thanks to the collaboration with Techgea S.r.l., a leading geophysical society at Regional scale (about 300 Vs profiles) and by performing specific field tests or implementing specific information from literature data (about 50 Vs profiles).

All the available data underwent specific Quality Control (QC) in order to consider only reliable and state of the art information. Data deriving from MASW tests (the most widely diffused technique for Vs profile determination) underwent a specific QC control consisting in checking: 1) the consistency of the dispersion curve, that should present a clearly visible and continuous fundamental mode in the frequency band of interest; 2) in case of presence of multiple modes of vibration, they should be well separable, well distinguishable and reliably interpretable independently; 3) the picking of the dispersion curve that should be reliable and fitting with the spectral maxima of the seismogram transform used for the analysis; 4) the inversion of the data should lead to a synthetic dispersion curve very close to the experimental data *i.e.* good correspondence between the experimental data and the results of the inversion; 5) the depth of the Vs profile should be compatible with the minimum frequencies observed in the analysis of the dispersion curve, *i.e.* investigation depth less than at least the maximum wavelength (preferably half the maximum wavelength); 6) the Vs profile should match the minimum parametrization criterion, *i.e.* number of analyzed layers compatible with the experimental information.
The results of the QC are about 1000 Vs profiles distributed over all the GDs (Figure 1), concentrated near the main urban settlements and most populated areas that are the main targets for such types of studies. The final step is the evaluation of specific Vs profile distribution within each GDs and their comparison among different GDs.

Results and Discussion

As an example, the results of the performed analysis over the GD 8 (Po plain fed by alpine rivers) are reported in Figure 2. In this GD 362 Vs profiles were available (Figure 2a) of which 66 reached the seismic bedrock (Figure 2b). The average Vs of the bedrock is 975 m/s and its depth is between 5 and 46 m. The Vs,z (harmonic average velocity) distribution of the non-bedrock layers was also computed for each profile (Figure 2c) together with the resulting Vs,h according to NTC (Figure 2d). The Vs,z is indeed usually considered as a closer representation of the physics of the problem than the Vs layered profile (Comina et al., 2022). This allowed also to obtain a representative median Vs,z profile for the GD (together with its standard deviation).
Median Vs,z profiles were then analysed in the different GDs (Figure 3). The distribution of the median Vs,z profiles show groups of GDs with very similar behaviours, reflecting the similarities in the properties of the non-bedrock deposits. Following a global approach to the data analysis the median Vs,z profiles, eventually merged between similar GDs, will be the basis for the following randomization and simulation steps. For this purpose specific randomization approaches, based on the same Vs,z (Passeri et al., 2020) or on usually adopted randomization criteria (e.g. Toro, 2022) will be evaluated. This proposed global approach allows to overcome the limitations inherited by the uncertainties of the specific litho-stratigraphic settings within each GD, due to the regionality scale of observations and the quality of the existing databases.

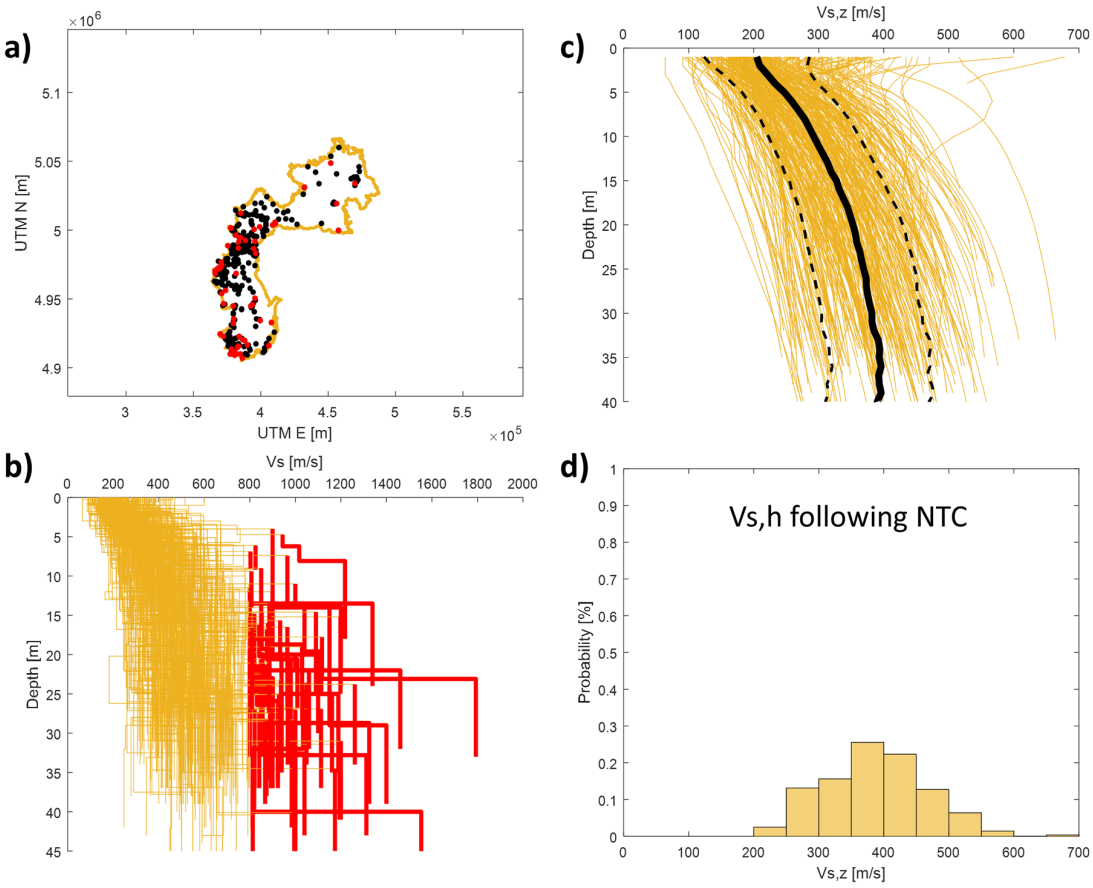

Figure 2 – Example results of the performed analysis over GD 8 – Po plain: a) Vs profile availability within the GD (black dots) and evidence of the Vs profiles reaching the seismic bedrock (red dots); b) All available Vs profiles (orange lines) with evidence of the bedrock velocities (red lines); c) Vs,z profiles for the non-bedrock units and their mean (continuous black line) and standard deviation (dashed black lines); d) Vs,h distribution following NTC.

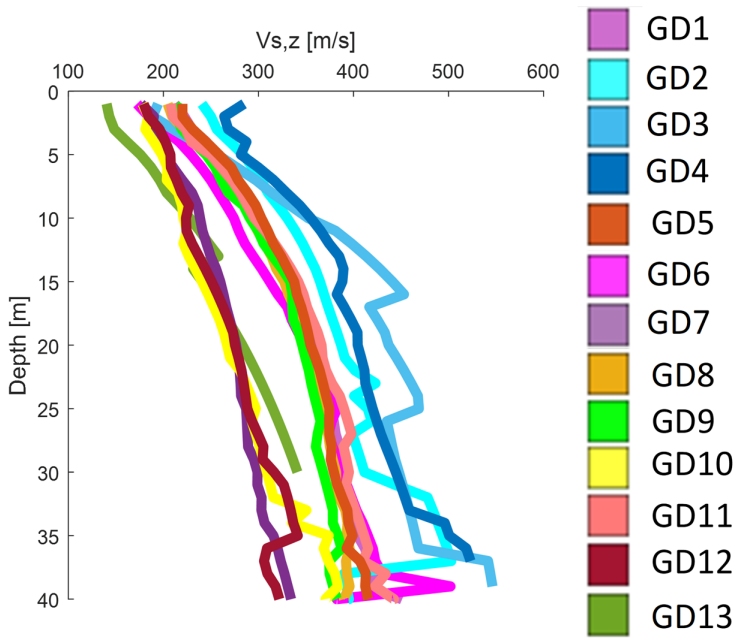

Figure 3 – Average Vs,z profiles for the non-bedrock units for each GD.

Conclusions and future work

The preliminary work done for the construction of the Piedmont Region amplification abacuses is presented and discussed in this study with particular attention in the definition of the shear wave velocity distribution of the different identified Geological Domains (GD). For this purpose, an extensive database of about 1000 Vs profiles was assessed for the randomization approaches to abacuses construction. Moreover, the median properties of the distribution of the Vs profiles within the GDs might provide useful data for similar materials in analogous geological contexts. Further work will include the analysis of available borehole logs in the Region and the definition of decaying curves to be adopted in the execution of specific numerical simulations.

Acknowledgements

Authors are indebted with the Seismic Sector of Piedmont Region for their support and data availability, with Techgea S.r.l. for the sharing of additional shear wave velocity profiles, fundamental to complement the data.

References

Acunzo G., G. Falcone, A. di Lernia, F. Mori, A. Mendicelli, G. Naso, D. Albarello, M. Moscatelli, 2023, NC92Soil: A computer code for deterministic and stochastic 1D equivalent linear seismic site response analyses, Computers and Geotechnics 165 (2024) 105857.

Comina C., Foti S., Passeri F., Socco L.V., 2022, Time-weighted average shear wave velocity profiles from surface wave tests through a wavelength-depth transformation, Soil Dynamics and Earthquake Engineering, 2022, 158, 107262.

Pagani M., Marcellini A., Crespellani T., Martelli L., Tento A., Daminelli R., (2006) Seismic microzonation regulations of the Emilia-Romagna Region (Italy). Third international symposium on the effects of surface geology on seismic motion, Grenoble, France, 30 August–1 September 2006.

Passeri F., Foti S., Rodriguez-Marek A., 2020, A new geostatistical model for shear wave velocity profiles, Soil Dynamics and Earthquake Engineering, 2020, 136, 106247.

Peruzzi G., D. Albarello, M. Baglione, V. D'Intinosante, P. Fabbroni, D. Pileggi, 2016, Assessing 1D litho-stratigraphical amplification factor for microzoning studies in Italy, Bull. Earthquake Eng. 14:373–389.

Pieruccini P., Paolucci E., Fantozzi P.L, Naldini D., Albarello D., 2022. Effectiveness of Geological-Geomorphological modelling for Seismic Microzonation studies. Nat Hazards 112, 451–474.

Toro G.R., 2002, Uncertainty in Shear-Wave Velocity Profiles, J Seismol (2022) 26:713–730.

Corresponding Author: cesare.comina@unito.it

Using data from CRISP database to infer site response behaviour

G. Cultrera[1] , A. Mercuri[1]

(1) Istituto Nazionale di Geofisica e Vulcanologia, Roma - Italy

The CRISP archive is a web portal that collects site information of the Italian National Seismic Network RSN (website crisp.ingv.it; Mercuri et al., 2023). It is organized to contain all the information useful for the site characterization, such as: thematic maps on geological characteristics; information on station and housing (location, instrumentation, data quality, housing type); geological data under and around the station (stratigraphy, geological review, morphological, lithological and geological classification, cross section); seismic analysis on recordings (spectral ratio on noise and earthquake, signal polarization); geophysical investigations (Vs profile, non linear curve); topography and soil class. CRISP is populated with heterogeneous data coming from pre-existing INGV archives or having different origins, such as: maps and geological description from ISPRA (https://www.isprambiente.gov.it/), results of seismological analyses and geophysical surveys specifically performed or inferred from literature, site and topography classification using different available information. It represents a continuously expanding database being updated with new stations added to the national network and with new data gradually becoming available from new sources.
With 340 stations present at the beginning of 2023, in the framework of the national research PRIN project SERENA - Mapping Seismic Site Effects at REGional and NATIONAL Scale, (WP6 - Empirical Testing and Calibration) CRISP represents a good starting point for systematising the information related to the site characterization with the aim to identify a site amplification model based on site condition indicators.
A preliminary selection of representative proxies drove us to extract and compare the indicators related to the morphological and lithological classification, site classification and seismological analysis. Specifically, we selected the slope of morphology, lithological type, soil consolidation degree, amplitude and frequency peaks of Horizontal-to-Vertical spectral ratio (HVSR) on noise and earthquakes, frequency and direction of polarization, topography class and site class from EC08 and NTC18.
In order to identify the significant indicators and recognize their dependencies, we first analysed the distribution of each indicator (see histograms of Lithological classification groupments and site class in Fig.1).

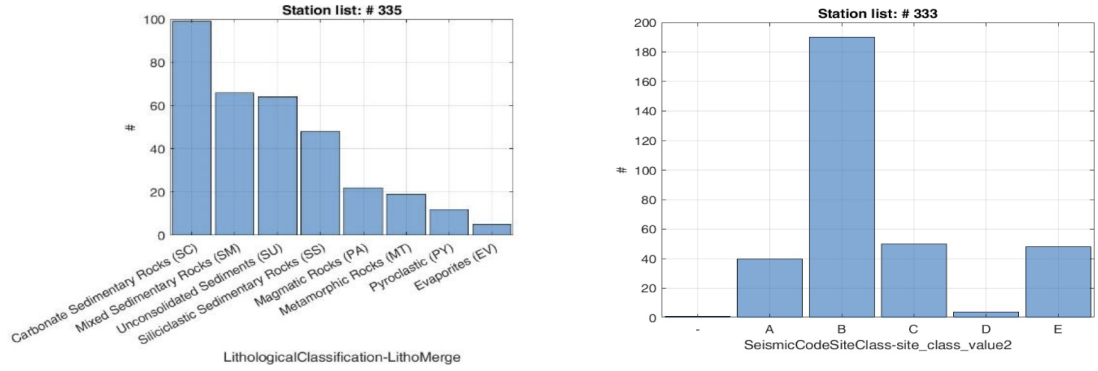

Fig. 1 – Data distribution for lithological classification grouped by rock categories with similar genesis(left) and Site classification from NTC18 (right).

We then looked for possible correlation between different parameters. Fig. 2 shows the comparison between the resonance frequency (f0) values from HVSR on noise and earthquakes at all stations: in general, for frequencies larger than about 2 Hz, the peak amplifications from noise are found at larger frequencies than from earthquakes.
Moreover these proxies are compared with magnitude residual from Di Bona et al. (2016), to look for an additional relationship helping to determine a site amplification model. For example the Fig.3 shows the distribution of f0 from HVnoise: the magnitude residuals tend to positive values as f0 increases.
Furthermore, the availability of numerous HVSR curves can be grouped by means of the cluster analysis for the recognition of similar characteristics.

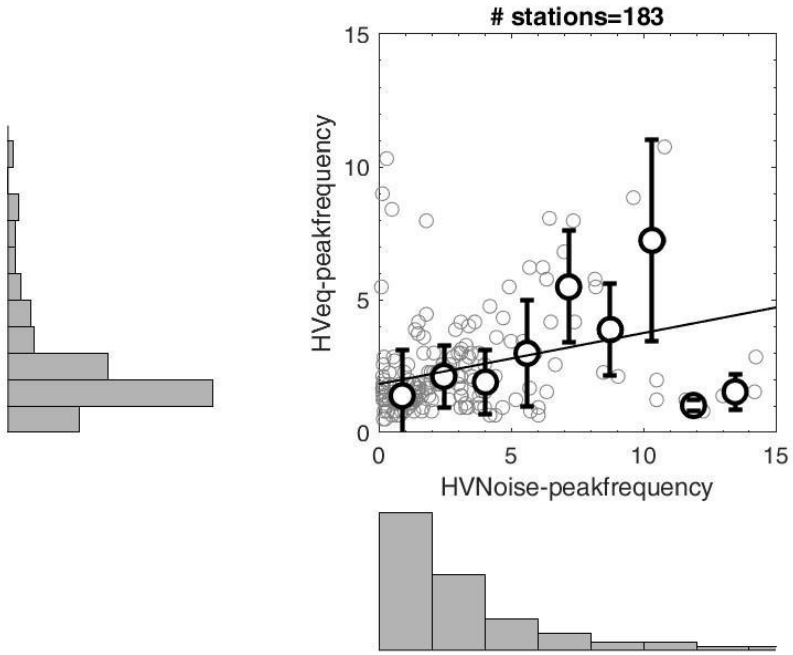

Fig. 2 – Example of correlation between f0 from HVSR on noise and earthquakes, having amplitude A0 >= 2.

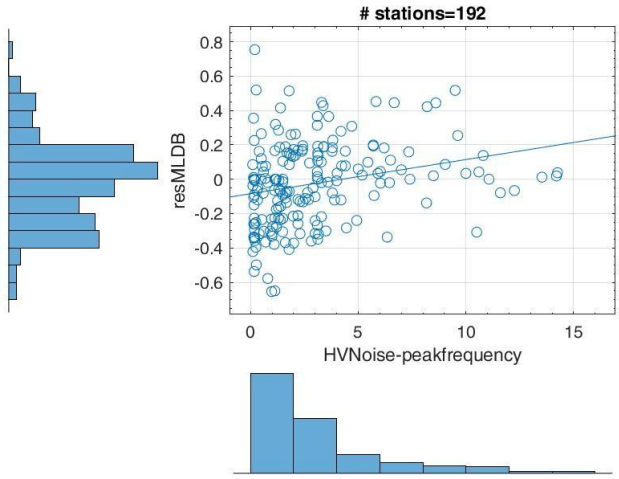

Fig. 3 – Distribution of f0 from HVnoise, with respect to the magnitude residuals.

References

Cultrera G., Bordoni P., Mercuri A., Quintiliani M., Minarelli L., Famiani D., Casale P., Pischiutta M., Ladina C., Cara F., Di Giulio G., Pucillo S., Monti G., and CRISP Working Group (2022). Database for site characterization of permanent seismic stations (CRISP). Istituto Nazionale di Geofisica e Vulcanologia (INGV). https://doi.org/10.13127/crisp

Mercuri A., G. Cultrera, L. Minarelli, M. Quintiliani, P. Bordoni, D. Famiani, P. Casale, M. Pischiutta, C. Ladina, F. Cara, G. Di Giulio, S. Pucillo, G. Tarabusi, and INGV CRISP Working Group. CRISP: an archive for the site characterization of permanent Italian seismic stations. Accepted by Bulletin of Earthquake Engineering (2022). https://doi.org/10.1007/s10518-023-01618-w

Russo E, Felicetta C, D Amico M, Sgobba S, Lanzano G, Mascandola C, Pacor F, Luzi L (2022). Italian Accelerometric Archive v3.2 - Istituto Nazionale di Geofisica e Vulcanologia, Dipartimento della Protezione Civile Nazionale. doi: 10.13127/itaca.3.2

Corresponding author: alessia.mercuri@ingv.it

Automated Stratigraphic Reconstruction and Spatialization for Seismic Site Effect Analysis

A. D'Agostino[1], A. Porchia[2], G. Cavuoto[3], F. Pavano[3], M. Moscatelli[2], G. Tortorici[2], S. Catalano[1,2]

[1] Department of Biological, Geological and Environmental Sciences (DBGES) – Section of Earth Science, University of Catania.
[2] IGAG-CNR - Institute of Environmental Geology and Geoengineering of the Italian National Research Council, Area Della Ricerca di Roma 1.
[3] ISPC-CNR - Institute of Heritage Science of the Italian National Research Council, Napoli.

In the frame of the PRIN project "Mapping seismic site effects at regional and national scale – SERENA", we have developed a set of Python scripts within a GIS environment, aimed at reconstructing and spatializing stratigraphies. These codes represent an integral part of a workflow designed to divide the territory into stratigraphically homogeneous areas, providing representative stratigraphic columns for modeling and determining seismic amplification factors.

The code set consists of two scripts for stratigraphic reconstructions and a third script for their spatialization. The first unsupervised script operates on a raster base and generates stratigraphies based on a predetermined total thickness. The second supervised script works on vector cartographic bases and produces stratigraphies through individual steps. This procedure allows a progressive verification of the stratigraphic column under construction. These first two scripts analyze the lateral contacts between the outcropping units, placing them in stratigraphic order based on a geometric position index (Cesarano et al., 2022) and calculating the cumulated thickness.

The third unsupervised script performs the spatialization by assigning the same ID to each unique reconstructed stratigraphic column. The final output is a 2D map made of polygons populated by the same column ID.

In order to generate and spatialize the stratigraphies, the employed raster or vector cartographic base must contain polygonal elements representing the Engineering-Geological Units – EGU (Technical Commission for Seismic Microzonation, 2020). Each polygon must include a unique geometric position index and a thickness value.

The scripts were validated on the 428 km^2 wide Territorial Context (TC) of Cariati (Calabria, Italy) (Regione Calabria DGR 498/2019), since the EGUs had already been geometrically indexed (Fig. 1) and the stratigraphic columns manually reconstructed by Cesarano et al. (2022). In this study, the stratigraphic columns were represented in a matrix form. The

developed scripts successfully reproduced the same stratigraphic columns manually obtained by Cesarano et al. (2022), confirming their efficiency (Fig. 2). The entire process required about ten minutes.

Currently, a fourth script for automated thickness calculation is under development with the main goal of defining realistic thickness values that take into account the effects of the erosional processes. This script, using the same cartographic base employed in the previous scripts along with a digital elevation model, analyzes the boundaries between different EGUs and reconstructs their subsoil geometry to assess the thickness of each outcropping unit.

These tools, combined with geophysical and geotechnical data, such as the variability of shear wave velocity in relation to EGUs (Romagnoli et al., 2022) and shear modulus reduction and damping ratio curves (Gaudiosi et al., 2022), represent a significant advancement in the analysis of seismic hazards on a large scale. Their ability to provide detailed and realistic stratigraphies for local seismic response analysis greatly contributes to improving the calculation of seismic amplification factors (AF). This refines the current procedure based on the identification at a national scale of homogeneous morphological-geological and lithological areas (Falcone et al. 2021).

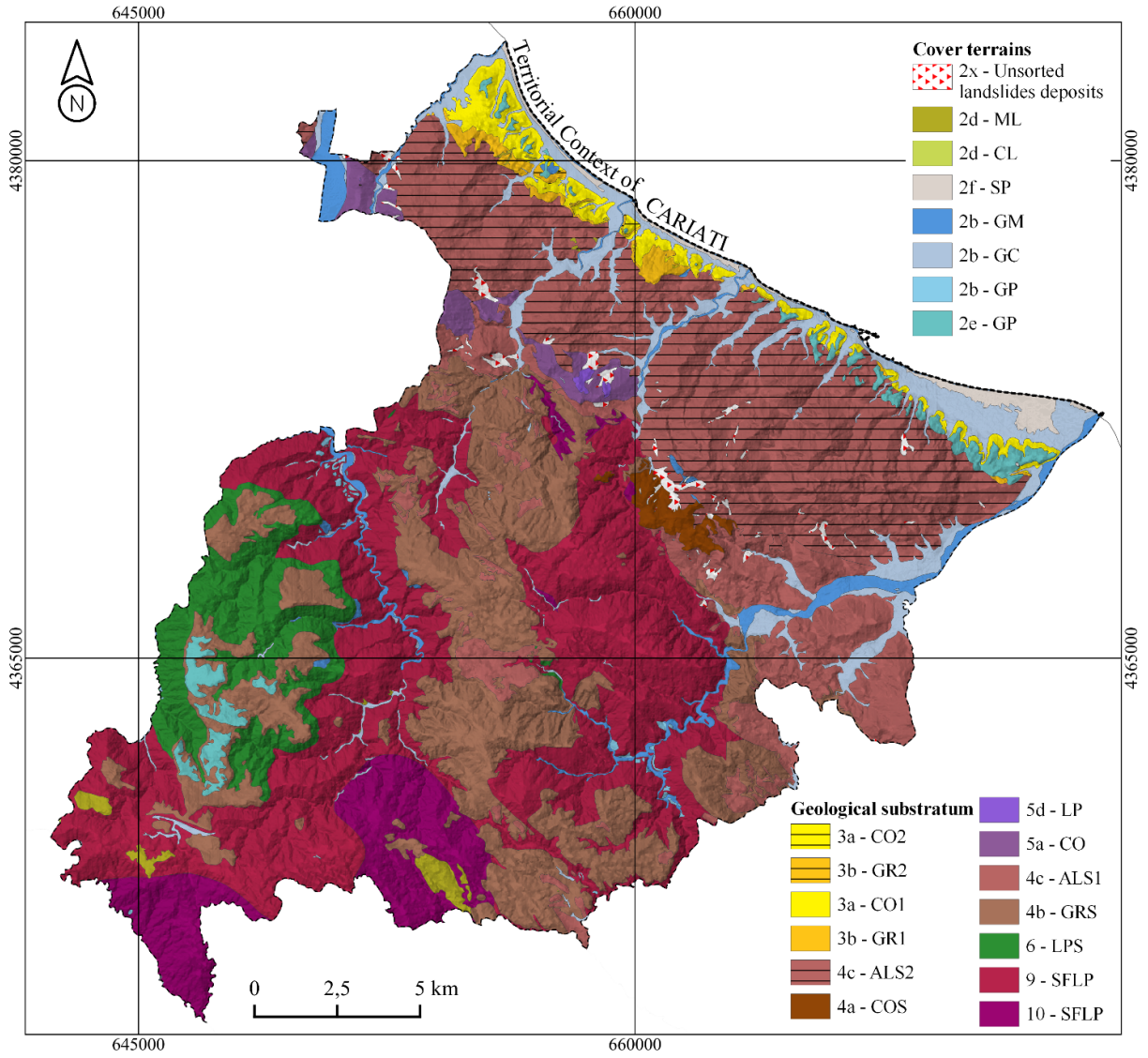

Fig. 1 – Engineering-geological map of the Territorial Context of Cariati (from Cesarano et. al, 2022).

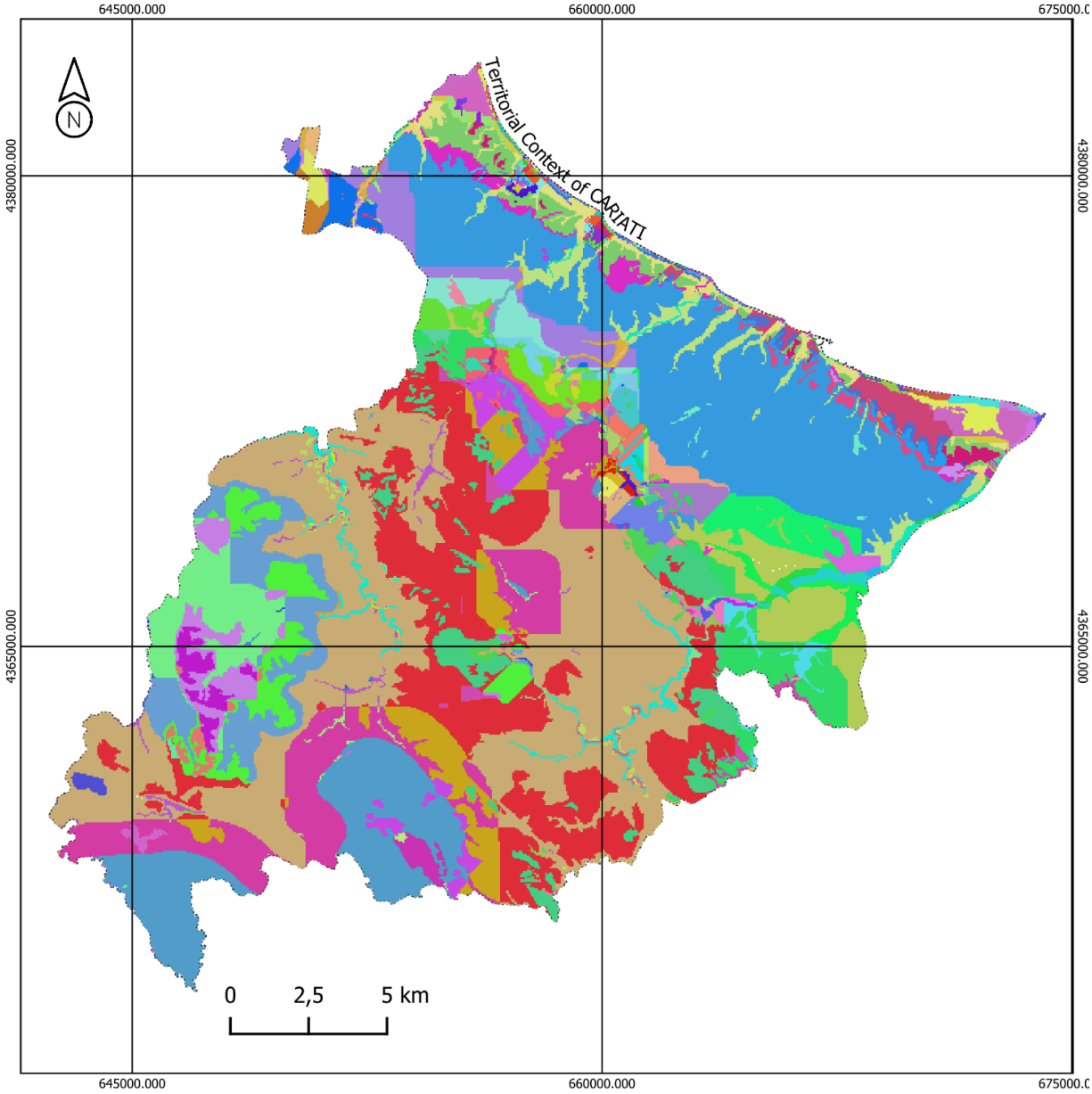

Fig. 2 – Result of the spatialization process in the Territorial Context of Cariati. Each color represents a unique stratigraphic column.

References

Cesarano M., Porchia A., Romagnoli G., Peronace E., Mendicelli A., Nocentini M., Naso G., Castenetto S., Catalano S. & Moscatelli M.; 2022: Multiscale geothematic maps for using the database from the Italian Seismic Microzonation Project: an example of application in the Calabria Region (Southern Italy). Ital. J. Geosci, 141(1), 35-52. https://doi.org/10.3301/IJG.2022.03.

Falcone G., Acunzo G., Mendicelli A., Mori F., Naso G, Peronace E., Porchia A., Romagnoli G., Tarquini E., Moscatelli M.; 2021: Seismic amplification maps of Italy based on site-specific microzonation dataset and one-dimensional numerical approach, Engineering Geology, 289, 2021, 106170, ISSN 0013-7952. https://doi.org/10.1016/j.enggeo.2021.106170.

Gaudiosi, I., Romagnoli, G., Albarello, D., Fortunato, C., Imprescia, P., Stigliano, F., Moscatelli, M.; 2023: Shear modulus reduction and damping ratios curves joined with engineering geological units in Italy. Sci Data 10, 625. https://doi.org/10.1038/s41597-023-02412-8

Regione Calabria; DGR n. 498 del 25 ottobre 2019: Prevenzione del rischio sismico. Adozione documento Contesti Territoriali e Comuni di Riferimento della Regione Calabria redatto dal Dipartimento Nazionale Protezione Civile. Revoca DGR n. 408 del 24.10.2016.

Romagnoli G., Tarquini E., Porchia A., Catalano S., Albarello D., Moscatelli M.; 2022: Constraints for the Vs profiles from engineering-geological qualitative characterization of shallow subsoil in seismic microzonation studies, Soil Dynamics and Earthquake Engineering, 161, 2022, 107347, ISSN 0267-7261. https://doi.org/10.1016/j.soildyn.2022.107347.

Corresponding author: alberto.dagostino@phd.unict.it

Site-dependency of fragility functions

M. Fasan[1], C. Bedon[1], F. Romanelli[2]

[1] University of Trieste, Department of Engineering and Architecture
[2] University of Trieste, Department of Mathematics and Geosciences

Introduction

This work focuses on investigating the potential impact of site conditions on fragility curves, considering factors like source effects, wave propagation, and local site characteristics. Utilizing physics-based numerical simulations, the study examines a hypothetical site using a single seismic source with varied crustal and stratigraphic models.

Through nonlinear dynamic analyses the response of a reinforced concrete frame structure is assessed, leading to the evaluation of fragility curves using the cloud analysis method. The study emphasizes the frequently overlooked impact of crustal models through comparisons among curves for various configurations. The primary objective is to comprehend physical parameter influences on the seismic response of buildings in a hypothetical setting.

Methodology

The methodology of this study delves into ground shaking simulation and seismic source modeling to explore the factors affecting seismic responses. Ground shaking, influenced by rupture processes, rupture propagation, and slip distribution on the fault plane, exhibits high variability in expected acceleration. Synthetic accelerograms are computed through the tensor product of earthquake source representation and Green's function of the medium, considering local site effects and crustal layer characteristics (Chieffo et al., 2021; Hassan et al., 2020). The simulations encompass a hypothetical seismic scenario, evaluating various configurations by employing two realistic deep crustal models (propagation effects) and two local stratigraphic models (site effects, within the same category according to EC8). The earthquake source is modeled as a distributed slip field on the fault surface, employing a Monte Carlo approach to account for spatiotemporal variability in rupture evolution. Seismogram calculations use two techniques, Modal Summation (MS) and Discrete Wave Number (DWN), ensuring accurate simulation of ground motion under different conditions. The limitation to a maximum frequency of 10 Hz is a compromise for simulation accuracy, available information, and computation time.

The fragility curves in this study are derived through the "cloud" methodology, employing unscaled signals and assuming a linear correlation between the logarithms of signal intensity

measures (IM) and engineering demand parameters (EDP)(Jalayer & Cornell, 2009). This linear relationship, expressed as:

is determined by parameters a and b through linear regression. Assuming a lognormal distribution, the fragility function can be expressed as:

Here, is the standard normal cumulative distribution and the logarithmic standard deviation of linear regression.

The methodology can accommodate aleatory and epistemic uncertainties, considering variations in structural response, mechanical properties, capacity thresholds, and model parameters.

Aleatory uncertainties, linked to record-to-record variability, mechanical properties, and capacity thresholds, contribute to fragility functions. Record-to-record variability is naturally considered by the initial data cloud .

Furthermore, epistemic uncertainty in model parameters is addressed through a bootstrap procedure involving resampling with replacement, resulting in n different realizations of , leading to n fragility curves and regressions. The report adopts n=1000 bootstrap samples, providing a comprehensive approach to assessing fragility curves that considers multiple uncertainties and enhances the understanding of probabilistic seismic vulnerability.

Modeling choices

Ground accelerations are influenced by source, path, and site effects. Key source modelling parameters include magnitude (M_w), source rupture process (nucleation point, rupture front evolution, slip distribution, depth), path effects, site stratigraphy, receiver-source distance (R), and source-receiver angle.

The seismic source, modeled after the "Medea" fault, undergoes one hundred different rupture process realizations (Fig.1). Parameters from the DISS database and source functions proposed by Magrin et al. (2016) are employed. Crustal models (CR1 and CR2) and local stratigraphies (L1 and L2) are used to capture the source-to-site path effects. The physical properties of the crustal models are extracted from literature (Brandmayr et al., 2010). These cellular structures represent realistic configurations present in the Italian territory and were obtained through a nonlinear optimized inversion of the dispersion curves of surface waves. Both local stratigraphies belong to category B according to Eurocode 8 classification, but L1 can be considered moderately faster (V30= 695 m/s), and L2 slower (V30= 366 m/s). As a result, in common practice, all the presented outcomes would represent equivalent scenarios in the selection of real signals to be used in nonlinear dynamic analyses. The receiver was placed approximately 26 km from the fault center.

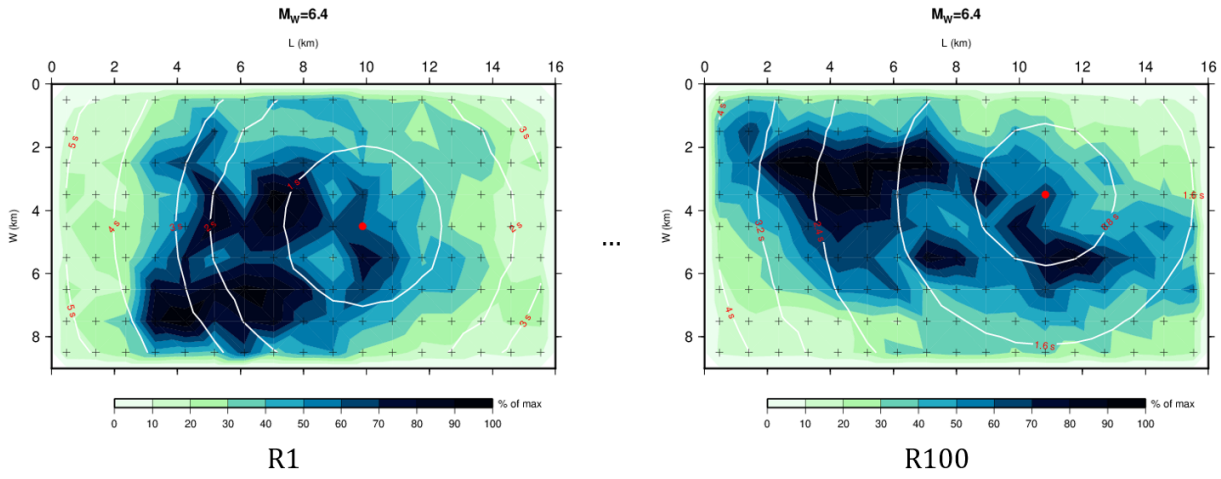

Fig. 1 – Example of different realizations of the rupture process

The reference structure is a five-story reinforced concrete frame designed according to Italian regulations. The structure has a 15m wide square plan with three bays, each 5m long. Each floor is 3m high, totaling 15m. Gravitational permanent loads include self-weight of structural elements, and an accidental load of 2 kN/m2 is applied to each floor. The roof has a snow load of 0.8 kN/m2. Seismic action is considered based on the Italian Building Code for a moderately hazardous site.

A spectral analysis determines maximum stress values, and beams and columns are designed with low ductility (Class B) and a behavior factor of 3.9. Design criteria ensure weak beam/ strong column capacity. Nonlinear time history analyses (NLTHA) are performed using Seismostruct software, considering both material and geometric nonlinearities. Inelastic force-based beam elements are used for material nonlinearities. Concrete strength class C28/35 and steel reinforcement class B450C are adopted.

Rayleigh damping is applied, and the Hilber-Hughes-Taylor integration scheme is used. The summary outlines the structural design, seismic considerations, material properties, and analysis methods employed in evaluating the behavior of the reinforced concrete frame under various conditions.

Scalar intensity measures such as peak ground acceleration (PGA), spectral acceleration at the first mode Sa(T1), and average spectral acceleration () are employed for fragility curve construction. Since the reference structure is 3D, the IM should account for the main vibrational properties in both directions. Therefore, here the spectral acceleration is evaluated for an average period calculated as the mean of the fundamental period values in each direction (FEMA, 2018):

$$S_a(T_{1m}) = S_a(\frac{T_{1x} + T_{1y}}{2})$$

Average spectral acceleration is defined as the geometric mean of spectral accelerations over a range of periods (Eads et al., 2015):

$$S_{a,avg}(T_i) = \left[\prod_{i=1}^{n} S_a(T_i)\right]^{1/n}$$

The period range is selected to including the effects of higher modes and period elongations due to damage accumulation. Five periods are selected, including modes with a mass participation greater than 10%:

$$T_i = \left[T_{2m}, min\left[(T_{2m} + T_{1m})/2,\ 1.5T_{2m}\right], T_{1m}, 1.5T_{1m}, 2T_{1m}\right]$$

Where is the mean of the second mode periods in the two orthogonal directions.

Results

The findings encompass accelerograms, intensity parameter distributions, regressions, and fragility curves derived from four distinct configurations. Various crustal and local models, yielding four configurations: CR1-L1, CR2-L1, CR1-L2, and CR2-L2. While the seismic source remains constant, 100 variations in rupture processes are considered to capture variability.

Accelerograms resulting from the combined models exhibit significant variations in shape and amplitude. Distributions of ground motion parameters, including Arias Intensity, Significant Duration, PGA, PGV, and Response Spectra in Acceleration, underscore the impact of the chosen configurations.

The Arias Intensity distributions highlight the influence of crustal model CR2 on signal energy, while the coupling of local model L2 with CR1 increases Arias. Signal duration, crucial for structures with cyclic strength degradation, shows greater dispersion in configurations coupling CR2 and L2. Notably, PGA, a historically pivotal intensity measure, displays no clear increase when transitioning from fast to slow B soil, emphasizing the intricate interplay between crustal and local models.

The fragility curves, representing the structure's vulnerability, reveal intriguing insights. For the sake of brevity only results for PGA are reported, hence for regressions of parameter MIDR (Maximum Interstorey Drift Ratio) as a function of $PGA_{GMRotD50}$ (median value of the geometric mean of the two horizontal components rotated through all nonredundant period-dependent angles (Boore et al., 2006)) in the bi-logarithmic plane. Regressions associated with crustal model CR1 appear less steep due to higher standard deviation, indicating greater uncertainty. Conversely, the reliability of estimates is higher for crustal model CR2, influenced by a more consistent distribution of intensity measures (Fig. 2).

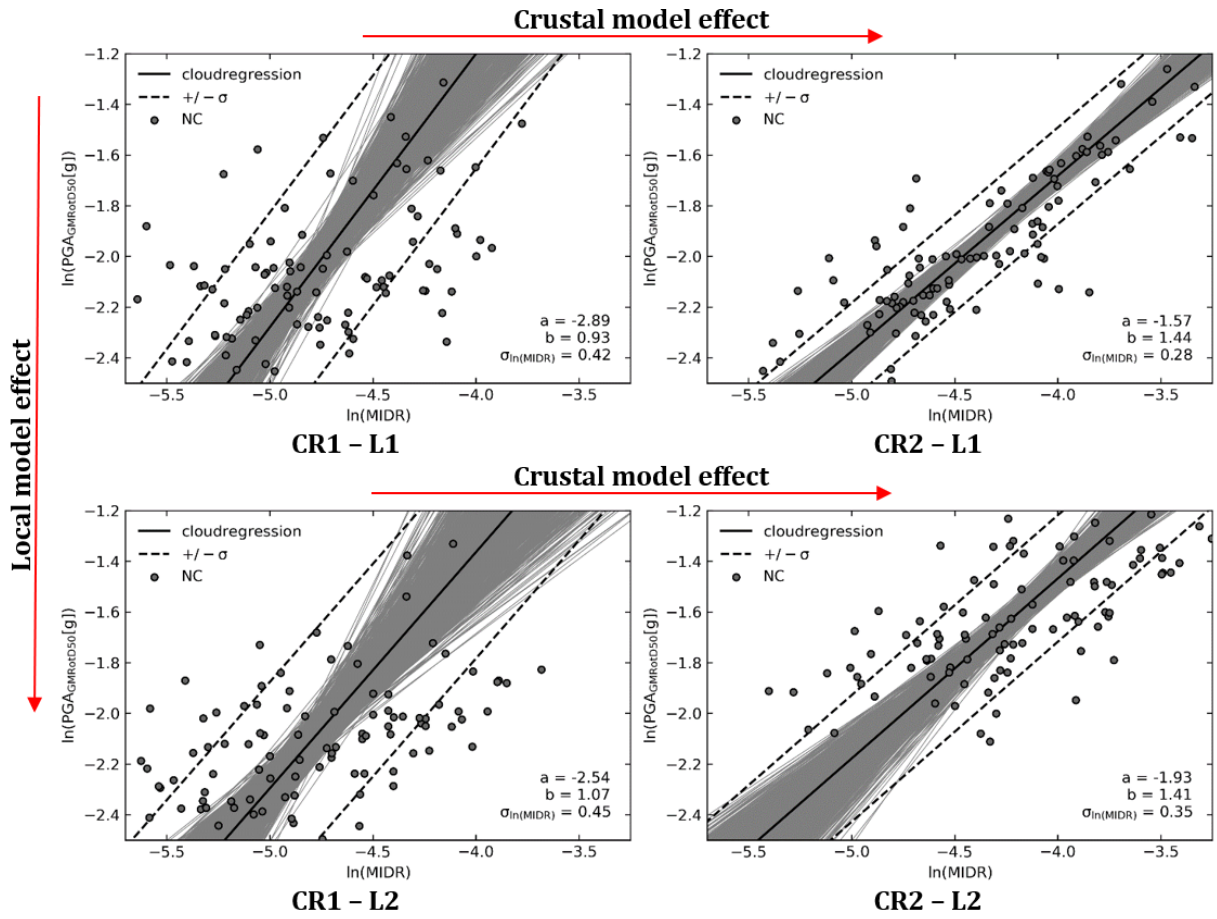

Fig. 2 – Cloud data (indicated with NC) and regressions obtained for the four studied configurations (PGA)

This study challenges the assumption that identical seismic scenarios, at least in terms of commonly used seismological parameters (magnitude, focal mechanism, site conditions, source-to-site distance) produce uniform structural responses. The observed variations in fragility curves, here reported only for the life safety (LS) performance level, underscore the need for an understanding of crustal and local model interactions in seismic risk assessment, emphasizing the importance of considering various configurations for a comprehensive analysis (Fig. 3).

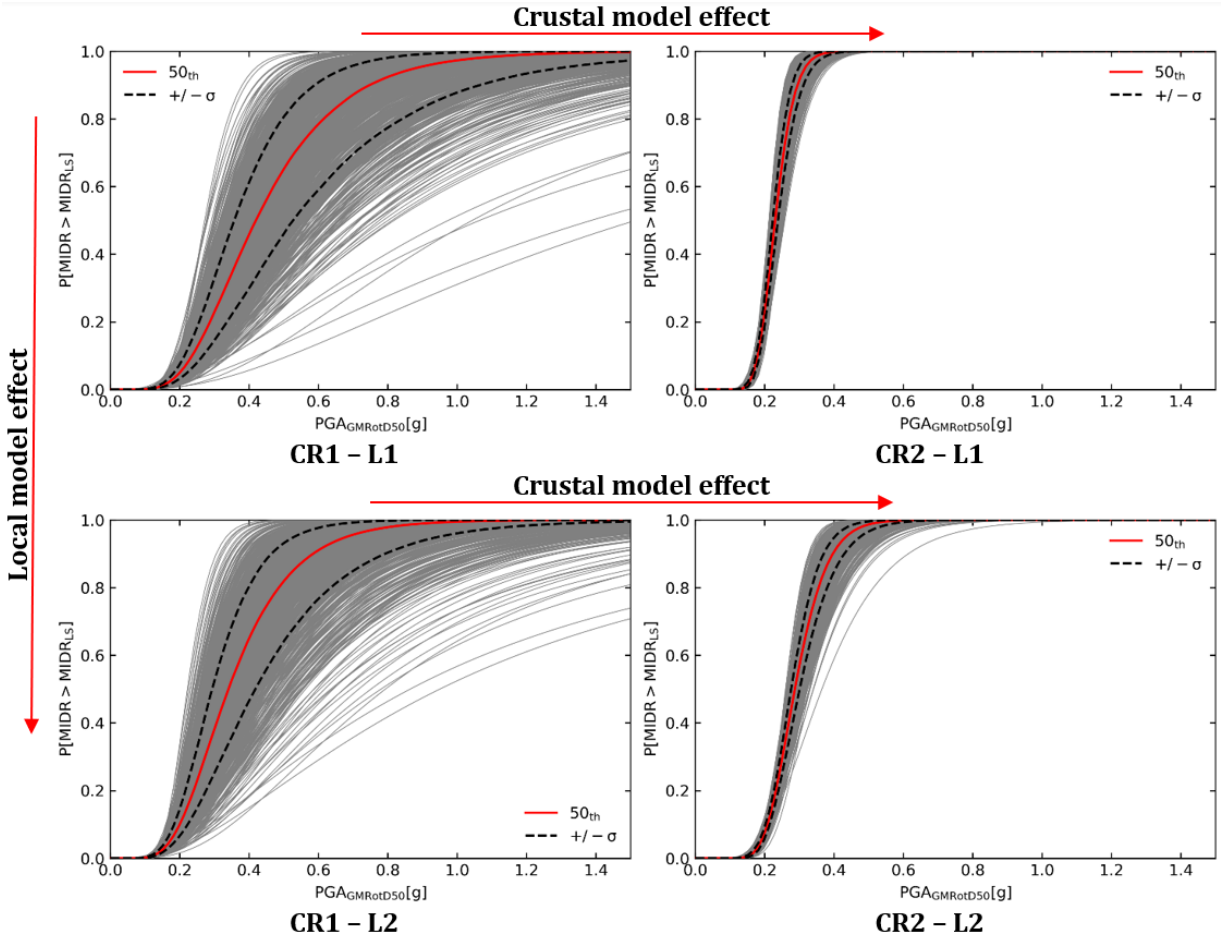

Fig. 3 - Fragility curves obtained for the four studied configurations (PGA)

Conclusions

In this work, four possible configurations of crustal and local structural models were analyzed to identify their influence on the IM-EDP relationship and, consequently, on fragility curves. In terms of demand, reflecting the distribution of possible signal intensity measures, configurations where crustal model CR2 is present showed higher values. The influence on the intensity measure values of crustal models seems to be, in the analyzed cases, more significant than that of local models.

Examining the IM-EDP relationship and consequently the fragility curves, it is observed that the regressions performed on IM-EDP pairs do not overlap. This implies that the intensity measures analyzed are not sufficient even in the studied case, where a single scenario is represented. In particular, the dependence of these measures on local and crustal structural models has been highlighted.

Acknowledgements

DPC-RELUIS is gratefully acknowledged for funding the present research activity under the MARS-2 research project.

References

Boore, D. M., Watson-Lamprey, J., & Abrahamson, N. A. (2006). Orientation-independent measures of ground motion. *Bulletin of the Seismological Society of America*, *96*(4 A), 1502–1511. https://doi.org/10.1785/0120050209

Brandmayr, E., Raykova, R. B., Zuri, M., Romanelli, F., Doglioni, C., & Panza, G. F. (2010). The lithosphere in Italy: structure and seismicity. *Journal of the Virtual Explorer*, *36*. https://doi.org/10.3809/jvirtex.2010.00224

Chieffo, N., Fasan, M., Romanelli, F., Formisano, A., & Mochi, G. (2021). Physics-Based Ground Motion Simulations for the Prediction of the Seismic Vulnerability of Masonry Building Compounds in Mirandola (Italy). *Buildings*, *11*(12), 667. https://doi.org/10.3390/buildings11120667

Eads, L., Miranda, E., & Lignos, D. G. (2015). Average spectral acceleration as an intensity measure for collapse risk assessment. *Earthquake Engineering & Structural Dynamics*, *44*(12), 2057–2073. https://doi.org/10.1002/eqe.2575

FEMA. (2018). *Seismic Performance Assessment of Buildings, FEMA P-58-1*.

Hassan, H. M., Fasan, M., Sayed, M. A., Romanelli, F., ElGabry, M. N., Vaccari, F., & Hamed, A. (2020). Site-specific ground motion modeling for a historical Cairo site as a step towards computation of seismic input at cultural heritage sites. *Engineering Geology*, *268*(February), 105524. https://doi.org/10.1016/j.enggeo.2020.105524

Jalayer, F., & Cornell, C. A. (2009). Alternative non-linear demand estimation methods for probability-based seismic assessments. *Earthquake Engineering & Structural Dynamics*, *38*(8), 951–972. https://doi.org/10.1002/eqe.876

Magrin, A., Gusev, A. A., Romanelli, F., Vaccari, F., & Panza, G. F. (2016). Broadband NDSHA computations and earthquake ground motion observations for the Italian territory. *International Journal of Earthquake and Impact Engineering*, *1*(1/2), 28. https://doi.org/10.1504/IJEIE.2016.10000979

Corresponding author: mfasan@units.it

Development of a hybrid method for ground shaking map reconstruction in near-real time

S. F. Fornasari , V. Pazzi , G. Costa

Dipartimento di Matematica, Informatica e Geoscienze (MIGE - Università degli Studi di Trieste, Italia)

Introduction

Real-time seismic monitoring is of primary importance for rapid and targeted emergency operations after potentially destructive earthquakes. A key aspect in determining the impact of an earthquake is the reconstruction of the ground-shaking field, usually expressed as the ground motion parameter. Traditional algorithms (e.g. ShakeMap®) compute the ground-shaking fields from the punctual data at the stations relying on ground-motion prediction equations (GMPEs) computed on estimates of the earthquake location and magnitude when the instrumental data are missing. The results of such algorithms are then subordinate to the evaluation of location and magnitude, which can take several minutes.

Since machine learning techniques have already been proven capable of estimating the ground motion parameters (Fornasari et al., 2023), a hybrid method has been developed to integrate neural networks in the ShakeMap® workflow to speed up the current ground-shaking map evaluation process.

The core idea is to adopt the ShakeMap® multivariate normal distribution (MVN) method for the intensity measure (IM) interpolation and use a neural network, in place of the ground motion prediction equations (GMPEs), to estimate the IM conditional expected value and uncertainty at the target sites based only on data available in real-time and thus do not wait for the magnitude and location estimates.

Furthermore, by reusing the ShakeMap® framework, the complexity of the model is reduced with improvements in the interpretability of the results.

Method

The proposed hybrid method consists of two steps: first, the expected IM values (and their uncertainties) are computed at the stations and target locations; then the recorded and expected IMs are passed to the MVN to compute the ground-shaking map (and its uncertainty).

The approach adopted to replace the GMPE is called Convolutional Conditional Neural Process (ConvCNP, Gordon et al., 2019): starting from sparse randomly sampled observations, a functional representation of them is computed, discretized to a regular grid and fed to a backbone neural network whose outputs are converted from the function space to the

original space of the intensity measures such that the output, for each target point, is a conditional distribution.

The input and output of the ConvCNP are expressed in log-units and thus assumed to be corrected for site effects: the effects of local geology are removed from the IMs recorded at the stations and reintroduced into the estimated IMs at the target points using the corresponding amplification factor by Falcone et al. (2021). The choice of using the amplification factors (instead of, for example, a Vs30-based approach) to address the site effects is double-fold: on one hand, it simplifies the ConvCNP process by operating on uniform inputs and outputs (which is especially useful since the encoder and decoder can seamlessly handle input and output points affected by different local effects); on the other hand, it improves the interpretability of the results by separating the contribution of local geology to the final results.

The implemented MVN is based on the formulation by Worden et al. (2018) and the correlation function by Loth and Baker (2013) is adopted: the choice of a correlation function independent of the epicentral distance and the event magnitude is required to obtain a workflow no longer dependant on the evaluation of the source parameters.

A flowchart of the hybrid method is shown in Fig. 1:

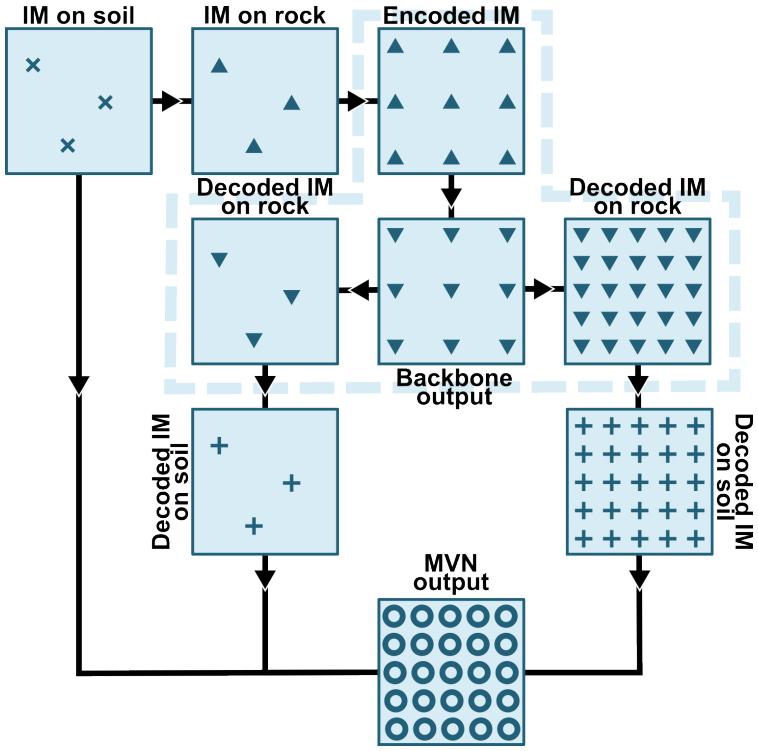

Fig. 1 – ShakeRec-hybrid flowchart: real-time data are corrected for the site effects with an amplification factor and passed to the ConvCNP (defined by the dashed line). IM values are estimated both at the station locations and the target points (here represented by a regular grid) and the soil effect is reintroduced by the corresponding amplification factors. These outputs and the real-time original inputs are then passed to the MVN to compute the ground-shaking maps.

The functional encoding and decoding are performed using rational quadratic kernels k_{rq} based on the great distances d_{ij} between the input and output points:

$$k_{rq}(d_{ij}) = (1 + \frac{{d_{ij}}^2}{2\alpha\lambda^2})^{-\alpha}$$

with $\lambda > 0$ and $\alpha > 0$ being two learnable parameters called length scale and the scale-mixture, respectively.

The backbone neural network has a custom architecture, shown in Fig. 2, consisting of a common sequential network that leads into two different branches for the evaluation of the mean IM values and the associated standard deviations, respectively.

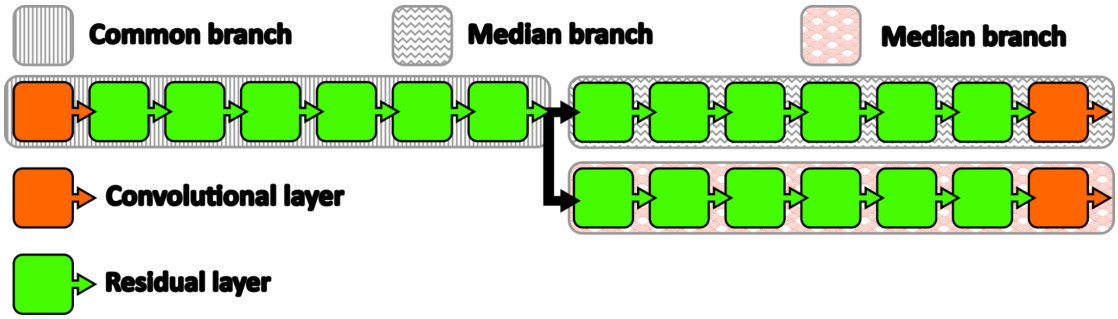

Fig. 2 – Schematic diagram of the ConvCNP backbone neural network architecture.

Model training

The model has been trained with a combination of synthetic and recorded data.

Numerical simulations provide a cost-effective way to acquire more data to train neural networks that allows building datasets whose dimension can meet the actual requirements for training and in which the distribution of the events can be balanced, generating more scenarios for rare events with high magnitudes (generally under-represented in recorded data). Furthermore, different scenarios can be generated including different noise levels in the input data leading to models more robust to input noise.

A synthetic dataset has been created by simulating multiple events over the Italian territory: the source characteristics have been taken within the ranges provided by the Database of Individual and Composite Seismogenic Sources, considering for each source multiple scenarios for different magnitudes.

The ShakeMap® INGV catalogue has been considered as the source for recorded data: specifically, the database considered contains 4925 events whose magnitude ranges between M3.0 and M6.5.

The model is trained to learn a conditional log-normal distribution over the expected GMPE output in two stages: first, a new model has been pre-trained on the synthetic dataset; then, the pre-trained model has been fine-tuned using the real data.

For each event (both synthetic or recorded), a variable number of context points (i.e., the IM values at the stations) and a fixed number of target points have been considered: the context points are corrected for the site effects using the amplification factors by Falcone et al. (2020) evaluated at the station locations.

The target points have been randomly selected with a radial uniform distribution around the epicentre.
To avoid any bias introduced by the training data, the "computational" grid is randomly shifted with respect to the epicentre position for each event.
The loss function L used to train the model is a linear combination of negative log-likelihood (NLL) and Frechet inception distance (FID): $L = w_{NLL}NLL + w_{FID}FID$.
Effectively, the adopted loss can be seen as a Wasserstein distance with a negative log-likelihood penalty term introduced to regularise the results and provide a better connection between the mean and standard deviation.

Results and Conclusions

The proposed hybrid method implements a multi-step approach in which the neural network performs a very specific task: while it still maintains some aspects of a black box-like algorithm, the results of this implementation are much more interpretable, specifically with the possibility to address the role of the different components in the final result.
The use of data augmentation is beneficial even in cases where a good amount of recorded data is available to train the models, because the greater control over synthetic data could allow the development of more balanced datasets that can, in turn, promote the model to learn more useful low-level features while the fine-tuning phase using real data seems promising in training models able to generate more realistic results.
The proposed method proved to be robust to network geometry changes (both in terms of the number of stations and their spatial distribution) and to noise.
The 30 October 2016 M_w6.5 Norcia earthquake has been chosen to benchmark the method against ShakeMap®.
Even though it doesn't represent an exhaustive analysis, the Norcia event, which required mobilisation of emergency response, is indicative of the behaviour of the method for the archetype of the seismic event it has been developed for, being a strong event recorded by a high number of stations with good coverage.
In Fig. 3, the PGA median and standard deviation obtained with the proposed method and ShakeMap® are compared. In the epicentral area, thanks also to the high density of stations, both methods provide similar results in terms of median values (panels a) and c) in Fig. 3). Considering the standard deviations, the hybrid method generates values that are overall more similar, although consistently greater, than ShakeMap® (panels b) and d) in Fig. 3). Given the PGA probability distributions at each target point from the hybrid method f_H and ShakeMap® f_{SM}, the map of the overlapping coefficient $OVL = \int_R min(f_1(x), f_2(x))dx$ has been computed (panel e) in Fig. 3) showing great compatibility between the two methods and thus the quality of the hybrid method.
Despite being non-predictive (i.e. it reconstructs the ground-shaking field to be consistent with the values recorded until that moment rather than foresee future ones), the hybrid

method allows to update the ground-shaking maps every few seconds and to obtain the final ground-shaking map for inland events within a minute of their origin time.

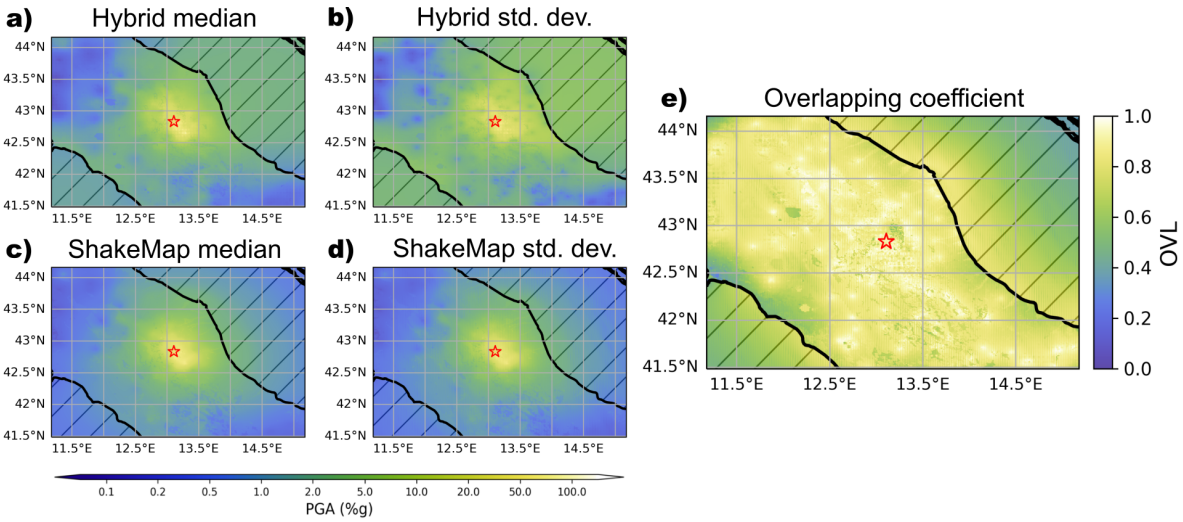

Fig. 3 – Reconstruction of the PGA median and standard deviation using the hybrid method (panels a) and b), respectively) and using ShakeMap® (panels c) and d), respectively) for the $M_w 6.5$ Norcia earthquake. Panel e) shows the overlapping coefficient between the PGA reconstructions obtained with the two methods.

Acknowledgement

This research received financial support from the Italian Civil Protection Department - Presidency of the Council of Ministers (PCM-DPC), to whom I am grateful, under the agreement “Accordo ai sensi dell’art. 15 della legge 7 agosto 1990, n. 241 e dell’art. 4 del decreto legislativo 2 gennaio 2018, n. 1 tra la Presidenza del Consiglio dei Ministri dipartimento della Protezione Civile e l’Università degli Studi di Trieste per il monitoraggio accelerometrico in Friuli Venezia Giulia e Veneto e la consulenza sull’elaborazione dei dati della rete accelerometrica nazionale" (2023-2024) between DPC and University of Trieste.

References

Falcone G., Acunzo G., Mendicelli A., Mori F., Naso G., Peronace E., Porchia A., Romagnoli G., Tarquini E., & Moscatelli M.; 2021: Seismic amplification maps of Italy based on site-specific microzonation dataset and one-dimensional numerical approach. Engineering Geology, 289:106170

Falcone, G., Boldini, D., Martelli, L., & Amorosi, A.; 2020: Quantifying local seismic amplification from regional charts and site specific numerical analyses: a case study. *Bulletin of Earthquake Engineering*, *18*, 77-107.

Fornasari, S. F., Pazzi, V., & Costa, G.; 2022: A Machine-Learning Approach for the Reconstruction of Ground-Shaking Fields in Real Time. Bulletin of the Seismological Society of America, 112(5), 2642-2652.

Gordon, J., Bruinsma, W. P., Foong, A. Y., Requeima, J., Dubois, Y., & Turner, R. E.; 2019: Convolutional conditional neural processes. arXiv preprint arXiv:1910.13556.

Loth C., and Baker J. W.; 2013: A spatial cross-correlation model of spectral accelerations at multiple periods. Earthquake Engineering & Structural Dynamics 42.3.

Worden, C. B., Thompson, E. M., Baker, J. W., Bradley, B. A., Luco, N., & Wald, D. J.; 2018: Spatial and spectral interpolation of ground-motion intensity measure observations. Bulletin of the Seismological Society of America, 108(2), 866-875.

Corresponding author: simonefrancesco.fornasari@phd.units.it

On the reconnaissance of slopes susceptible to co-seismic failures in Daunia (Apulia, Southern Italy)

F. Fredella[1], V. Del Gaudio[1], N. Venisti[1], J. Wasowski[2]

[1]Dipartimento di Scienze della Terra e Geoambientali, Università degli Studi di Bari "Aldo Moro", Bari

[2]Consiglio Nazionale delle Ricerche, Istituto di Ricerca per la Protezione Idrogeologica, Bari

Introduction

Co-seismic landslides are capable of causing significant damage even to structures and infrastructures that resist the direct effects of earthquake ground shaking. It is therefore important to identify the slopes potentially exposed to seismic destabilization for hazard mitigation and prevention. A regional- to local-scale investigation of sites susceptible to co-seismic failure requires allocation of considerable resources, which should be prioritized by focusing attention on slopes with greater probability of being mobilized by seismic shaking.

Here we explore the potential of reconnaissance-type identification of slopes susceptible to co-seismic failures in the Daunia Mountains, at the NW border of the Apulia region. This is done by comparing the resistance demand placed by local seismicity on slope sites and the actual slope resistance. To this end, we take into account i) the basic seismic hazard inferred at regional scale from earthquake records, ii) the local effects of site amplification phenomena and iii) expeditious estimates of slope resistance to seismic shaking.

Our study benefits from the large amount of data acquired in the ongoing seismic microzonation (SM) studies of the Apulia region. We focus on the Daunia Mts., which are known for the widespread presence of marginally stable slopes consisting of clay-rich flysch materials and rainfall-triggered landsliding (e.g., Wasowski et al. 2010). Although Daunia is exposed to earthquakes generated in the surrounding areas, little is known about the susceptibility of its slopes to seismic failure.

Basic slope resistance demand

A first stage for the identification of slopes subject to seismically induced landslides consists in defining the resistance demand placed on slope by the regional seismicity. For this purpose, the starting point is the assessment of the basic seismic hazard, represented as a probabilistic

estimate of seismic shaking expected at a site. This depends on the location of the surrounding seismogenic zones, whose seismicity rate can be inferred from historical and instrumental records. Then, ground motion prediction equations (GMPE) are used to estimate the probability of a site to experience seismic shaking of different levels on a flat surface with outcropping stiff lithology. These site conditions, however, differ from those of slopes susceptible to seismically induced landslides, where the slope response to seismic waves can considerably aggravate the destabilizing effects of shakings.

A method for a probabilistic evaluation of the resistance demand was proposed by Del Gaudio et al. (2003) through the quantity $(A_c)_x$, which represents the critical acceleration A_c that a slope must have to keep the probability of landslide triggering, for expected earthquakes, within a pre-defined probability level (e.g., 10% in 50 years). The condition of landslide triggering is identified by the exceedance of a critical threshold x of the permanent displacement induced by seismic shaking, measured, according to the Newmark (1965) model, as Newmark displacement D_N. The calculation of $(A_c)_x$ is based on an empirical relation calibrated by Romeo (2000), in which D_N is expressed as a function of the Arias Intensity (Arias, 1970) (which measures the ground shaking) and of the slope critical acceleration a_c (which measures the slope resistance to failure).

In their first application of the proposed method Del Gaudio et al. (2003), produced a map of slope resistance demand in terms of $(A_c)_x$ values for the area of Daunia Mts. (Fig. 1 a). They exploited the following data and tools available at that time: the ZS4 seismogenic zonation (Scandone, 1997), a GMPE for Arias Intensity published by Sabetta and Pugliese (1996) and the SEISRISK III software (Bender and Perkins, 1987) to calculate the seismic shaking probabilities. The map shows the results in terms of critical acceleration that slopes must have to keep within 10% in 50 years the probability that D_N exceed 10 cm. Site amplification effects were not considered.

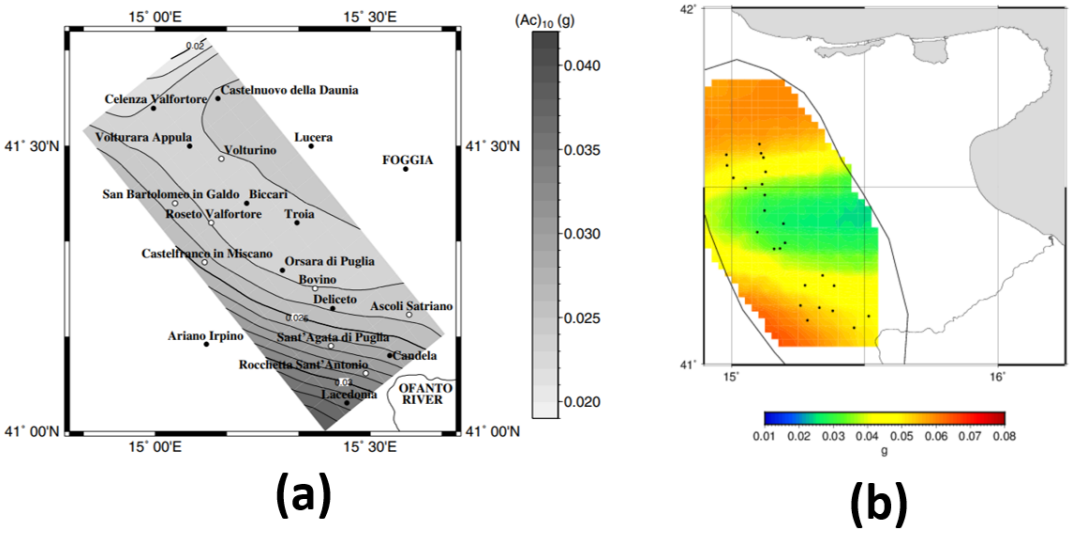

Fig. 1: Basic resistance demand maps calculated for the Daunia area, expressed through the quantity $(A_c)_{10}$: (a) results obtained by Del Gaudio et al. (2003); (b) new version of the same map obtained using updated versions of the seismogenic zonation and of the earthquake catalogue.

Figure 1b shows an updated version of the map of slope resistance demand. It relies on more recent information and tools, namely the ZS9 seismogenic zonation (Meletti et al., 2004), the latest attenuation relation for Arias Intensity published by Sabetta et al., (2021) and the software R-CRISIS for the seismic hazard assessment (Ordaz et al., 2017).

A comparison of the two maps reveals significant differences, in particular an increase of the maximum value of $(A_c)_{10}$ from 0.04 to 0.06 g. The spatial distribution of $(A_c)_{10}$ values is strongly influenced by the geometry of the seismogenic zones, which cause a minimum in the central part of Daunia and higher values both in the northern and southern parts. Higher $(A_c)_{10}$ values coincide with the areas including many old, large deep-seated landslides of unknown origin (Ardizzone et al., 2023). These landslides are generally larger than the recent slope failures triggered by rainfall, and Wasowski et al. (2022) presented circumstantial evidence for their co-seismic origin.

Data on site resonance properties

Our previous study on slope resistance demand in Daunia have not incorporated the effect of site amplification. At present, a software package like R-CRISIS allow taking into account the site effects providing in input a matrix of the spatial distribution of amplification factors. A detailed evaluation of such effects requires the acquisition of many data, which is not feasible for regional scale studies. Thus, for a preliminary estimate of the influence of site effects on slope resistance demand, we explore the utility of information on site resonance properties obtained from ambient noise analysis carried out during the 1st level of Seismic Microzonation of the Daunia urban and peri-urban areas.

A large set of noise recordings (about 1000) have been acquired on different lithologies and slope stability conditions. We initially examined the results obtained from their processing with the HVNR method (Nakamura, 1989), which identifies local site conditions from peak values in the ratios between the spectral amplitudes of the horizontal and vertical components of the recordings. For each Daunia municipality, the resonance amplitudes and frequencies and the lithology at the measurement sites were identified, distinguishing whether these sites are on landslide or stable areas.

The following flysch formations are most common at the measurement sites:

FAE - **Flysch di Faeto** (Upper Burdigalian-Lower Tortonian). Limestone-marly-clayey alternation with a bentonite base. It is divided into a predominantly pelitic facies (FAEp) and a predominantly calcarenitic facies (FAEc).

FYR – **Flysch Rosso** (Cretaceous-Aquitanian). Grey-green to reddish mudstones alternating with blackish layers of jaspers, with intercalations of breccias, calcarenites and calcilutites.

Fig. 2 shows the distribution of resonance frequencies and H/V peak amplitudes resulting from noise measurements. The most recurring frequencies are between 0.9 and 4 Hz, while the most recurrent peak amplitudes are between 2 and 4. The attention is focused on sites

where H/V peak values are greater than 3, which should indicate a significant level of site amplification. Peak values of this amount are found to be slightly more frequent for the sites on landslides (44%) than on stable areas of (38%). This can be expected because a pre-existing landslide creates velocity contrasts with the substratum.

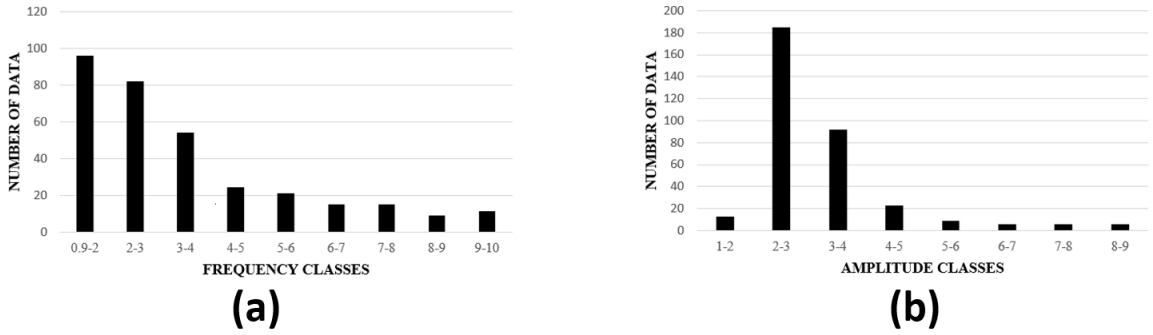

Fig. 2: Distribution of resonance frequency (a) and H/V peak amplitude (b) based on ambient noise in Daunia.

However, resonance conditions are not ubiquitous and 7.9% of landslide and 6.9% of stable ground areas showed no site effects. Furthermore, resonances appeared rather weak and this could be the effect of the “slow” flysch substratum, which causes weak velocity contrasts with the surficial material.

Between the two most common flysch formations, FAE appear characterized by a slightly greater diversity of resonance frequencies with higher mean amplitudes, in comparison to FYR whose resonance frequencies are concentrated around lower values and amplitudes. The sites on landslides in FAE, however, show a larger recurrence of lower frequency and higher amplitude, likely as an effect of the reduced velocity of slope materials. The sites on FYR, besides an increase of mean amplitude, show a frequency re-distribution towards intermediate frequency from the lowest (< 2 Hz) and the highest (> 8 Hz) frequencies. Furthermore, resonance is absent in 9.4% of FAE and 22.5% of FYR sites.

Given the differences in dynamic response, the estimates of amplification factors from the results of noise analysis may require the use of differentiated relations for the two units. However, additional efforts are needed considering that, with regard to H/V peak amplitude measurements, the HVNR technique suffers from a strong dependence on environmental conditions. For this reason the recordings are being reanalysed with the HVIP technique (Del Gaudio, 2017), which extracts from the noise the Rayleigh waves and measures their ellipticity, thus providing more stable H/V values better correlated to the local amplification factor. Fig. 3 shows a comparison between the results obtained by the two types of noise analyses.

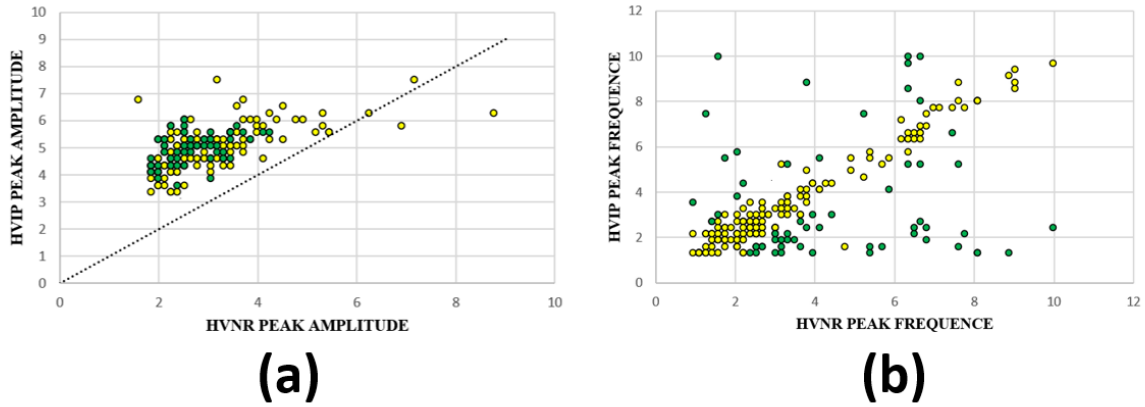

Fig. 3: Comparison of the results of HVIP and HVNR analysis of Daunia noise recordings: (a) peak frequencies and (b) peak amplitudes. Green dots mark the cases for which the main resonance frequency identified by the two techniques differs by more than 1 Hz.

The amplitudes of the HVIP peaks (which represent Rayleigh wave ellipticity) are usually greater than those of the HVNR peaks. The main peak frequency identified by the two techniques differs by more than 1 Hz in about 40% of sites. This seems related to the complex resonance pattern of flysch units, with multiple peaks of similar amplitude.

Future work

The results of ambient noise analysis will be compared with the outcomes of numerical modeling of the local seismic response in order to seek possible correlations useful to estimate the amplification factors from ambient noise data. Such modelling will rely on the detailed auxiliary data collected for Seismic Microzonation of the Daunia Mts urban and peri-urban areas, including borehole stratigraphies and results of geophysical surveys. A major contribution is expected from the study sites which, thanks to a large availability of data, will allow a 3D modelling of the local seismic response, to be compared with the results of simplified (1D and 2D) modelling; this will help evaluating uncertainties introduced by the simplification. The objective is to expand as much as possible the data set for the calibration and validation of empirical relation providing estimates of amplification factors in terms of Arias Intensity. Where the presence of site amplification effects will be recognised through the noise measurements, the resistance demand values $(A_c)_x$ will be accordingly modified, introducing the estimated amplification factors in the calculation of exceedance probability of Arias Intensity.

Finally, the $(A_c)_x$ values corrected for site amplification effects will be compared with the slopes' critical acceleration values a_c based on local topography and geotechnical properties of slope material. This should allow us to identify slopes most susceptible to co-seismic failure.

Acknowledgements

Study carried out within the RETURN Extended Partnership with funds from the European Union Next-Generation EU (National Recovery and Resilience Plan – NRRP, Mission 4, Component 2, Investment 1.3 – D.D. 1243 2/8/2022, PE0000005). Data acquired within the seismic microzonation studies of Apulia supported by the National Department of Civil Protection and the Civil Protection Office of the Apulian Regional Administration.

References

Ardizzone F., Bucci F., Cardinali M., Fiorucci F., Pisano L., Santangelo M. and Zumpano V.; 2023: Geomorphological landslide inventory map of the Daunia Apennines, southern Italy. Earth System Science Data, 15, 2, pp. 753-767.

Arias A.; 1970: A measure of earthquake intensity, in Seismic Design for Nuclear Power Plants, R. J. Hansen (ed), MIT Press, Cambridge, Massachusetts, pp. 438-483.

Bender B. and Perkins B.; 1987: SEISRISK III: A Computer Program for Seismic Hazard Estimation. U.S. Geological Survey Bulletin 1772.

Del Gaudio V.; 2017: Instantaneous polarization analysis of ambient noise recordings in site response investigations. J. Geophys. Int., 210, pp. 443-464.

Del Gaudio V., Pierri P. and Wasowski J.; 2003: An Approach to Time-Probabilistic Evaluation of Seismically Induced Landslide Hazard. Bulletin of the Seismological Society of America, 93, 2, pp. 557-569.

Meletti C., Galadini F., Valensise G., Stucchi M., Basili R., Barba S., Vannucci G. and Boschi E.; 2004: Zonazione sismogenetica ZS9 [Data set]. Istituto Nazionale di Geofisica e Vulcanologia (INGV).

Nakamura Y.; 1989: A method for dynamic characteristics estimation of subsurface using microtremor on the ground surface. Q. Report Railway Tech. Res. Inst., 30, pp. 25-33.

Newmark N. M.; 1965: Effects of earthquakes on dams and embankments, Geotechnique, 15, pp- 139-160.

Ordaz M., Martinelli F., Aguilar A., Arboleda J., Meletti C. and D'Amico V.; 2017: R-CRISIS. Program and platform for computing seismic hazard.

Romeo R.; 2000: Seismically induced landslide displacements: a predictive model. Eng. Geol., 58, 3-4, pp. 337-351, doi:10.1016/S0013-7952(00)00042-9.

Sabetta F. and Pugliese A.; 1996: Estimation of response spectra and simulation of nonstationary earthquake ground motions. Bull. Seism. Soc. Am., 86, 2, pp. 337-352.

Sabetta F., Pugliese A., Fiorentino G., Lanzano G. and Luzi L.; 2021: Simulation of non-stationary stochastic ground motions based on recent Italian earthquakes. Bull. Earth. Eng., 19, pp. 3287-3315, doi.org/10.1007/s10518-021-01077-1.

Scandone P.; 1997: Linea di ricerca 2 "Sismotettonica". In: Corsanego A., Faccioli E., Gavarini C., Scandone P., Slejko D. and Stucchi M. (eds), L'attività del GNDT nel triennio 1993 -1995, CNR-GNDT, Roma, pp. 67-96.

Wasowski J., Lamanna C. and Casarano D.; 2010: Influence of land-use change and precipitation patterns on landslide activity in the Daunia Apennines, Italy. Quarterly J. Eng. Geology and Hydrogeology, 43, 4, pp. 387–401.

Wasowski J., Del Gaudio V., Pisano L., Fazio N. L., De Lucia D., Ugenti A., Zumpano V., Filice F., Casarano D., Santaloia F., Gallicchio S. and Lollino P.; 2022: Unravelling the origin of large ancient landslides in low elevation Daunia Mountains, Italy. AGU Fall Meeting Abstracts, NH22A-07.

Corresponding author: flaviana.fredella@uniba.it

Temporal and Spatial Variability of Anelastic Attenuation and Its Effects on Ground Motion Characteristics in Central Italy

Simona Gabrielli (1), Aybige Akinci (1), Carolina Gutierrez (2), Javier Ojeda Vargas (2), Sebastian Arriola (3) and Sergio Ruiz (2)

1 Istituto Nazionale di Geofisica e Vulcanologia (INGV), Via di Vigna Murata 605, 00142, Rome, Italy

2 Departamento de Geofísica, Universidad de Chile, Blanco Encalada, 2002, Santiago, Chile

3 Centro Sismológico Nacional Universidad de Chile, Santiago, Chile

In recent decades, Central Italy has experienced seismic sequences resulting in casualties and significant building damage, as the one of 2016-2017, started with the Amatrice mainshock (Mw6.2) in August 2016, followed by the Visso (Mw5.9) and Norcia (Mw6.5) events in October 2016 (hereafter, AVN). Considering the frequent seismic activity and elevated seismic risk in the region, employing ground-motion simulations is essential for assessing seismic risk and earthquake engineering applications. Previous studies focused on ground motion characteristics of the Mw6.2 Amatrice and Mw6.5 Norcia earthquakes using stochastic and numerical approaches (Pischiutta et al., 2020; Ojeda et al., 2021; Pitarka et al., 2021).

The definition of attenuation characteristics and their relationship with ground motion models have already been used for predicting ground motions from hypothesized events, which are fundamental to defining the accuracy of seismic assessments. Recent studies applied non-ergodic approaches to reduce the uncertainties in ground motion models, taking into account a range of physical parameters linked to both the seismic source and wave propagation, along with heterogeneities specific to the path.

Here, we explore the seismic wave attenuation variability on strong-ground motion simulation in the Central Apennines, using stochastic simulations (Ojeda et al., 2021). First, we calculate the quality factor Q values for the area, obtaining the total attenuation Q as a function of frequency for the 2016-2017 seismic sequence. In order to map this variation, we applied a 2D kernel-based imaging of coda-Q space variation, which confirmed the differences in attenuation between the pre-sequence and the AVN, with an increment in attenuation during the 2016 time period in the fault plane zones.

Then, we integrate the obtained frequency-dependent Q value as input parameters for strong-ground motion simulations, considering earthquake-induced ground motions. This stochastic methodology simulates the strong-ground motion at high frequencies, mimicking

the source rupture fault mechanisms, slip distribution, stress drop and radiation pattern, and obtaining horizontal and vertical accelerograms. The estimations are correlated and validated against observed peak ground accelerations and spectral acceleration for the Amatrice and Norcia fault plane, and then compared with the ground motion prediction equations used for the region (Lanzano et al., 2019).

Stochastic modelling as a method for providing seismic hazard estimates of site effects over wide areas

I. Gaudiosi[1], G. Acunzo[2], D. Albarello[3], M. Moscatelli[1]

[1] Istituto di Geologia Ambientale e Geoingegneria (CNR, Italy)
[2] Theta Group (Italy)
[3] Dipartimento di Scienze Fisiche, della Terra e dell'Ambiente (Università degli Studi di Siena, Italy)

Numerical simulations of seismic site response require the characterization of the nonlinear behaviour of shallow subsoil and their mechanical characterization. When extensive evaluations are of concern, as in the case of seismic microzonation studies, funding problems prevent a systematic use of laboratory tests or S-waves velocity profiles to provide detailed evaluations.

For this purpose, we investigate the use of statistical laws for both the main mechanical and dynamic parameters. A statistical analysis of the data were carried out in previous studies (Romagnoli et al., 2021; Gaudiosi et al., 2023) with the aim of shedding light on the significant difference between the laboratory and in situ classification of samples and soils and the macroscopic/engineering geological one, provided during seismic microzonation studies.

Since the engineering geological classification plays a prominent role in extensive site response evaluations, the outcomes of the present work may be of help at least when preliminary seismic response estimates are of concern. The preliminary tests carried out in the framework of the PRIN SERENA Projects provide reference information that can serve as key data for large-scale hazard assessments in the Italian territory.

The variability of the synthetic hazard parameters may be modelled throughout the NC92 code (Acunzo et al., 2024) by considering the probability distributions obtained for each seismo-stratigraphy. These probability distributions may be combined in the frame of a Bayesian approach to determine a probabilistic estimate of the hazard parameters at output nodes, as well as its variability range.

References

Acunzo G., Falcone G., di Lernia A., Mori F., Mendicelli A., Naso G., Albarello D., Moscatelli M.; 2024. *NC92Soil: A computer code for deterministic and stochastic 1D equivalent linear seismic site response analyses*. Computers and Geotechnics, **165**, 105857.

Gaudiosi I., Romagnoli G., Albarello D., Fortunato C., Imprescia P., Stigliano F., Moscatelli M.; 2023. Shear modulus reduction and damping ratios curves joined with engineering geological units in Italy. Scientific Data **10**, 625. https://doi.org/10.1038/s41597-023-02412-8

Romagnoli G., Tarquini E., Porchia A., Catalano S., Albarello D., Moscatelli M.; 2022. *Constraints for the Vs profiles from engineering-geological qualitative characterization of shallow subsoil in seismic microzonation studies*. Soil Dynamics and Earthquake Engineering, **161**, 107347. https://doi.org/10.1016/j.soildyn.2022.107347

Acknowledgments

This research was supported by the PRIN SERENA project (scientific coordinator: D. Albarello; Prot. 2020MMCPER; Decreto 374 Direttoriale n. 223 del 18/02/2022 del Ministero dell'Università e della Ricerca, Segretariato Generale Direzione Generale della 375 ricerca).

Corresponding author: iolanda.gaudiosi@cnr.it

Testing synthetic site amplification maps through comparison with empirical estimates in Central Italy

S. Hailemikael[1], G. Cultrera[1], C. Barnaba[2], G. Laurenzano[2], G. Martini[1,3], A. Peloso[3], F. Cara[1], G. Di Giulio[1], D. Famiani[1]

[1] Istituto Nazionale di Geofisica e Vulcanologia (INGV), Rome, Italy.
[2] Istituto Nazionale di Oceanografia e di Geofisica Sperimentale (OGS), Trieste, Italy.
[3] Agenzia Nazionale per le Nuove Tecnologie, l'Energia e lo Sviluppo Economico Sostenibile (ENEA), Frascati, Italy.

In the framework of the national research project SERENA - Mapping Seismic Site Effects at REGional and NATIONAL Scale, the work package 6 (WP6) aims to test the ground motion amplification maps developed within the project by means of empirical estimates. The target maps will be mainly generated by a hybrid geological-geomorphological classification of the national territory and stochastic 1D equivalent linear numerical simulations (synthetic approach) based on seismic microzonation data collected over the last decade (Moscatelli *et al.*, 2020).

To this end, we collected and enriched the database of experimental site-specific amplification estimates originally gathered by Priolo *et al*. (2020) for Central Italy and compared these estimates with those obtained in a study preceding this project by implementing a synthetic approach similar to what will be developed in SERENA (Falcone *et al.*, 2021). In particular, the empirical estimates for about 240 seismic monitoring sites in Central Italy were obtained by evaluating more than 45000 seismic records processed with a standardised approach to derive site amplification factors (FA). The FA values are calculated within three period intervals, defined by the current seismic microzonation guidelines (SM Worging group 2015) and representative of short, medium and long period ground-motion amplification (namely 0.1s-0.5s, 0.4s-0.8s, 0.7s-1.1s).

We calculated and compared the statistical distributions of experimental and synthetic FA (FA_exp and FA_syn, respectively) for the 240 sites in Central Italy, also by means of specifically developed GIS tools. We found that the FA_syn distributions are within the range 1-2 for all considered periods, while all FA_exp distributions have median values equal to or greater than 2 and large upper tails, with amplification values up to 7.5. The distribution of FA_exp also shows values below 1 for a few sites, indicating de-amplification compared to the considered reference motion.

The distributions of the residuals between FA_exp and Fa_syn (in natural logarithmic units) were then evaluated for each considered site and the influence of the period interval and the

available site parameters on the residual value were investigated. The distributions of the residuals (Fig. 1) show a positive mean term, which clearly indicates an underestimation of empirical amplification by the synthetic approach. The mean underestimation term increases with the considered period interval, while the associated uncertainty (σ of such distributions) is almost constant with respect to the period. The distributions also show negative tails, which are related to those sites having experimental de-amplification of ground motion.

Despite the lack of detailed geological information for the studied sites, the uniform geo-lithological classification of the national map at 1:100.000 scale (http://www.pcn.minambiente.it/mattm) revealed that most of the sites (65%) for which the synthetic approach underestimates the observed amplification are located on alluvial deposits and chaotic sedimentary complexes, while the sites for which an overestimation was calculated by FA_syn are located on bedrock formations and mostly correspond to sites with the FA_exp < 1.

These preliminary results suggest that the amplification maps produced prior to the SERENA project using the synthetic approach may significantly underestimate the experimental ground-motion amplifications. Therefore, the approach should be improved so that the FA_syn values can cover a wider range (max FA_syn >> 2). Furthermore, the analysis of the residuals suggests that larger discrepancies between the experimental and synthetic estimates occur for long-period amplifications, which may be caused by: i) bedrock definition in 1D simulations for those sites located on large intermountain basins characterised by large bedrock depths (> 100 m) and ii) 2D/3D site effects.

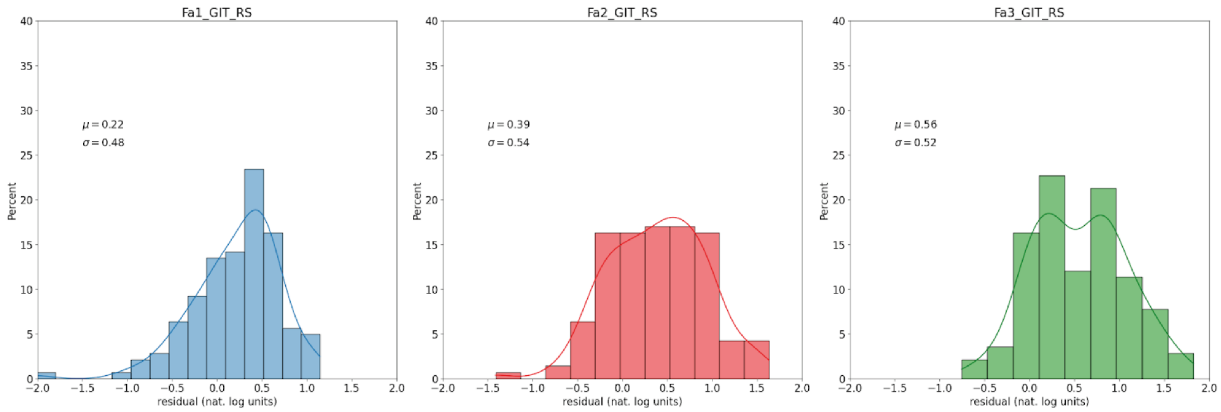

Fig. 1 - Distribution of residuals between median FA_exp and Fa_syn values (in natural logarithmic units) as a function of period: short (FA1 blue), intermediate (red) and long periods (green).

References

Falcone G., Acunzo G., Mendicelli A., Mori F., Naso G., Peronace E., Porchia A., Romagnoli G., Tarquini E. and Moscatelli M.; 2021: *Seismic amplification maps of Italy based on site-specific microzonation dataset and one-dimensional numerical approach*. Engineering Geology, Vol. 289, 106170, https://doi.org/10.1016/j.enggeo.2021.106170.

Moscatelli M., Albarello D., Scarascia Mugnozza G. and Dolce M.; 2020: *The Italian approach to seismic microzonation*. Bull Earthq Eng 18, 5425–5440. https://doi.org/10.1007/s10518-020-00856-6

SM Working Group; 2015: *Guidelines for seismic microzonation, conference of regions and autonomous Provinces of Italy—Civil Protection Department, Rome*. http://www.protezionecivile.gov.it/httpdocs/cms/attach_extra/GuidelinesForSeismicMicrozonation.pdf.

Priolo E., Pacor F., Spallarossa D., Milana G., Laurenzano G., Romano M.A., Felicetta C., Hailemikael S., Cara F., Di Giulio G., Ferretti G., Barnaba C., Lanzano G., Luzi L., D'Amico M., Puglia R., Scafidi D., Barani S., De Ferrari R. and Cultrera G.; 2020: Seismological analyses of the seismic microzonation of 138 municipalities damaged by the 2016–1017 seismic sequence in Central Italy. Bull Earthq Eng 18:5553–5593. https://doi.org/10.1007/s10518-019-00652-x

Corresponding author: salomon.hailemikael@ingv.it

Site Response Analysis in the Agri valley (Basilicata) using the Generalized Inversion Technique

G. Laurenzano[1], N. Tragni[2], P. Klin[1], TA Stabile[2], MR Gallipoli[2] & *PRIN SERENA WP06 WG*

[1] Istituto Nazionale di Oceanografia e di Geofisica Sperimentale – OGS (Triste, Italy)
[2] National Research Council of Italy - CNR-IMAA (Tito Scalo, Italy)

The inclusion of site amplification effects caused by local geo-lithological features could bring a considerable improvement in the assessment of seismic hazard (e. g. Mascandola et al., 2023). A wide range of approaches is used today to analyze the site response, but the modalities for their optimal application are still under debate. As part of the work package "Empirical testing and calibration" of the ongoing PRIN project "Mapping seismic site effects at regional and national scale - SERENA", this study presents the application of the Generalized Inversion Technique - GIT (Castro et al., 1990) to evaluate the frequency-dependent local seismic amplification at 24 sites in the Agri Valley (southern Basilicata). The Agri Valley is a NW-SE trending intermontane basin, which mainly developed during Quaternary draining of a large sector of the Southern Apennines. The High Agri Valley is a tectonically active area characterized by high seismic hazard related to fault systems capable of generating up to M = 7 earthquakes (i.e., the 1857 Mw = 7 Basilicata earthquake). The analyzed sites are distributed over an area of about 800 km^2 and correspond to the locations of seismic stations that belong to three permanent seismic networks. The sites are characterized by a variety of lithologies, ranging from alluvial, lacustrine, swamp and marine deposits to eluvial and colluvial deposits, siliciclastic sedimentary rocks and carbonate rocks. Site amplification functions are estimated by means of an implementation (Klin et al., 2021) of the one-step nonparametric GIT based on the conventional decomposition of the S-wave phase in terms of source, propagation, and site response. The used database of earthquake recordings consists of more than 2000 waveforms recorded between 2016 and 2018 and includes local and regional events in a distance range of up to 400 km, ensuring good azimuthal coverage for each station. The evaluated site amplification functions are compared to both earthquake and micro-tremor horizontal-to-vertical spectral ratios. Finally, the amplification functions are used to evaluate the FA amplification factors in three period bands of engineering interest (0.1 – 0.5 s, 0.4-0.8 s, and 0.7-1.1 s). The results evidence high FA amplification factors (up to values of the order of 5) in the low and medium period bands for stations located on sedimentary deposits. A more detailed investigation on possible correlations between the measured amplification and the site geomorphological characteristics is under progress.

References

Castro R.R., Anderson J.G. and Singh S.K.; 1990: Site response, attenuation and source spectra of S waves along the Guerrero, Mexico, subduction zone. Bull. Seismol. Soc. Am., 80 no. 6A, 1481–1503.

Klin P., Laurenzano G., Barnaba C., Priolo E. and Parolai S.; 2021: Site Amplification at Permanent Stations in Northeastern Italy. Bull. Seismol. Soc. Am., 111 no. 4, 1885–1904, DOI 10.1785/0120200361.

Mascandola C., Barani S. and Albarello D.; 2023: Impact of Site-Response Characterization on Probabilistic Seismic Hazard in the Po Plain (Italy). Bull. Seismol. Soc. Am., 113 no. 3, 1269–1285, DOI 10.1785/0120220177.

Corresponding author: nicolatragni@cnr.it

MUDA: a new geophysical and geochimical MUltiparametric DAtabase for real-time multidisciplinary monitoring networks

Massa M.[(1)], Rizzo L.A.[(2)], Ferrari E.[(1)], Lovati S.[(1)], Scafidi D.[(3)] and MUDA working group

[(1)] Istituto Nazionale di Geofisica e Vulcanologia, sezione Milano
[(2)] Università di Milano Bicocca, DISAT
[(3)] Università di Genova, DISTAV

MUDA (geophysical and geochemical MUltiparametric DAtabase) is a new infrastructure of the National Institute of Geophysics and Volcanology (INGV, www.ingv.it) serving geophysical and geochemical multiparametric data, designed as part of the INGV Pianeta Dinamico (PD) 2020-2022 project and now implemented as a part of the ongoing INGV Pianeta Dinamico 2023-2025 PD-GEMME (Integrated Geological, gEophysical and geocheMical approaches for 3D Modeling of complex seismic site Effects) project.

MUDA is a dynamic and relational database based on MySQL (https://www.mysql.com) with a web interface realised in php (https://www.php.net) using a responsive design technique. The multi-parametric data are stored and organised using a table-structure able of correlating different types of data that allow possible future integration with new type of data acquired through both real-time and off-line transmission vectors.

MUDA collects information from different types of sensors, such as seismometers, accelerometers, hydrogeochemical sensors, sensors for measuring the flux of carbon dioxide on the ground (CO_2), sensors for detecting the concentration of Radon gas and weather stations with the aim of making possible correlations between seismic phenomena and variations in environmental parameters such as the level of groundwater as well as its temperature and electrical conductivity (e.g, Barberio et al. 2017; Chiodini et al., 2020; Mastrorillo et al. 2020).

MUDA archives and publishes data of multiparametric stations belonging both to permanent (e.g. National Seismic Network, RSN-INGV, https://www.fdsn.org/networks/detail/IV/) or temporary (e.g. PDnet, Massa et al., 2021, https://www.fdsn.org/networks/detail/ZO_2021/) INGV seismic networks, as well as data from a multi-parametric Salse di Nirano Reserve (MO) site in cooperation with the PD PROMUD 2023-2025 (Definition of a multidisciplinary monitoring PROtocol for MUD volcanoes) project and two additional multi-parametric sites installed in the inter-mountain basin of Norcia, as a part of the GEMME 2023-2025 project. Data from Radon stations belong to the INGV-IRON national network (Italian Radon Monitoring Network, https://www.ingv.it/en/monitoring-and-infrastructure/monitoring-networks/ingv-and-its-networks/iron).

MUDA daily publishes multi-parametric data updated to the previous day and offers the chance to view and download dynamic time series for all available data and for different periods, up to a maximum of 30 days. For longer periods, users can request data to muda@ingv.it.

MUDA is now published at http://muda.mi.ingv.it (doi.org/10.13127/muda)

Bibliografia

Barberio M.D., Barbieri M., Billi A., Doglioni C., Petitta M. (2017), Hydrogeochemical changes before and during the 2016 Amatrice-Norcia seismic sequence (central Italy). Scientific Reports, 7:11735, doi:10.1038/s41598-017-11990-8.

Chiodini G., Cardellini C., Di Luccio F., Selva J., Frondini F., Caliro S., Rosiello A., Beddini G., Ventura G. (2020), Correlation between tectonic CO2 Earth degassing and seismicity is revealed by a 10-year record in the Apennines, Italy. Sci. Adv. 2020; 6 : eabc2938

Massa M., Rizzo A.L., Lorenzetti A., Lovati S., D'Alema E., Puglia R., Carannante S., Piersanti A., Galli G., Cannelli V., Luzi L. (2021), La rete del lago di Garda: una nuova infrastruttura dell'INGV per il monitoraggio multiparametrico, blog INGV dipartimento terremoti, https://ingvterremoti.com/2021/12/10/la-rete-del-lago-di-garda-una-nuova-infrastruttura-dellingv-per-il-monitoraggio-multiparametrico/

Mastrorillo L, Saroli M, Viaroli S, Banzato F, Valigi D, Petitta M. (2020), Sustained post-seismic effects on groundwater flow in fractured carbonate aquifers in Central Italy. Hydrological Processes, 34:1167–1181. https://doi.org/10.1002/hyp.13662

Correponding author: marco.massa@ingv.it

In-plane strengthening of timber floors to improve the seismic response of masonry structures: a 18thcentury case-study

A. Mazelli[1,2], C. Bedon[2], A. Morassi[1]

[1] University of Udine, Polytechnic Department of Engineering and Architecture, Udine, Italy
[2] University of Trieste, Department of Engineering and Architecture, Trieste, Italy

Introduction

Existing masonry buildings are often complex structures, and their seismic performance evaluation represents a challenge. The high variability of mechanical characteristics of unreinforced masonry and the presence of flexible floors that are poorly anchored to the walls make identifying their dynamic behaviour tough.

A solution to improve the seismic behaviour of existing / historic masonry structures is the floor reinforcement, by stiffening and connecting them efficiently to vertical structures, and facilitating an effective distribution of the seismic action with a box-like behaviour. Various solutions have been proposed over the years, using steel, wood or fibre-reinforced materials, and their effectiveness on the building seismic behaviour has been addressed by push-over (Ortega et al. 2018, Jiménez -Pacheco et al. 2020) or nonlinear dynamic analyses (Scotta et al. 2018, Gubana and Melotto 2019).

The main goal of current work is to evaluate the effectiveness of several floor stiffening solutions, by means of push-over analysis, to improve the seismic performance of a case-study historic building.

Description of the case-study building

The case-study building is a noble Villa in north-eastern Italy (Pordenone) built in the early 18th century (Fig. 1a,b). The building has a compact rectangular plan shape (16x15 m) and four levels. The upper floors were added after a renovation (end of 18th century), and for this reason the internal walls layout of new and lower floors has no correspondence (Fig. 1c,d). Moreover, the floor at the tympanum level has smaller dimensions.

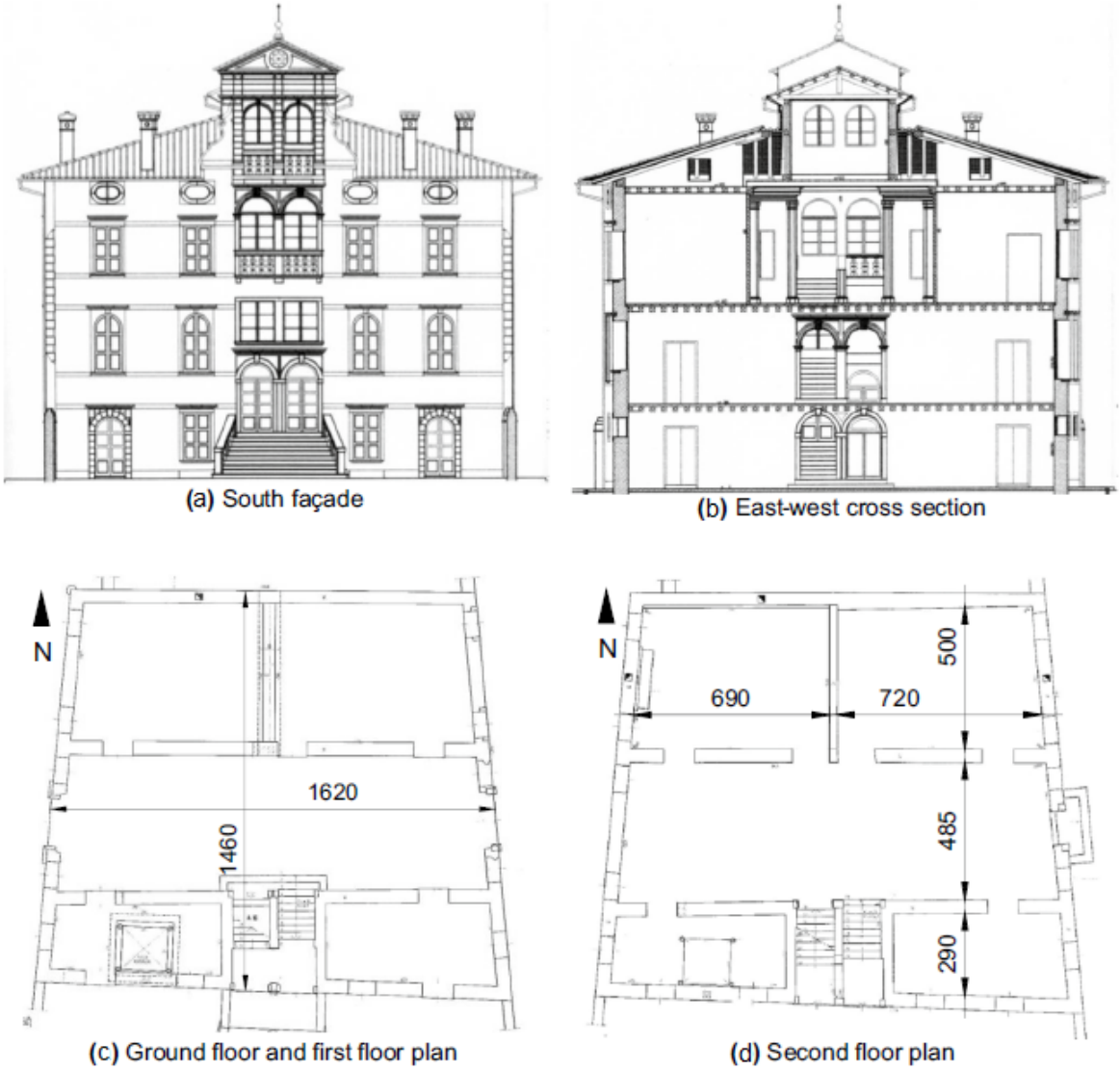

Fig. 1 – Drawings of the case-study historic Villa (measurements in centimetres).

The walls are made of rubble stone masonry (mean compressive strength f_c=2.17 MPa, elastic modulus E=1500 MPa, shear modulus G=500 MPa) varying in thickness from 50 cm (ground floor) to 42 cm (upper storeys). The existing floors consist of timber joists and nailed planks, with beams oriented North-South.

Structural numerical model

The case-study villa was modelled in Sap2000 using a simplified but efficient approach, which was validated towards the earlier DEM modelling strategy presented in (Gubana and Melotto 2021a). To this aim, the façade shape was slightly simplified in geometry, in accordance with (Gubana and Melotto 2021a). Moreover, the roof and the 4th storey were described in terms of equivalent masses only (applied to the 3rd floor). The tympanum floor consists in a timber reticular system with negligible contribution to the overall stiffness of the building (Gubana and Melotto 2021a).

The walls were modelled with an equivalent frame strategy (Fig. 2). Each pier and spandrel were associated with two flexural hinges at the ends, and a shear hinge at mid-span. Ultimate bending moment, shear and corresponding drifts were assumed in accordance with the Italian Building Code and the CNR-DT 212/2013.

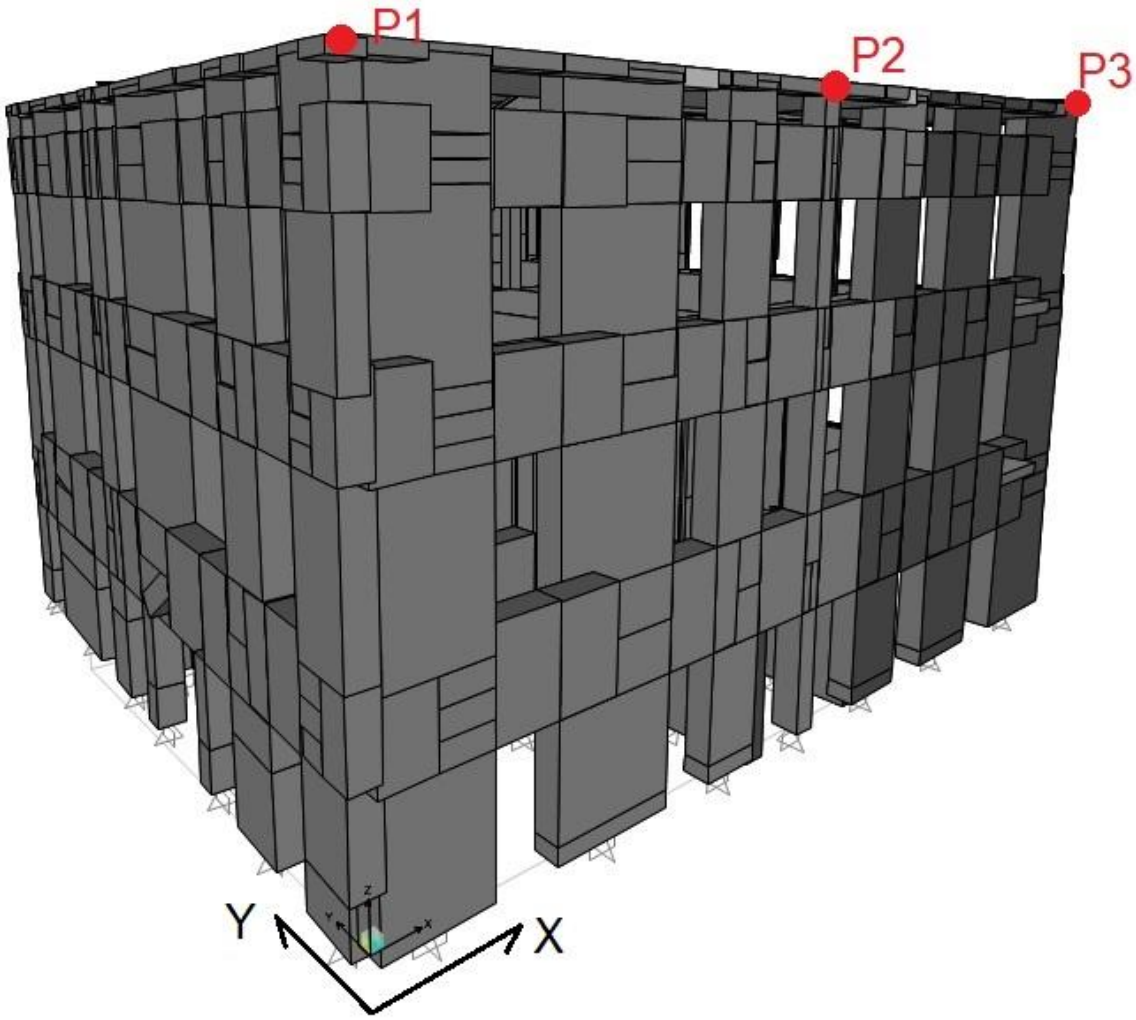

Fig. 2 – Structural FEM model of the Villa and control points on the top floor (Sap2000).

Six different models of the Villa were developed, by varying the in-plane reinforcement strategy for timber floors (Table 1). The mechanical parameters for the reinforcement characterisation were taken from a previous extensive experimental campaign (Gubana and Melotto 2021b). The equivalent stiffness of the floor was evaluated by means of equation 1:

$$G = \frac{F/B}{\gamma} = \frac{F/B}{\frac{\sqrt{B^2 + H^2}}{BH}\frac{d_1 - d_2}{2}} \quad (1)$$

Where F is the applied load, B and H are the floor dimensions parallel and orthogonal to the orientation of the beams respectively, and d_1 and d_2 are the length variation of the diagonals. Values of the equivalent stiffness are shown in Table 1. A first shear stiffness $G_{0\text{-}30}$ was calculated between 0% and 30% of the maximum shear load carried by the sample, while a second value ($G_{10\text{-}40}$) between 10% and 40% of the maximum load, in accordance to UNI-EN12512 (2006). Two non-reinforced floors (TF-UR-G and TF-UR-NG) were selected for the analyses: the first with gaps between the planks and the second without gaps. Their difference is emphasized by the $G_{0\text{-}30}$ stiffness, which is eighteen times higher for the NG case, where the friction between the parts of the floor plays an important role. The influence of the initial stiffness is partially lost when evaluating $G_{10\text{-}40}$. Three types of reinforced floors were considered. TF-OSB-N and TF-OSB-S were stiffened with 25 mm thick OSB panels and ringed-nails (N case) or screws (S case). On the other hand, TF-CLT-S floor was reinforced with 60 mm thick CLT panels, which were fastened with screws. Each floor was modelled as an equivalent shell element with an elastic behaviour. Furthermore, the case of rigid diaphragm was also taken into account (TF-RIGID).

Table 1 – Timber floor typologies considered for the non-linear analysis of the case study Villa, as derived from the experimental investigations in (Gubana and Melotto 2021b)

ID	Features	Reinforcement type	Connectors	$G_{0\text{-}30}$ [kN/mm]	$G_{10\text{-}40}$ [kN/mm]
TF-UR-G	With gaps	-	-	0.09	0.06
TF-UR-NG	No gaps	-	-	1.66	0.65
TF-OSB-N		OSB panel	Ringed-Nails	19.52	5.92
TF-OSB-S		OSB panel	Self-tapping screws	10.49	3.81
TF-CLT-S		CLT panel	Self-tapping screws	5.69	2.83
TF-RIGID		-	-	-	-

Results

The parametric numerical results were analysed in term of displacements. A comparison between base shear and top displacement obtained for each configuration of Table 1 was also carried out.

Pushover analyses were performed in the North-South direction (Y direction according to Fig. 2), which corresponds to the orientation of timber joists. In accordance with the Italian Building Code, a mass proportional (Group 1) and an acceleration proportional (Group 2) configuration were considered for loading.

Fig. 3 shows the displacements on the top storey of the South façade of the Villa for all floor configurations, normalized to the displacement of control point P2 in the TF-UR-NG arrangement ($d_{P2,TF\text{-}UR\text{-}NG}$). A red dot highlights the control point P2 defined in Fig. 2. The graphs in Fig. 3 confirm the significant contribution of the interventions in reducing the out-of-plane bending of the south wall, and so the possibility to avoid the activation of local out-of-plane mechanisms. The effect can also be seen graphically, considering the less convex shape of the deformed curves in the reinforced cases.

In the TF-UR-G case, the structure exhibits a different behaviour, where in Fig. 3a,d a considerable slip is visible at x = 0 m, due to the collapse of the corresponding shear wall.

For each type of floor, the ratio between the out-of-plane deflection of the south façade and the total displacement was evaluated, referring to control point P2. For the TF-UR-NG case, the ratio varies between 20% (Group 2 negative) and 46% (Group 1 negative). These percentages drop significantly for strengthen floors.

When the floor is reinforced with OSB panels and ringed-nails, the incidence of the out-of-plane bending varies between 11% and 22% for Group 2 and Group 1 in the positive direction respectively. The results are further improved if OSB panels and screws are considered: in this case, the incidence is limited between a minimum of 7% (Group 2 negative) and a maximum of 15% (Group 1 positive).

In the TF-CLT-S case, the ratio varies between 7% (Group 2 negative) and 30% (group 1 positive). It is worth noticing that this solution allows achieving higher global displacements in the negative direction.

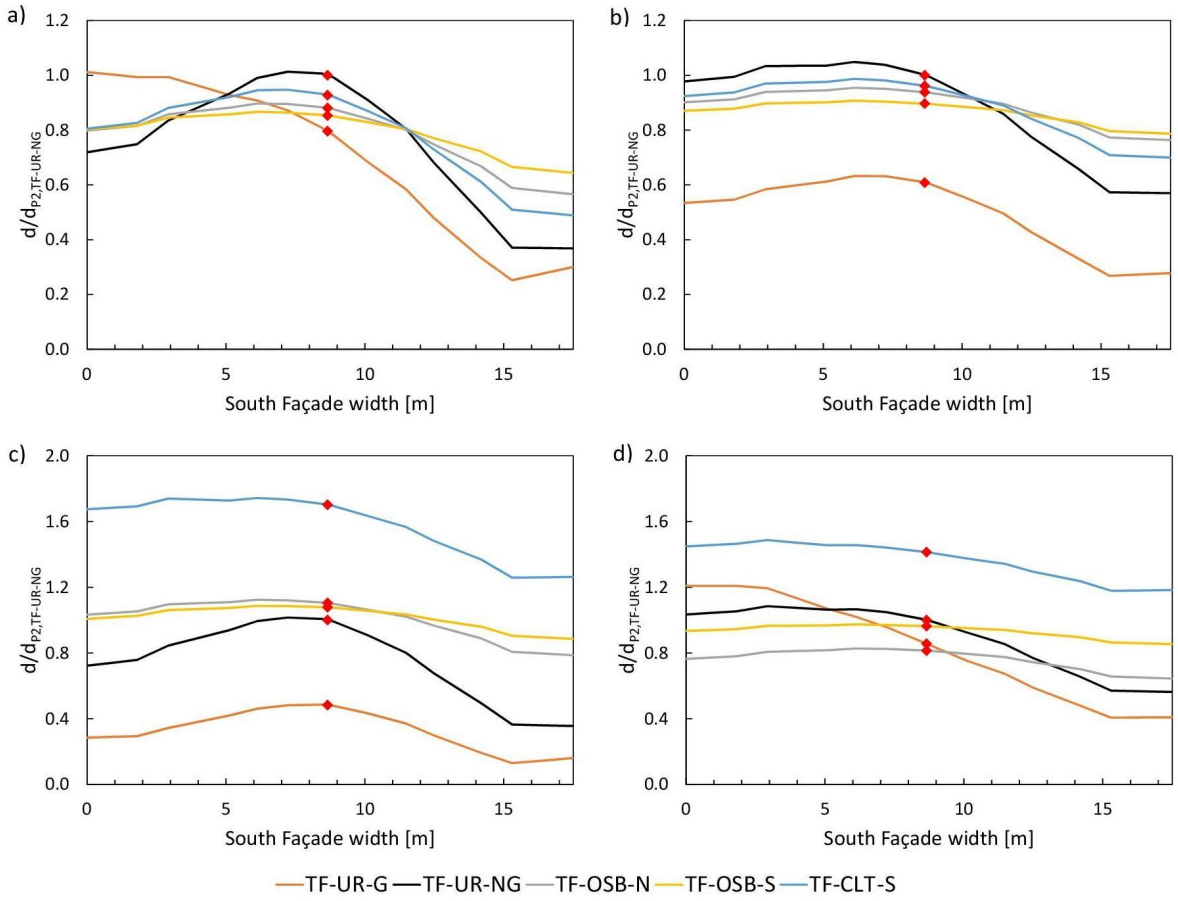

Fig. 3 – Normalised displacements of the main South façade for Group 1 and Group 2 loading configurations in positive (a and b) and negative (c and d) directions.

Furthermore, Table 2 shows the influence of the reinforcement on the maximum base shear F_{max} and the maximum displacement d_{max} of the control point in the center of mass of the top floor. The results were considered in terms of percentage variation compared to the TF-UR-NG case.

The high displacements of the TF-UR-G case are due to the premature collapse of a shear wall, as already seen in Fig. 3. The effect is visible in the decrease in the total force at the base compared to the TF-UR-NG case.

The reinforced cases exhibit a slight increase in the maximum base shear, due to the improved distribution of the seismic forces on the resistant structures. Furthermore, in most cases, the ultimate displacement decreases. It is worth noticing that this is not a decrease in the ductility of the structure, which is low because its global response is governed by brittle shear failures. The smaller displacement is due to the greater stiffness of the reinforced floors.

As already seen in Fig. 3, the CLT case in the negative direction has an excellent performance. It limits the out-of-plane displacements of the south façade and, at the same time, the

maximum shear obtained is increased. Among all cases, the TF-CLT-S is the one more similar to the ideal behavior of a rigid diaphragm, as already noted in (Gubana and Melotto 2021a).

Table 2 – Influence of the reinforcement of the floors on the base shear F_{max} and on the maximum displacement d_{max} with respect to the TF-UR-NG case.

	GROUP 1				GROUP 2			
	Positive		Negative		Positive		Negative	
	ΔF_{max} [%]	Δd_{max} [%]	ΔF_{max} [%]	Δd_{max} [%]	ΔF_{max} [%]	Δd_{max} [%]	ΔF_{max} [%]	Δd_{max} [%]
TF-UR-G	-8.6	131.2	-28.7	47.6	-16.7	24.7	-5.6	74.7
TF-UR-NG	-	-	-	-	-	-	-	-
TF-OSB-N	7.0	-33.2	12.0	-16.7	5.7	-24.4	1.8	-35.5
TF-OSB-S	7.9	-37.4	14.4	-21.7	7.1	-29.4	8.8	-25.1
TF-CLT-S	5.5	-25.8	24.6	34.8	4.4	-19.4	10.4	17.5
TF-RIGID	91.0	83.0	48.2	-34.6	37.4	52.7	22.6	-21.9

Conclusions

Pushover numerical analyses to evaluate the influence of the in-plane strengthening of timber floors were carried out on a historical masonry Villa.

Three cases of reinforcement with OSB and CLT panels, with nails and screws, were considered, and their performances were compared with two unreinforced cases. The equivalent stiffness of the floors was assumed from experimental tests.

The investigation confirms the capacity of the reinforced floors to limit the out-of-plane bending of the Villa's façade. The incidence of out-of-plane on the total displacement varies from 20-46% in the unreinforced case to 7-15% in the case reinforced with OSB panels and screws. This reduction indicates that it is possible to avoid the activation of local out-of-plane mechanisms with a timber reinforced floor. Furthermore, the proposed stiffening interventions allows to obtain a slight increase in the maximum base shear, between 2% and 25% with respect to the unreinforced case.

References

CNR-DT 212/2013 Instructions for the Reliability Assessment of Seismic Safety of Existing Buildings, National Research Council, Rome 2013 (in italian)

CS.LL.PP. 2018 Ministery Decree 17/01/2018 - Italian National Building Code NTC 2018 (in Italian).

Gubana A., Melotto M.; 2019: Discrete-element analysis of floor influence on seismic response of masonry structures. Proceedings of the Institution of Civil Engineers - Structures and Buildings 174:459-472. doi.org/10.1680/jstbu.19.00099

Gubana A., Melotto M.; 2021a: Evaluation of timber floor in-plane retrofitting interventions on the seismic response of masonry structures by DEM analysis: a case study. Bull Earthquake Eng 19, 6003–6026. https://doi.org/10.1007/s10518-021-01190-1

Gubana A., Melotto M.; 2021b: Cyclic numerical analyses on wood-based in-plane retrofit solutions for existing timber floors. Structures 33:1764-1774. doi.org/10.1016/j.istruc.2021.05.037

Jiménez-Pacheco J., González-Drigo R., Pujades Beneit L.G., Barbat A.H., Calderón-Brito J.; 2020: Traditional High-rise Unreinforced Masonry Buildings: Modeling and Influence of Floor System Stiffening on Their Overall Seismic Response. International Journal of Architectural Heritage. doi:10.1080/15583058.2019.1709582

Ortega J., Vasconcelos G., Rodrigues H., Correia M.; 2018: Assessment of the influence of horizontal diaphragms on the seismic performance of vernacular buildings. Bulletin of Earthquake Engineering. doi:10.1007/s10518-018-0318-8

Scotta R., Trutalli D., Marchi L., Pozza L.; 2018: Seismic performance of URM buildings with in-plane non-stiffened and stiffened timber floors. Engineering Structures 167:683–694.

UNI-EN 12512:2006 Timber structures. Test methods. Cyclic testing of joints made with mechanical fasteners.

Acknowledgment

This work was carried out as part of the DPC-ReLUIS 2022-2024 project financed by the Department of Civil Protection.

Corresponding author: alessandro.mazelli@phd.units.it

Mapping recent flood covers using machine learning techniques.

A. Mendicelli[1], F. Mori[1], C. Varone[1], M. Simionato[1], M. Moscatelli[1]

1 CNR-IGAG, Istituto di Geologia Ambientale e Geoingegneria, Area della Ricerca di Roma 1, Via Salaria km 29.300, 00015 Monterotondo Stazione, Rome, Italy)

Abstract

At present, the most detailed geological map covering the entire Italian national territory is the 1:100,000 scale geological map of Italy created by ISPRA. To estimate the stratigraphic amplification of seismic motion at the surface over a large area, it is crucial to better define the geological and lithotechnical characteristics of covering soils and geological bedrocks. This work is aimed at improving the definition of recent alluvial covers (Holocene and Upper Pleistocene deposits) compared to the 1:100,000 geological map of Italy. For this purpose, a methodology based on machine learning models has been developed. It considers both categorical and numerical variables to predict the presence/absence of recent flood coverage with good accuracy.

To train the machine learning model, both geomorphometric parameters and geological databases at different scales were used. Initially, the methodology was tested in the Calabria Region and in the Marche Region, for which promising results were obtained with good performances in the external test. The next step, still in the development phase, consists in the application of the methodology in a wider area which includes not only the Calabria and Marche regions but also Tuscany, Emilia-Romagna and Umbria. The model thus obtained will be tested across the entire national territory.

Acknowledgements

This research was supported with funds from the PNRR, from the project: “National Center for HPC, Big Data and Quantum Computing – HPC – SPOKE 5” – CN00000013.

Corresponding author: amerigo.mendicelli @cnr.it

Local seismic effects forecast supporting risk mitigation in the Ferrara area.

L. Minarelli[1], M. Stefani[2], S. Amoroso[3-1], G. Tarabusi[1]

[1]*Istituto Nazionale di Geofisica e Vulcanologia, Italy*
[2]*University of Ferrara, Italy*
[3] *University of Chieti-Pescara, Italy*

Introduction

The history of Ferrara has been marked by many significant earthquakes, documented since 1117 (Guidoboni 1984; Locati et al. 2016; Guidoboni et al. 2018 and Guidoboni et al. 2019). The worst documented damage occurred during the 1570 earthquakes. The seismic activity was generated by reverse and, sometimes, strike-slip faults of the Apennines chain front, buried under thick Plio-Pleistocene foredeep deposits. The damage to the anthropic structures was modulated by local seismic effects, reflecting the complex stratigraphical, geophysical, and geotechnical features of the area. The subsurface architecture induced seismic wave amplification and, at sites, coseismic liquefaction of water-saturated granular sediments, as occurred in the urban area of Ferrara during the 1570 earthquakes (Guidoboni and Valensise 2023), and in adjacent areas in the year 2012 (Minarelli et al. 2022). For developing the research, over 4,000 pre-existing geophysical, stratigraphical, and geotechnical investigations were collected into a homogeneous database, and analyzed together with the new investigations we carried out, such as seismic noise measurements, seismic piezocone, and seismic dilatometer tests. Numerical modeling for the seismic response analysis was also performed.

Geology and Stratigraphy

The distribution and properties of the outcropping fluvial sediments were reconstructed through remote sensing, field investigation, and geotechnical testing. The Po channel sands (Fig. 1a), mainly Medieval in age, form elongated bodies in northern areas, whereas, in southern zones, the Reno channel silty sand and silts accumulated during the XVII century. In south-eastern areas, Roman Times Po and Reno channel bodies are sub-outcropping. The fluvial channel deposits are flanked by finely granular natural levee belts. Most of the study area consists of mainly cohesive, argillaceous sediments, accumulated into interfluvial settings (Fig. 1a). The conceptual correlation of the abundant cone penetrations tests and stratigraphic cores generated a subsurface geological model, developed throughout the wide Ferrara Municipality area, integrated, in the urban and peri-urban zone, by a lithostratigraphy 3D model, produced by automated interpolation techniques. To generate the model, synthetic lithological columns were derived from the comparison of the tip resistance and lateral friction values, interpreted according to the Roberston classes (Robertson 1990, 2009). The synthetic lithological logs and the actual stratigraphic cores were then laterally correlated, using trilinear and tricubic interpolation algorithms, to generate continuous 3D subsoil models of the first 40 m of subsurface (Fig. 1b, c).

In northern areas, the lower part of the study stratigraphic interval consists of Wuermian synglacial sands, sedimented by the river Po, which southward give way to finer grained units, mainly accumulated by Apennines rivers (Fig. 1c). Throughout the area, the synglacial units are topped by a terraced discordance surface, followed by syn-transgressive continental silty deposits, and by Holocene highstand fine grained sediments, associated with Po River channel sands and, in southern areas, with finer grained sediments of Apennines provenance. Based on the two geological models, 21 stratigraphic microzones (MOPS), homogeneous from a seismic response point of view, have been defined in the first 30 m of subsurface. The petrophysical properties of the microzones control the near surface seismic wave amplification and liquefaction hazard.

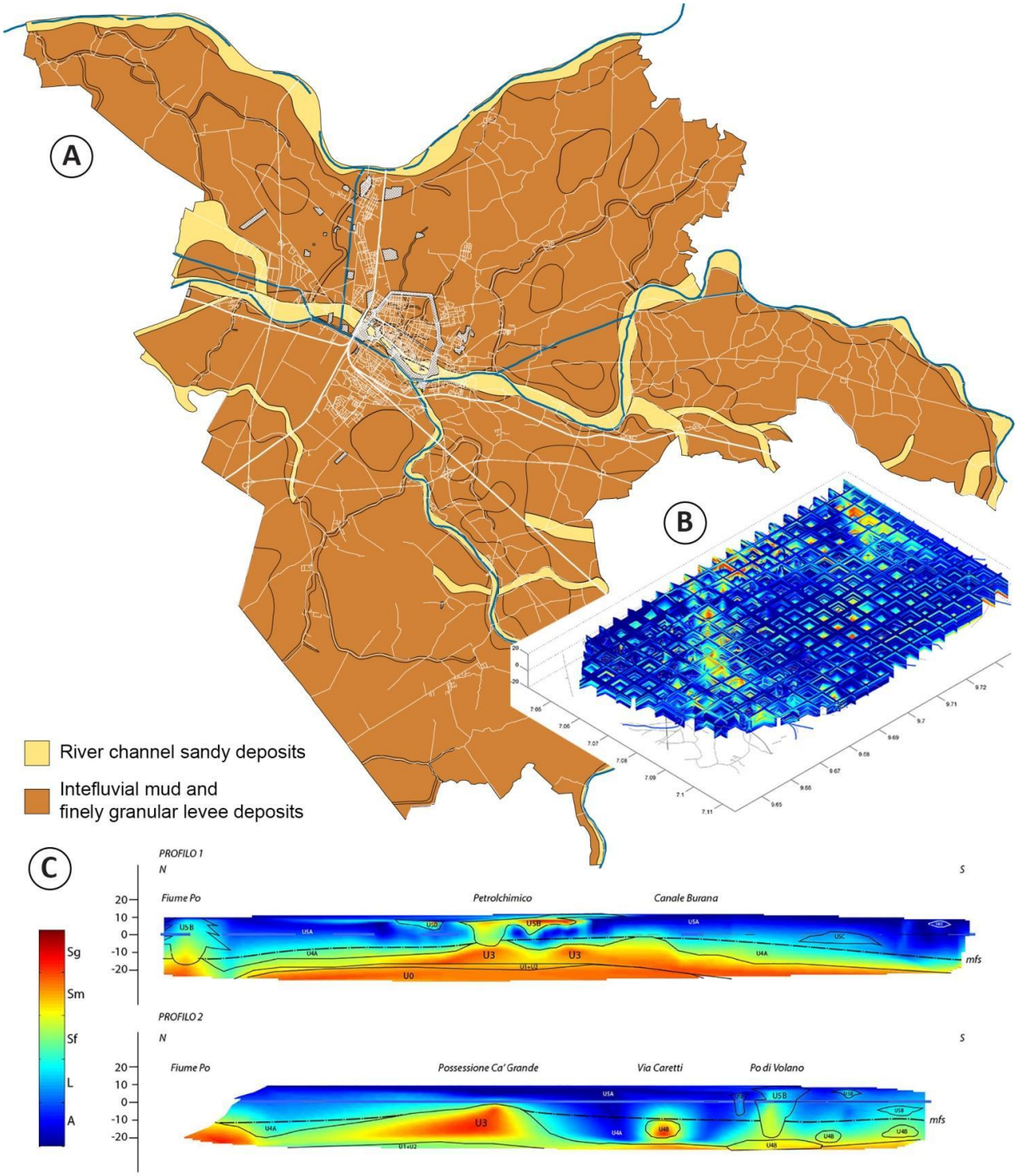

Fig. 1 – (A) Engineering-geological map of the Ferrara municipality area, the yellow ribbons depict Po and Reno channel sand bodies; (B) enclosure diagram extracted from the the 3D model of the first 40 m of the urban area subsurface, derived from the automated tricubic interpolation of more than 1000 subsurface logs; (C) N-S sections extracted from the same model, sand lithologies are depicted in red, cohesive muds in blue, late Pleistocene synglacial sands are covered by Holocene lower alluvial plain deposits.

Seismic amplification and local response

The spectral selective amplification of seismic waves shows rapid spatial variations, even within the comparatively small urban area of Ferrara, due to the complex geological architecture. The seismic bedrock, defined by rocks with S-waves speed exceeding 800 m/s, is everywhere covered by thick unlithified late Quaternary units. The bedrock rises in the

anticline area (Casaglia) to its minimum depth, at about 100 m, and largely sinks towards the subsiding southern syncline zone, where normally exceeds 300 m in depth. The deepening of the seismic substratum shifts the amplification peaks toward lower frequencies. To evaluate the forecasted acceleration at the surface, seismic microzonation studies require to input the seismic intensity, estimated on the bedrock top, with a 10% occurrence probability, over a 50-year time interval, which is provided by the Italian seismic hazard map (Meletti et al. 2006; Stucchi et al, 2011).

To evaluate the seismic motion amplification induced by the unlithified stratigraphic units overlaying the bedrocks, the amplification factor abacuses proposed by the Emilia-Romagna Region for alluvial plain areas were initially used. Two separate abacuses were applied. The "Pianura 2" abacus was used for the areas where the bedrock top is less than 150 m deep, while for the greater portion of the municipal area, with bedrock exceeding 300 m in depth, the "Pianura 3" one was applied. The amplification factors predicted by the abacuses were compared with those derived from our detailed local seismic response analyses (Fig. 2). The good match of the results supports the use of the abacuses approximation. The response analyses was performed in the anticline area and in different portions of the historic center, developed on fluvial sands or on interfluvial muds (Fig. 1, 2). We then forecasted the areal distribution of damage, according to the "synthetic damage constrained parameter" (HSM, Naso 2019), related to the forecasted site shaking, expressed in cm/s^2. The HSM values in turn support the damage estimation. Medium to severe damage is expected for the largest portion of the Municipality of Ferrara, including the whole urban area.

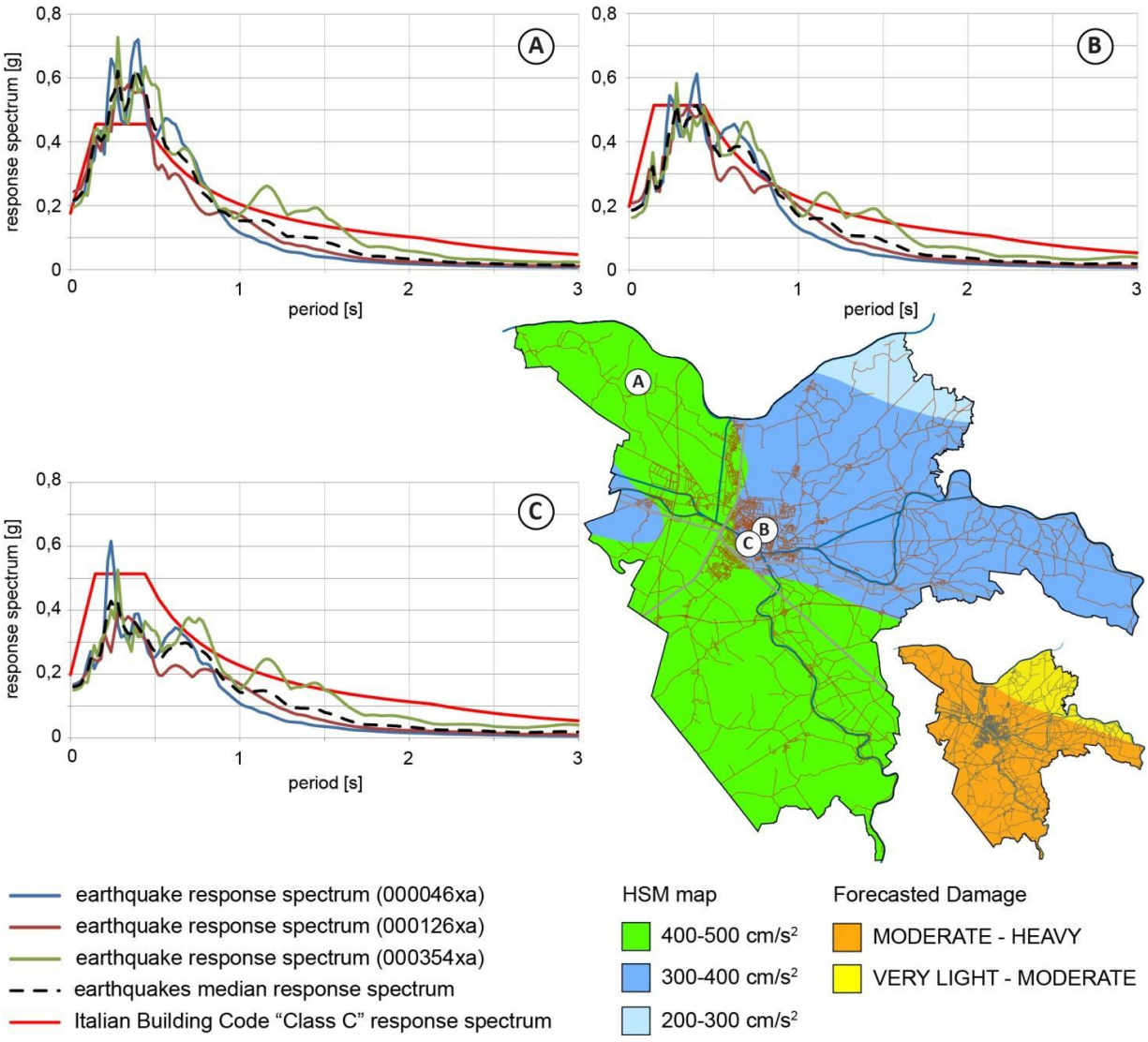

Fig. 2 – Distribution of the damage parameter expressed as acceleration in cm/s² and of the expected damage estimation: Medium-Severe damage is forecast for the urban area. Green areas indicate higher acceleration values than in the blue ones, orange zones more severe damage than the yellow ones. The three graphs illustrate the different spectrally selective amplification responses to the seismic acceleration, in the structural high area (A), and in the urban center, respectively on the Po channel sand body (B) and on interfluvial mud areas (C).

Coseismic liquefaction hazard

To evaluate the local liquefaction hazard, more than 400 punctual analyses were performed, processing cone penetration data through the Boulanger and Idriss (2014) "simplified method". Liquefaction hazard maps were then generated through the geology-based surface interpolation of the punctual estimations. The Liquefaction Potential Indexes LPI (Iwazaki et al., 1982) were subdivided into classes (Sonmez, 2003), to distinguish areas of low ($0 < LPI \leq 2$), moderate ($2 < LPI \leq 5$), and high ($5 < LPI \leq 15$) hazard. A high liquefaction susceptibility is mainly confined to the channel sand bodies deposited by the Po. The sites where the 1570 liquefaction is documented show medium to high hazard index values, validating the estimation procedure, as in the southern portion of the Medieval town and at Torre Fossa (Fig. 3). The forecasted effects of the liquefaction will be largely increased by the presence of

slopes and artificial embankments, which can trigger gravitational lateral spreading. The remaining portions of the study area are generally spared from the liquefaction hazard but are subject to seismic settlements and significant seismic amplification factors.

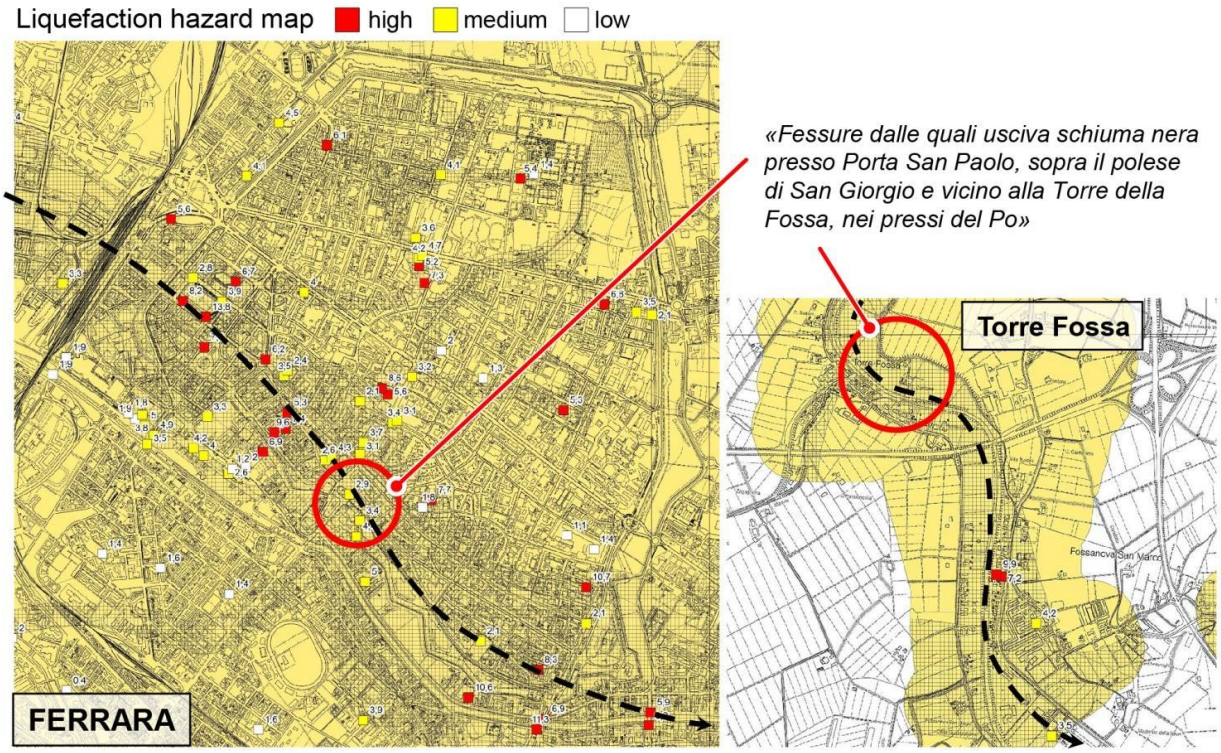

Fig. 3 – Liquefaction hazard map, red squares indicate points of high liquefaction hazard, the Po channel sands always show high or intermediate values. The circles indicate areas where liquefaction was reported in November 1570, near Castel Nuovo – Porta San Paolo and Torre Fossa. The quotation is from a manuscript describing the November 1570 earthquake (Guidoboni 1984).

Conclusions

Interdisciplinary research, integrating geological, geotechnical, geophysical, and computational geostatistics techniques, supported an accurate microzonation of the seismic hazard of the study area. Large spectral selective amplification was demonstrated, showing strong spatial variation gradients. Medium-severe damage is forecasted throughout much of the municipality area. Moderate to high liquefaction hazard characterizes the late Holocene Po channel sand bodies, on which the southern portion of the Medieval town developed. The outskirt areas built on both Po and Reno granular sediments are also subject to significant liquefaction hazard. The impact of the coseismic liquefaction will be multiplied by the lateral spreading of embankments and ridges. The remaining portions of the municipality are developed on cohesive interfluvial sediments and are therefore spared from liquefaction hazard, but still subject to significant seismic wave amplification. The research was aimed at supporting the development of appropriate urban planning and politics. The spatial distribution of the areas subject to liquefaction must be considered in the design of anti-seismic buildings and architecture restoration procedures. The increased knowledge of the risk affecting the town should prompt a massive effort to mitigate the expected damage, by improving the seismic response of both ancient and modern buildings, especially for the many of them built before the Italian seismic code implementation. Improved public

awareness should spur action to mitigate the serious risks to which both buildings and people's lives are now subject.

References

Boulanger R. W., Idriss I. M.; 2014: CPT and SPT based liquefaction triggering procedures. Report No. UCD/CGM-14/01, Center for Geotechnical Modeling, Department of Civil and Environmental Engineering, University of California, Davis, CA, 134 pp.

Guidoboni E.; 1984: Riti di calamità: terremoti a Ferrara nel 1570-74, Quaderni storici 55/ a. XIX, n. 1.

Guidoboni E., Valensise G.; 2023: *L'Italia dei Terremoti, l'Azzardo Sismico delle Città*. Vol. 2, Centro-Nord. Fondazione CNI, 668 pp.

Guidoboni E., Ferrari G., Mariotti D., Comastri A., Tarabusi G., Sgattoni G., Valensise G.; 2018: *CFTI5Med, Catalogo dei Forti Terremoti in Italia (461 a.C.-1997) e nell'area Mediterranea (760 a.C.-1500).* Istituto Nazionale di Geofisica e Vulcanologia (INGV). Guidoboni E., Ferrari G., Tarabusi G., Sgattoni G., Comastri A., Mariotti D., Ciuccarelli C., Bianchi M.G., Valensise G.; 2019: *CFTI5Med, the new release of the catalogue of strong earthquakes in Italy and in the Mediterranean area.* Scientific Data 6, Article Number: 80 (2019).

Iwasaki T., Arakawa T., Tokida K.; 1982: Simplified procedures for assessing soil liquefaction during earthquakes. Proceedings of the Conference on Soil Dynam, p. 49-58.

Locati M., Camassi R., Rovida A., Ercolani E., Bernardini F., Castelli V., Caracciolo C.H., Tertulliani A., Rossi A., Azzaro R., D'amico S., Conte S., Rochetti E.; 2016: *DBMI15, the 2015 version of the Italian Macroseismic Database*. Istituto Nazionale di Geofisica e Vulcanologia.

Meletti C., Montaldo V., Stucchi M., Martinelli F.; 2006: *Database della pericolosità sismica MPS04*. Istituto Nazionale di Geofisica e Vulcanologia (INGV).

Minarelli L, Amoroso S., Civico R., De Martini P.M., Lugli S., Martelli L., Molisso F., Rollins K.M., Salocchi A., Stefani M., Cultrera G., Milana G., Fontanta D.; 2022: *Liquefied sites of the 2012 Emilia earthquake: a comprehensive database of the geological and geotechnical features (Quaternary alluvial Po plain, Italy)*. BULLETIN OF EARTHQUAKE ENGINEERING, v. 20, p. 3659-3697.

Naso G., Martelli L., Baglione M., Bramerini F., Castenetto S., D'Intinosante V., Ercolessi G.; 2019: *Maps for land management: from geology to seismic hazard*. Boll. Geof. Teor. App. Vol. 60, n.2, June 2019, p. 277-294.

Robertson P.K.; 1990: *Soil classification using the cone penetration test*. Canadian Geotechnical Journal, 27(1), p. 151-158.

Robertson P.K.; 2009: *Interpretation of cone penetration tests — a unified approach*. Can. 34 650 Geotech. J. 46, p. 1337–1355.

Stucchi M., Meletti C., Montaldo V., Crowley H., Calvi G.M., Boschi E.; 2011: *Seismic Hazard Assessment (2003-2009) for the Italian Building Code.* Bull. Seismol. Soc. Am. 101(4), p. 1885-1911.

Sonmez H.; 2003: Modification to the liquefaction potential index and liquefaction susceptibility mapping for a liquefaction-prone area (Inegol-Turkey). Environ. Geology 44(7), p. 862-871.

Corresponding author: luca.minarelli@ingv.it

Seismic-induced Landslide Scenarios with Physically-based Models at Regional Scale

N. Monte, I. Marchesini, P. Reichenbach , M. Alviol , F. Bucci, M. Santangelo

CNR IRPI, via della Madonna Alta 126, I 06128 Perugia, Italy

The software r.slope.stability (M. Mergili et al, 2014a; M. Mergili et al, 2014b) is a tool for evaluating regional-scale slope stability (up to hundreds of square kilometers) perfectly integrated within a GIS environment (GRASS GIS – GRASS GIS Developers team, 2024). This software considers multiple potential sliding surfaces, three-dimensional in nature (more precisely, 2.5D), approximated by portions of ellipsoids or truncated ellipsoids. It also relies on the characterization of key geotechnical features of materials and layers used to describe variations in mechanical properties with depth. It employs a limit equilibrium approach and the Mohr-Coulomb criterion to assess the stability factor or, considering uncertainty in input parameters, to define a landslide susceptibility.

The software is freely accessible (https://www.slopestability.org) and constantly evolving. Recently, thanks to collaborations between CNR IRPI and Mundialis GmbH & Co. and the significant contribution of the University of GRAZ, it has been enriched with new functionalities aimed at evaluating the propensity of the territory to experience landslides under the influence of seismic forces (Mergili, M., 2014-2021). The seismic input is integrated via pseudo-static analysis, where seismic forces are directly included in the calculation of destabilizing and resisting forces, utilizing peak ground acceleration and a seismic coefficient. A Newmark approach is also applicable when the hipocenter of the earthquake is known or supposed.

This contribution outlines the software's characteristics and presents preliminary results of its expedited application over an area covering almost the entire region of Molise.

Reference

Mergili, M., 2014-2021. r.slope.stability - The slope stability model. https://www.slopestability.org

GRASS Development Team 2024. Geographic Resources Analysis Support System (GRASS GIS) Software, Version 8.3 https://grass.osgeo.org

Corresponding author: nunzia.monte@irpi.cnr.it

Towards a multi-risk deterministic scenario in the Mt. Etna area

V. Pessina[1], F. Meroni[1], E. Varini[2], M. Longoni[1], R. Rotondi[2], S. D'Amico[3], A. Cappello[3] e Panacea Group*

[1] Istituto Nazionale di Geofisica e Vulcanologia – INGV, Milan, Italy
[2] CNR Istituto di Matematica Applicata e Tecnologie Informatiche "Enrico Magenes", Milan, Italy
[3] Istituto Nazionale di Geofisica e Vulcanologia – INGV, Catania, Italy

* *A full list of authors appears at the end of the abstract*

1. Multi-risk analysis in the Panacea project

Etna (Sicily, Italy) is an active volcano characterized by effusive and explosive eruptions, often accompanied by intense seismic activity. Its densely urbanized territory on the eastern flanks can suffer severe impacts due to lava flows, earthquakes, and tephra, while pyroclastic flows only affect the summit area of the volcano.
As part of the Panacea project (Probabilistic AssessmeNt of volCano-related multi-hazard and multi-risk at Mount EtnA), seismic and volcanic hazard scenarios were generated; consequently risk scenarios for built-up places, lifelines and communication systems were assessed at very different scales, from local to sub-regional. In general, in case of a multi-risk project, it is necessary to identify the elements exposed to the volcano's effects, assess their vulnerability to each different hazard and proceed to complex risk analyses (Meroni et al., 2022, Pessina et al., 2022).
Mt. Etna's hazard studies provided interesting insights (Del Negro et al., 2019) but it is the first time that a multi-risk analysis has been carried out in the area. For this reason, in this study the analyses have been limited to the estimation of direct losses (in terms of structural damage, victims, and loss of functionality) and more complex risk analyses, such as multi-risk and cascade assessments, have not yet been taken into consideration.

2. The hazard scenarios

During the three years of the project, deterministic damage scenarios were created for the calibration and development of damage estimation methods. In this short note, we present

the risk results for 6 municipalities in the Etna area (Milo, Giarre, Riposto, Santa Venerina, Zafferana Etnea, Acireale) for a hypothetical reference scenario.

Two days after the Etna eruption of 24 December 2018 (Alparone et al., 2020), a strong earthquake (M_W 5.0) hit the lower south-eastern flank of the volcano, causing extensive damage in the area between the municipalities of Acireale and Zafferana, with over 1,100 homeless (Pessina et. Al, 2021). It represents the largest event occurred in the area in the last 70 years.

The flank eruption at the volcano started with an intense degassing from the summit craters, an opening of eruptive fissure with a lava flow that ended on December 27.

The (hypothetical) Tephra and Lava scenarios were generated assuming that the 2018 eruption was not interrupted, and significant values of input parameters were assumed in the simulation process to create realistic scenarios of lava invasion and ash ground loads, which are sufficiently important to cause damage to buildings and infrastructure. Fig. 1 shows the seismic scenario of December 26th 2018, and hypothetical scenarios for lava and tephra loads. More comprehensive studies are being published (Sandri et al.)

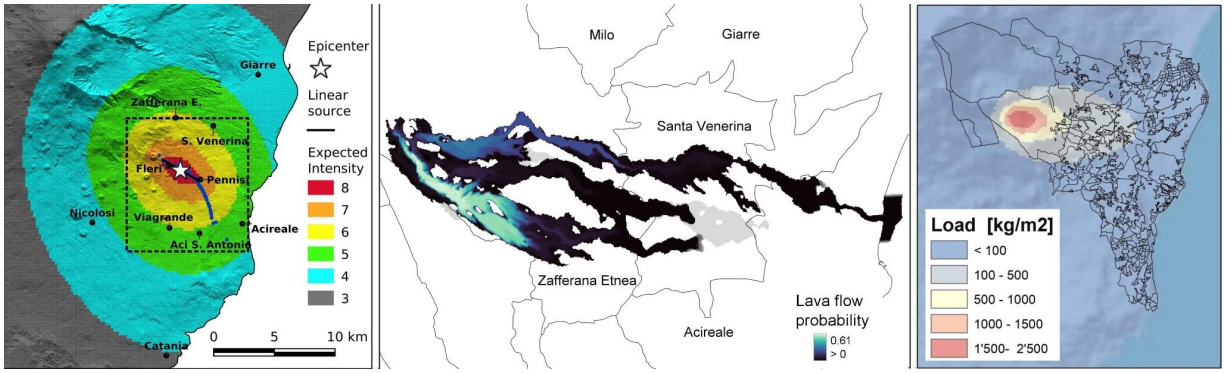

Fig.1 – From left to right: seismic scenario, represented in terms of EMS-98 Intensity, for the December 26, 2018 earthquake, and hypothetical scenarios for lava flow and tephra loads.

3. The risk scenarios

Damage assessment was calculated for residential buildings. Using data collected by the Italian Institute of Statistics (ISTAT, 2011), that are updated and spatially detailed, residential buildings were classified as masonry, reinforced concrete (RC) and other construction type, according to the method illustrated in Dolce et al. (2021). For the assessment of the seismic vulnerability and damage we used the model of Lagomarsino et al. (2021) for masonry buildings and that of Rosti et al. (2021) for RC ones.

Since the new models use both pga values, it was necessary to develop an ad hoc conversion relationship between EMS98 intensity and pga, for this type of event of volcanic origin in the Etna area. The new conversion relationship is the following:

$$\log_{10}(pga) = 0.346\ I_{EMS\text{-}98} - 0.190$$

With reference to the definition of the 5 damage levels of the EMS-98 scale (Grünthal, 1998), Fig. 2a shows the number of heavy damaged buildings (damage level (D4 + D5) in each census tract).

Through remote sensing analysis, the project's colleagues estimated the percentage of pitched and flat terrace roofs of the buildings. These distributions, together with the analysis of AeDes data for the identification of building types and their vulnerability, made it possible to identify the distribution of roofs in four vulnerability classes (Spence et al., 2005). The distribution of buildings with total collapse of the roof due to tephra load – if no cleanup action is taken- is shown in Fig 2c, but it is necessary to highlight the very low probability to have such a level of loads.

In case of lava flow hazard, the level of risk is independent of the vulnerability of the buildings. For each ISTAT census section, the number of buildings damaged by lava is calculated proportionally to the percentage of the section's area occupied by the flow (Fig. 2b).

Once assessed the damage level of the buildings, the totally collapsed buildings, the unusable one, the number of the possible victims or of homeless are calculated in each census section.

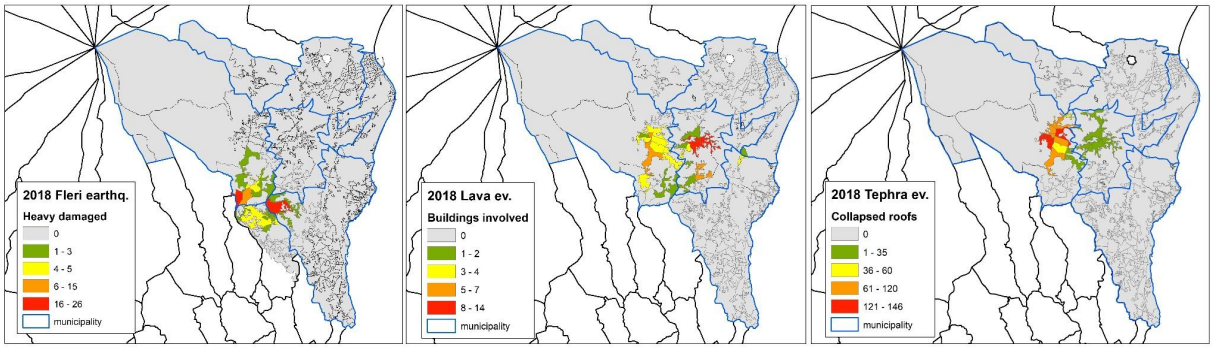

Fig.2 – Damage map of residential buildings due to the earthquake, lava and tephra flows scenarios.

Damage scenarios due to ash loads, lava flows and earthquakes have been estimated to road and power systems, too. Tab. 1 illustrates damage to the power system (pylons, medium voltage (MV) and high voltage (HV) substations and transformers) reach by lava flow with different probability of invasion, as well as the length of invaded road and number of affected buildings.

Tab. 1 – Damage due to the 2018 lava flow scenario

POWER SYSTEM	Road system	Residential

Probability	Pylons	Power MV	Power HV	Transformer	[km]	buildings
0.000358	15	52	1	10	23.82	737
0.005	2	10	-	1	6.27	181
0.01	4	23	-	2	12.61	596
0.025	3	20	-	4	15.69	639
0.05	2	3	-	3	5.37	148
0.1	4	14	-	1	8.31	205
0.3	0	4	-	-	0.74	1
0.5	1	1	-	-	0.79	2
Tot	31	127	1	21	73.6	2509

4. Conclusions

High-impact deterministic scenarios were generated to test the models to be applied for the seismic and volcanic risk of buildings (residential and strategic) and lifelines (electricity grid, roads, etc.) in the Etna area.This exercise, among other things, led to the implementation of a PGA-intensity conversion relationship for Etna earthquakes, as well as the characterization of roof vulnerability in the study area.

Apart from earthquake, expected damage from tephra and lava flow are unlikely to reach high level of damage(D4 and D5). Anyway the interruption of services and other inconveniences are foreseeable at lower damage levels (D2 and D3).

Due to the characteristics of Mount Etna eruptions, lava flow (which are slow) or ash accumulation does not generate victims. Instead, it is possible to find an interdependence on risk scenarios: even a thickness of a few centimetres of ash can make roads dangerous or even just unusable, making rescue operations difficult in the event of an earthquake or in the event of a fire triggered by the eruption.

Thanks to a probabilistic estimate of the expected damage, still in progress, it will be possible to quantify the influence of seismic hazard, lava flow and tephra accumulation in appropriate exposure times.

Acknowledgements

This work was carried out within the PANACEA project that benefited from funding provided by the MIUR (Minitero Istruzione Università e della Ricerca) - Decreto MIUR 1118 del 04/12/2019, within the Pianeta Dinamico project.

References

Alparone, S., Barberi, G., Giampiccolo, E.,Maiolino, V., Mostaccio, A., Musumeci, C., et al.; 2020: Seismological constraints on the 2018 Mt. Etna (Italy) flank eruption and implications for the flank dynamics of the volcano. Terranova 32, 334–344. doi: 10.1111/ter.12463

Del Negro C., Cappello A., Bilotta G., Gangi G., Hérault A., Zago V.; 2019: *Living at the edge of an active volcano: Risk from lava flows on Mt. Etna.* GSA Bulletin; Month/Month 2019; 0; p. 1–11; https://doi.org/10.1130/B35290.1

Dolce, M., Prota, A., Borzi, B., da Porto, F., Lagomarsino, S., Magenes, G., Moroni, C., Penna, A., Polese, M., Speranza, E., Verderame, G. M., Zuccaro, G.; 2021: *Seismic risk assessment of residential buildings in Italy*. Bull Earthquake Eng 19, 2999–3032, https://doi.org/10.1007/s10518-020-01009-5

Grünthal, G.; 1998: *European macroseismic scale 1998 (EMS-98)*. In: Cahiers du Centre Européen de Géodynamique et de Séismologie, Vol. 15. Luxembourg: Conseil de l'Europe

ISTAT (2011) 15° Censimento generale della popolazione e abitazioni.Retrieved February, 2022, from http://dati-censimentopopolazione.istat.it/Index.aspx?lang=it

Lagomarsino S., Cattari S., Ottonelli D.; 2021: *The heuristic vulnerability model: fragility curves for masonry buildings*. Bull Earthquake Eng 19, 3129–3163. https://doi.org/10.1007/s10518-021-01063-7

Meroni F., Pessina V., Azzaro R., D'Amico S., Scollo S.; 2022: *From seismic damage assessment to a risk volcanic scenarios in the area of Mount Etna (Sicily)*. 2nd Int. Conf. on Urban Risk, 30 june-2 July, Lisbon

Pessina V., Meroni F., Azzaro R., D'Amico S.; 2021: *Applying simulated seismic damage scenarios in the volcanic region of Mount Etna (Sicily): a case-study from the MW 4.9, 2018 earthquake*. Front. Earth Sci. 9:629184. doi: 10.3389/feart.2021.629184 https://www.frontiersin.or g/articles/10.3389/feart.2021.629184/full

Pessina, V., Garcia, A., Meroni, M., Sandri, L., Selva, J., Azzaro, R., Bevilacqua, A., Bilotta, G., Branca, S., Coltelli, M., D'Amico, S., de' Michieli Vitturi, M., Esposti Ongaro, T., Ganci, G., Mereu, L., Scollo S., and Cappello, A.; 2022: *From multi-hazard to multi-risk at Mount*

Etna: approaches and strategies of the PANACEA project, 3rd Int. Workshop on Natural Hazards, 26-27 May, Terceira Island, Azores, 6 pp

Rosti A., Del Gaudio C., Rota M., Ricci P., Di Ludovico M., Penna A., Verderame G.M.; 2021: *Empirical fragility curves for Italian residential RC buildings*. Bull Earthquake Eng 19, 3165–3183, https://doi.org/10.1007/s10518-020-00971-4

Sandri L. , Garcia A., Proietti C., Branca S., Ganci G., Cappello A.; :*Where will the next flank eruption at Etna occur? An updated spatial probabilistic assessment*. Preprint (on Discussion) https://doi.org/10.5194/egusphere-2023-2624

Spence R., Kelman I., Petrazzuoli S., Zuccaro G.; 2005: *Residential Buildings and Occupant Vulnerability to Tephra Fall.* Nat. Hazards Earth Syst. Sci. Eu.Geosciences Union, 1–18.

PANACEA GROUP

Azzaro R., Bilotta G., de' Michieli Vitturi M., Esposti Ongaro T., Ganci G., Garcia A., Mereu L., Sandri L., Scollo S., Tuvé T., Zuccarello F.

Corresponding author: vera.pessina@ingv.it

SISMIKO: the operational task force for seismic networks rapid deployments and integration in the INGV monitoring system.

D. Piccinini[1], E. D'Alema[1], S. Marzorati[1], M. Moretti[1], L. Margheriti[1] and SISMIKO Group

[1] *Istituto Nazionale di Geofisica e Vulcanologia (Italia)*

SISMIKO is the operational group within the Istituto Nazionale di Geofisica e Vulcanologia responsible for deploying a temporary seismic network as a rapid response to significant seismic events [Moretti et al., 2023; https://sismiko.ingv.it/]. The purpose of the temporary seismic network is to complement the RSNi (Rete Sismica Nazionale integrata) by reducing the inter-station distances of permanent stations, where necessary. SISMIKO has a distributed structure across various INGV headquarters nationwide and in recent years has equipped itself with a consistent set of around 50 seismo-accelerometric stations and an autonomous acquisition system. This system makes the acquired data available, without restrictions, to the entire scientific community through the Italy node of the European Integrated Data Archive (EIDA [Danecek et al., 2021]) portal, ensuring a high level of data quality.

To ensure a rapid response following an earthquake and rapid integration of data collected by emergency stations, a codified procedure has been established. Through this procedure, the metadata of each station is pre-configured and the data flow coming from these stations is collected within an acquisition system [D'Alema et al., 2022]. This setting allows the rapid use, if necessary, of the data obtained by SISMIKO - after a quality control - by the seismologists on duty at the INGV Operations Room [Margheriti et al., 2021].

Today, over 100 INGV personnel join SISMIKO group: technicians, technologists and researchers from each of the headquarters distributed across the national territory. A new configuration in Activity Groups allows to coordinate the distributed personnel and to cover all the aspects in the preparation of the emergency such as the technical management of the instrumentation, the field operations, to maintain contacts with the INGV Crisis Unit and the other Operational Groups and to develop automatic procedures to analyse real time seismic data (Fig 1).

Besides the operational aspects, in recent years SISMIKO has promoted the recovery of continuous data recorded by temporary seismic stations installed during past seismic sequences such as in L'Aquila 2009, Po Plain 2012 and Central Italy 2016. By reconstructing the complete station's metadata, it is now possible to distribute the data to the scientific community through the EIDA portal.

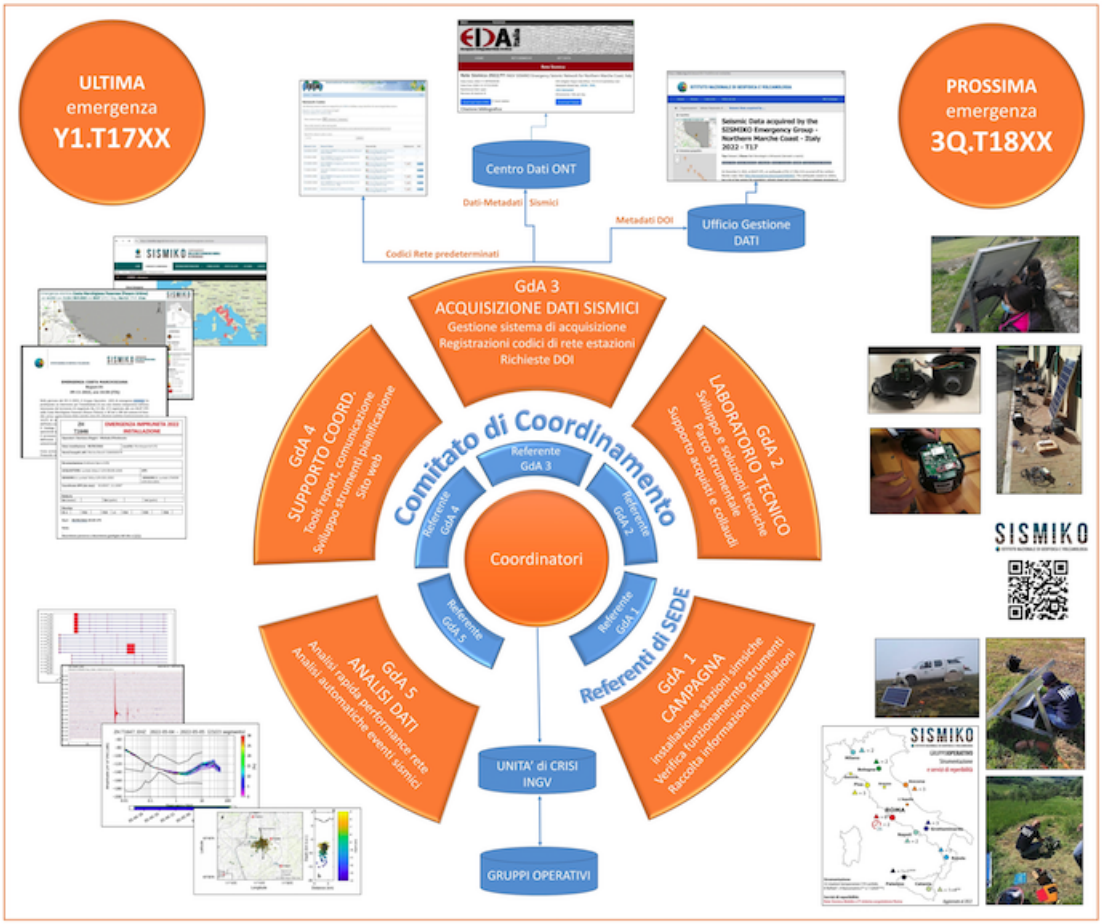

Fig. 1. Schematic representation of the current structure and activities of the SISMIKO Operational Group.

References

D'Alema E., Giunchi C., Marzorati S., Piccinini D., Moretti M.; 2022: SISMIKO: il nuovo sistema di acquisizione dati sismici in tempo reale. Rapp. Tec. INGV, 445: 1-126, https://doi.org/10.13127/rpt/445.

Margheriti, L., et al.; 2021: Seismic Surveillance and Earthquake Monitoring in Italy. Seismological Research Letters. 2021; 92 (3): 1659–1671. doi: https://doi.org/10.1785/0220200380.

Moretti M., Margheriti L., D'Alema E. and Piccinini D.; 2023: SISMIKO: INGV operational task force for rapid deployment of seismic network during earthquake emergencies. Front. Earth Sci. 11:1146579. doi: 10.3389/feart.2023.1146579.

Danecek, D., Pintore, S., Mazza, S., Mandiello, A., Fares, M., Carluccio, I., et al.; 2021: The Italian Node of the European Integrated Data Archive. Seismological Research Letters 92 (3): 1726–1737. doi: https://doi.org/10.1785/0220200409.

Corresponding author: davide.piccinini@ingv.it

Software applications for multi-level safety management of healthcare facilities network

Sandoli[1,2], D. Gargaro[3], D. Gentile[4], M. A. Notarangelo[3], G. Fabbrocino[1,2]

[1] University of Molise, Dept. of Biosciences and Territory, Campobasso, Italy
[2] Institute for Construction Technologies ITC-CNR, National Research Council, L'Aquila, Italy
[3] S2X S.r.l., Campobasso, Italy
[4] University of Molise, Dept. of Medicine and Health Sciences, Campobasso, Italy

Introduction

Earthquakes occurred worldwide demonstrated that hospital infrastructures have often experienced significant damage to structural and non-structural components, producing difficulties during the post-event emergency management phases and economic losses [1]. Collapses or severe damage of hospitals in a given area have had tremendous consequences on both injured peoples, which need immediate medical attention, and patients in the hospitals, thus reducing the resilience of the communities. This phenomenon is particularly felt in the so called Inner or Peripheric Areas, where the health infrastructure network is composed with few hospitals often not well interconnected among them, making difficult the emergency management.

In this framework, it appears evident the needs of identifying safety management strategies of the health infrastructure network, based on multi-level approach, i.e. involving management strategies from large scale (Regional or sub-Regional) up to single-scale building approach. On the other hand, it is also true that the management of healthcare facilities engages a transversal concept of safety which must be regarded at different levels: it involves the safety of structural and non-structural elements under severe and moderate seismic events and that of workers in workplaces in the sense of the Italian Legislative Decree n.81 released in 2008 [2]. The LD81/08 supplies general measures aimed at protecting the safety and the health of workers in workplaces, valid for all private and public activity sectors and for all types of risk [3]. These measures - of primary importance for developing a complete framework for seismic risk assessment of health services in the post-event and for strategizing risk mitigation plans - should be conveniently implemented in probabilistic safety assessment methods. This paper presents an operational framework supported by software applications aimed at approaching from an engineering perspective the management of the occupational health and safety in critical infrastructures [4]. Attention herein is focussed on the multi-level safety management of health services network. The first part is devoted to data collection regarding safety assessment of workers conditions in the workplace, while the second part is devoted at performing Probabilistic Structural Safety Assessment (PSSA) of health facilities with an integrated approach at different scales.

Definition of a comprehensive framework for occupational safety and health management

Safety management of existing health facility structures represents a complex task, because involving the “container” (i.e., structural and non-structural components) and the “content” i.e., safety of workers in workplaces as defined by the LD 81/08. In this regard, a general multi-scale framework to support the safety management of the health facility structures is proposed in Fig. 1, discussed in the following. With the term “multi-level” is here intended scalable datasets and procedures oriented to safety assessment at different levels of deepening. The scales can be substantially organized in three different macro-levels: large- (Level 1), medium- (Level 2) and single-scale buildings (Level 3). The large-scale evaluations involve the safety assessment of a network of heath facility structures located in a given area whose extension coincides with Regional of sub-Regional boundaries; medium scale concerns a group of building constituting the hospital campus, while a single-scale refers to single building belonging to the health facility.

For safety management purposes involving the Levels 1 and 2, data can be conveniently collected in remote through web-based crowd-sourcing technologies, eventually complemented with data coming from on-site surveys. In the case of the Level 3, on-site inspections - eventually integrated with data coming from structural health monitoring - are necessary to collect structural-typological information and details regarding the building characteristics. In addition, on-site inspections to collect data regarding the condition of workers on workplaces are necessary.

Once the data are collected, different procedures of data treatment can be adopted depending on the scale level required to conduct safety assessment. Less detailed data in the case of procedures involving probabilistic-based structural safety evaluations at large and medium scale are required, while more detailed information in the case of single-scale building are necessary (both from structural and safety on workplace point of view). Data, collected and filtered as a function of the considered scale-level, represent the input for implementing multi-level safety assessment methodologies, the latter chosen among those available in literature. As a result, a baseline for defining risk mitigation strategies against natural events of health facilities network is obtained. Note that, data collection, data treatment and safety assessment are procedures which can be by automated through digital tools, facilitating the multi-level management phases of the infrastructure network from the Authorities both in case of emergency or in to plan mitigation strategies.

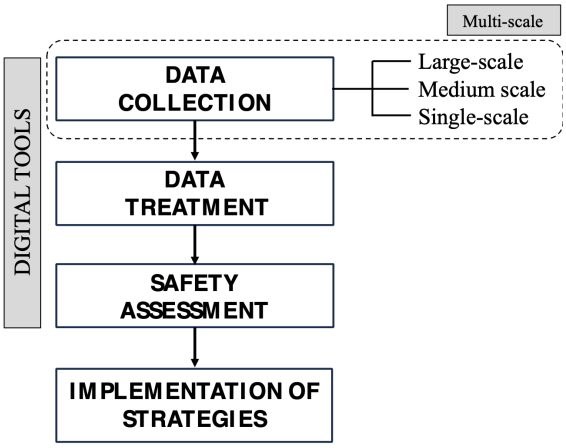

Fig. 1 – Multi-level framework for safety management of health facilities structures

Digital tools for safety assessment and management

In this paper two software devoted to support the implementation of safety management strategies of health facility structures are presented. The software are named as follows:

HF-INSPECT, allows on-site data collection regarding (i) risks related to safety of workers in workplaces as defined by the LD81/08 (electric, biologic attacks, fire, etc.) and (ii) structural typological characteristics of buildings (material-type, age of construction, structural details).

HF-ALL RISKS, enables a comprehensive PSSA of the health facilities (i.e., referred to a network of structures or to single buildings). Data to be included in the software can be collected through web-mapping procedures, eventually combined with on-site surveys.

HF- INSPECT includes a digital form to support on site census activity. Data collection regards: (i) information on personnel working inside the structure, (ii) metric data (i.e. plan and sections) of the structure and their use destination, (iii) layout of the installations, (iv) list of electromedical devices, (v) identification of the risks affecting the specific working place according to LD81/08 (Fig. 2). This survey activity is integrated with interviews to medical personnel operating in the structure. Moreover, HF-INSPECT includes a specific layout called as “structural form” which allows to collect data related to safety and operational conditions of the structure. In particular, the form allows to upload data relative to age of construction, structural characteristics, type of soil, presence of structural interventions and seismological data. Information relative to structural characteristics are of paramount importance to implement PSSA analysis and they are directly interconnected with the HF-ALL RISKS software.

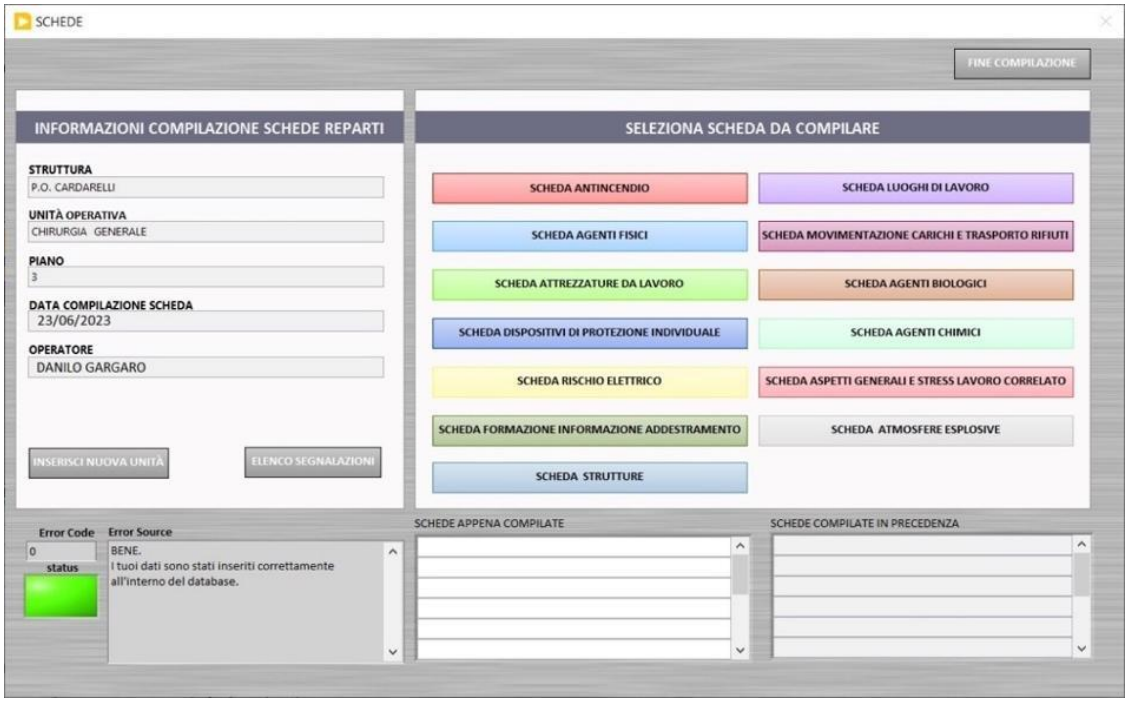

Fig. 2 – HF-INSPECT software

HF-ALL RISKS generates multi-scale PSSA of health facility structures using the Typological Fragility Matrices (TFM) [5]. Typically, such type of analysis is conducted by developing typological fragility curves, which provide the exceedance probability of a Limit State threshold associated with conventional earthquakes conditioned to an IM parameter described through peak-ground, spectral or macroseismic parameters. Instead, TFM computes the exceedance probability using a vectorial form of the IM, for instance composed by magnitude M and distance R, leading to a three-dimensional representation of the fragility (Fig. 3). The change of variable from a single peak-ground/spectral or macroseismic

parameter to (M-R) is obtained by disaggregating the ground motion through Ground Motion Prediction Equations (GMPE). To develop the software, the GMPE provided by Bindi et al. 2011 [6] was used, which consider the magnitude of the event, the epicentral distance, type of soil and type of fault.

The software allows to estimate the PSSA based on the three fundamental steps: a) structural-typological classification of the building classes, b) computation of fragility, c) definition of a safety threshold defining a demand-to-capacity ratio.

As far as the building classes is concerned, each analysed hospital structure is associated to a structural-typological building class. Basically, within the software, the five classes of masonry buildings and the four classes of reinforced concrete ones defined in [7] have been considered, but they can be also changed with other building classes available in the literature. The association to the building class is based on the information available in HF-INSPECT integrated with web-mapping cataloguing procedures. For each building class, the software estimates the TFM computing the Cumulative Density Function (CDF), as follows [5]:

$$CDF = P\left[PGA^{-}\right] = \int_{0}^{PGA^{-}} f(im)dim = \int_{0}^{PGA(M,R)} f(im)dim$$

where PGA is the peak-ground acceleration threshold, M the magnitude of the event, R the epicentral distance, LS the Limit State considered for the structure (in this case the Ultimate Limit State). By cutting the TFM with a M-CDF or R-CDF plane the corresponding fragility curves are also provided by the software. Moreover, the report of the conducted analysis can be downloaded in *.pdf* format. Finally, by selecting a set of earthquake scenarios in terms of (M, R), for instance those provided by the Probabilistic Seismic Hazard Analysis (PSHA) or with reference to an earthquake occurred at a given epicentral distance between with respect a hospital infrastructure and characterized with a given magnitude, the probabilistic structural safety level of the investigated structure can be identified.

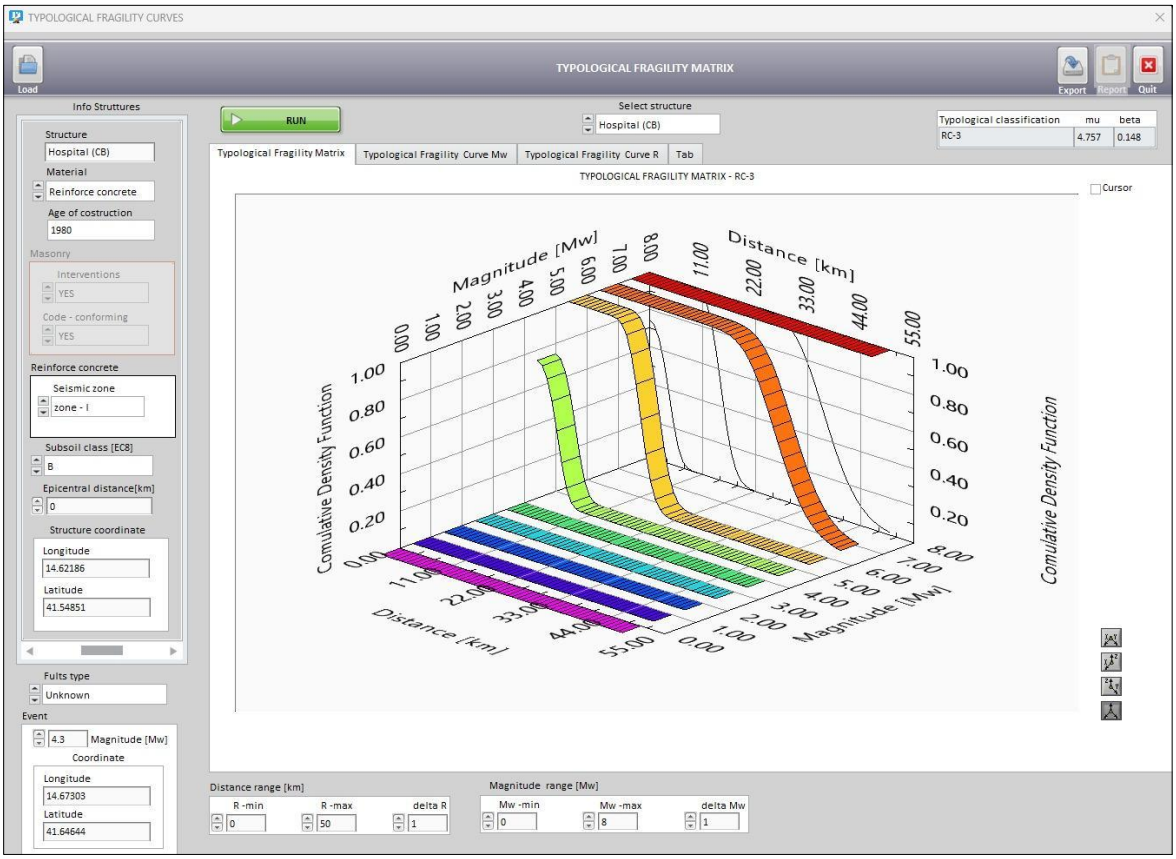

Fig. 3 – HF-ALL RISKS software (the figure illustrates the TFM for the hospital of Campobasso)

Acknowledgements. This study received financial support by research project PON CADS 2020–2023 (Creating a safe home environment) promoted by the Italian Ministry of University and Research.

References

[1] Miranda E, Taghavi S. 2003. Estimation of seismic demands on acceleration-sensitive nonstructural components in critical facilities, Proc. of the seminar on seismic design, performance, and retrofit of non- structural component in critical facilities, ATC 29-2, Newport Beach.

[2] Legislative Decree LD 81/08 – Ministry of work. DL 9 Aprile 2008 n. 81. Testo unico sulla salute e sicurezza sul lavoro. Gazzetta ufficiale n. 101 del 30 aprile 2008- suppl. ordinario n. 108.

[3] Notarangelo MA, Rainieri C, Fabbrocino G. 2016. Strumenti informatici integrati per le indagini conoscitive finalizzate alla valutazione dei rischi sul logo di lavoro in strutture sanitarie e presidi ospedalieri. Proc. of Conf. Proc of the Conf Valutazione e Gestione del Rischio negli Insediamenti Civili ed Industriali VGR 2016. Rome, Italy, 13-15 September 2016.

[4] Ghasemi F, Doosti-irani A, Aghaei H. 2023. Applications, Shortcomings, and new advances of job safety analysis (JSA): findings from a systematic review. Safety and Health at Work 14, 153-162.

[5] Sandoli A, Lignola GP, Prota A, Fabbrocino G. 2023. Seismic fragility assessment of inner peripheries of Italy through crowd-sourcing technologies. Buildings, 13(2), 562.

[6] Bindi D, Pacor F, Luzi L, Puglia R, Massa M, Ameri G, Paolucci R. 2011. Ground motion prediction equations derived from the Italian strong motion database. Bull of Earth Eng 9, 1899-1920.

[7] Sandoli A, Lignola, GP, Calderoni B.; Prota, A. 2021. Fragility curves for Italian URM buildings based on a hybrid method. Bull Earth Eng 19, 4979–5013.

Corresponding author: antonio.sandoli@unimol.it

Capturing spatial variability of empirical site amplification functions δS2S: a case-study in Central Italy

S. Sgobba[1], C. Felicetta[1], G. Lanzano[1], F. Pacor[1] , T. Bortolotti[2], A. Menafoglio[2]

1. *Istituto Nazionale di Geofisica e Vulcanologia, INGV (Milan, Italy)*
2. *MOX, Department of Mathematics, Politecnico di Milano (Milan, Italy)*

Among the techniques for predicting seismic shaking for damage scenarios or regional hazard and risk assessment, the empirical methods based on the use of a ground motion model (GMM) are probably the most rapid and widespread. However, to produce the estimates at ground-level, we need a key-proxy to describe the effect of the local site response, which is usually represented by the shear wave velocity in the first 30 m depth (Vs30) from in situ geophysical measurements or inferred from other proxies (geology, topography, etc.). Although Vs30 has the advantage of being a synthetic predictor, on the other hand it has been shown that it is not truly representative of site response (Castellaro et al., 2008; Luzi et al., 2011; Bergamo et al., 2021), thus, alternative site proxies called site-to-site terms (δS2S) are being explored; they represent systematic deviations of observed amplification at a site from the median values predicted by a partial or fully non-ergodic GMM calibrated on a set of reference rock sites (Lanzano et al., 2022; Kotha et al., 2020). To date δS2S can be considered the most reliable representation of empirical site response if estimated from a sufficient number of site-specific ground-motion observations (Bard et al., 2020; Loviknes et al., 2021).

To increase the use of δS2S for site characterization studies, there is a need to map this parameter at locations in space that lack direct observations. Geostatistical methods, such as the simple Kriging technique, are commonly used for this purpose, but limitations arise in less densely sampled areas or in complex regions (e.g. characterized by the presence of different geological and tectonic structures, alluvial basins, mountain chains, etc. within a few kilometers) due to a too coarse interpolation.

To address this issue, we explore the statistical correlations of δS2S in terms of PGA and elastic spectral acceleration (SA) up to 2s, with other mappable site proxies, in order to calibrate a parametric model capable of constraining the spatial predictions to other proxies or geological/lithological information that are available in the area. In our case the proxies are: Vs30 measurements, high-frequency attenuation decay parameter κ0 (Anderson and Hough, 1984), topographic slope from the Tinitaly DEM at 40m (Mascandola et al., 2021) and local descriptions of the litho-stratigraphic units of the region from large-scale maps (i.e. the

chart of ISPRA 1:100.000 and the classification provided by Forte et al., 2019). On the basis of the resulting correlations, we construct a geostatistical methodology to model the spatial dependencies observed in the site terms, testing both the spatial stationary and non-stationary hypotheses; for the latter, we apply the Universal Kriging technique that captures the local variability and allows us to produce high-resolution maps of δS2S that are constrained to other parameters; i.e. the Vs30 data and the other site-related proxies.

The need for dense information in the region and low-uncertain estimates of ground motion parameters, motivates the choice of central Italy as a case-study area. In this region, in fact, we dispose of a very high number of seismic events recorded in the last 20 years (more than 30.000 records of events with magnitude ranging from 3.2 and 6.5) and the calibration of specific regional GMMs in a completely non-ergodic framework (Sgobba et al., 2021; Sgobba et al., 2023).

Key-findings

- The statistical correlation analysis shows that the δS2S estimates at different spectral periods are mostly correlated with Vs30 measurements, especially at longer periods (from about 0.3s), while are less dependent on the other investigated proxies (κ0, slope, lithology, etc.);
- The best model of δS2S (**Figure 1**) is obtained with a non-stationary parametrization based on geographical coordinates (x, y) and a combined Vs30-map *ad-hoc* developed for the study . The parametric functional form (the same for all spectral parameters) is the following: $\delta S2S \sim \beta0 + \beta1x + \beta2\ y + \beta3\ (x*y) + \beta4\ (Vs30\text{-}map)$ + model error.

  Note that the Vs30-map was constructed by combining the dataset of observations and estimates inferred from the topographic slope (Vs30-WA), according to Wald and Allen's global empirical relationship (Wald and Allen, 2007), and the Italian map (Vs30-Mori) provided by Mori et al. (Mori et al., 2020); indeed, we observed that neither Vs30-WA nor Vs30-Mori alone were able to capture the full range of variability of Vs30 observations;

- Non-stationary spatial models including lithology were also tested but they are not able to significantly improve the predictions of δS2S, suggesting that the current lithological classification or resolution may not be useful for constructing spatial models of the investigated parameters;
- The final optimal model is able to capture the main trend of the empirical site response in central Italy, but it shows some limitations in reproducing the full range of local amplifications and the observed variability between different frequencies, suggesting that additional key-proxies are needed, such as the fundamental frequency of soil deposit f0, the sediment thickness, as well as alternative maps of geo-lithological complexes.

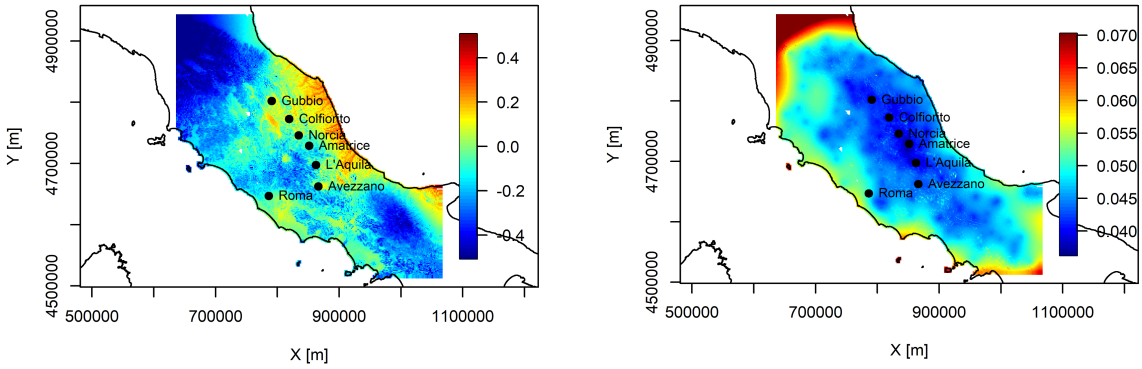

a) **b)**

Figure 1. Maps (coordinate system UTM zone N32) of the best δS2S model: median predictions (log10 units) (a) and associated variance (b) for PGA.

Acknowledgements

This work was partially supported by the Italian Ministry of University and Research (MIUR) in the framework of the project PRIN-SERENA, coordinated by Prof. Dario Albarello of the University of Siena and by the Centrum of Seismic Hazard (CPS, INGV) within the WP4 - Shaking Scenarios. The authors wish to thank the Working Group of Work Package 06 “Empirical Testing and Calibration” and their coordinator Giovanna Cultrera of INGV-Roma.

References

Anderson, J., Hough, S. (1984). *A model for the shape of the Fourier amplitude spectrum at high frequencies.* Bulletin of the Seismological Society of America. 74. 1969-1993.

Bard P. Y. Bora S. S. Hollender F. Laurendeau A., and Traversa P. (2020). *Are the standard Vs30-kappa host-to-target adjustments the only way to get consistent hard-rock ground motion prediction?* Pure Appl. Geophys. 177, 2049–2068.

Bergamo, P., C. Hammer, and D. Fäh (2021). *Correspondence between Site Amplification and Topographical, Geological Parameters: Collation of Data from Swiss and Japanese Stations, and Neural Networks-Based Prediction of Local Response*, Bull. Seismol. Soc. Am. 112, 1008–1030, doi: 10.1785/0120210225

Castellaro S. Mulargia F., and Rossi P. L. (2008). *Vs30: Proxy for seismic amplification?* Seismol. Res. Lett. 79, 540–543, doi: https://doi.org/10.1785/gssrl.79.4.540

Forte, G., Chioccarelli, E., De Falco, M., Cito, P., Santo, A., & Iervolino, I. (2019). *Seismic soil classification of Italy based on surface geology and shear-wave velocity measurements*. Soil Dynamics and Earthquake Engineering, 122, 79-93.

Kotha, S.R., Cotton, F., Bindi, D. (2018). *A New Approach to Site Classification: Mixed-effects Ground Motion Prediction Equation with Spectral Clustering of Site Amplification Functions*. Soil Dynamics and Earthquake Engineering. 10.1016/j.soildyn.2018.01.051.

Lanzano G, Felicetta C, Pacor F, Spallarossa D, Traversa P. (2022). *Generic-to-reference rocks scaling factors for seismic ground motion in Italy*. Bull Seismol Soc Am. https://doi.org/10.1785/0120210063.

Loviknes, K., Kotha, S. R., Cotton, F., Schorlemmer, D. (2021): *Testing Nonlinear Amplification Factors of Ground-Motion Models*. - Bulletin of the Seismological Society of America, 111, 4, 2121-2137.

Luzi, L., Puglia, R., Pacor, F., Gallipoli, M.R., Bindi, D., Mucciarelli, M. (2011). *Proposal for a soil classification based on parameters alternative or complementary to Vs,30*. Bulletin of Earthquake Engineering 9, no. 6, 1877-1898

Mascandola, C., Luzi, L., Felicetta, C., Pacor, F. (2021). *A GIS procedure for the topographic classification of Italy, according to the seismic code provisions*. Soil Dynamics and Earthquake Engineering. 148. 106848. 10.1016/j.soildyn.2021.106848.

Mori, F., Mendicelli, A., Moscatelli, M., Romagnoli, G., Peronace, E., & Naso, G. (2020). *A new Vs30 map for Italy based on the seismic microzonation dataset*. Engineering Geology, 275, 105745.

Sgobba S., Lanzano G. and Pacor F. (2021). *Empirical nonergodic shaking scenarios based on spatial correlation models: An application to central Italy*. *Earthq. Eng. and Struct. Dynam*., 50(1), 60-80. https://doi.org/10.1002/eqe.3362.

Sgobba S., Lanzano G., Colavitti L., Morasca P., D'Amico M. C., Spallarossa D. (2023). *Phyics-based parametrization of a FAS nonergodic ground motion model for Central Italy.* Bull. Earthq. Eng., 21, 4111-4137. https://doi.org/10.1007/s10518-023-01691-1.

Wald DJ, Allen TI (2007). *Topographic slope as a proxy for seismic site conditions and amplification*. Bulletin of the Seismological Society of America, 97(5), 1379-1395.

Corresponding author: sara.sgobba@ingv.it

GIS spatial modelling for seismic exposure assessment: a case study over Central Asia.

A. Tamaro, C. Scaini

National Institute of Oceanography and Applied Geophysics - OGS, Trieste, Italy

Introduction

Exposure assessment is of paramount importance in order to produce reliable risk estimates. However, there are many challenges associated with exposure assessment, in particular due to the lack of data on the spatial distribution of assets. Exposure analyses, in fact, identify the main exposed assets and their spatial location. In addition, it allows the assessment of the reconstruction costs for each asset.

Here, we present a methodology to assess exposed population and residential buildings based on a combination of regional-scale and national-scale data, and apply it to Central Asia. The adopted approach combines the most recent datasets and technologies, which allowed the development of high-resolution datasets (e.g., the Facebook high-resolution population grid, https://data.humdata.org/organization/facebook) and local-scale official data (e.g., population census). All collected data were harmonized in order to produce a regionally-consistent exposure database for Central Asia. The exposure database was developed during the project "*Regionally consistent risk assessment for earthquakes and floods and selective landslide scenario analysis for strengthening financial resilience and accelerating risk reduction in Central Asia*" funded by the European Community and implemented by the World Bank. The project saw the development of multiple exposure layers for the different exposed asset types identified in Central Asia:

- · population
- · residential buildings
- · non-residential buildings (schools, healthcare facilities, industrial and commercial buildings)
- · transportation system (roads, railways and bridges)
- · croplands
- A more detailed explanation of the methodology and the results obtained can be found in Scaini et al. (2023, a,b) In this short note we will only present the methods and results of the exposure model for the population and residential buildings, discussing the applicability of this method to other contexts.

Methodology

The methods adopted in this project allowed us to combine the available exposure data at different spatial resolutions (global, regional, national and sub-national) and produced under several past projects based on cutting-edge technologies. In particular, remote sensing data are very important in order to derive exposure datasets that allow covering large areas, but also allow to assess the location and specific characteristics of selected sites. These data were combined with local-scale information provided by local partners in each of the 5 Central Asia countries that enabled us to grasp the differences among the national contexts. The collected information was then homogenized in order to provide regionally-consistent aggregated results for the entire Central Asia region.

Exposure datasets are, by definition, spatial datasets, that is, digital maps where the exposure information is associated to spatial coordinates. In fact, the location of exposed assets (e.g., where different building types are located within a country) is required in order to perform the risk assessment. In absence of information on the asset location (e.g., address, coordinates), a common method to infer the buildings' or facilities' location is to distribute them spatially based on proxies such as population or land use maps. This operation, also called 'spatial disaggregation', and other spatial operations of the kind (e.g., merging of databases, intersection of different maps) were performed using the QGIS open-source program (https://www.qgis.org/en/site/).

Population

In this project, we developed a population dataset at 100m resolution that includes specific demographic attributes (age, gender) for the whole Central Asia. This dataset was based on data from several data sources, used as a starting point for the development of the exposure layers. In particular, the consortium used the Facebook high-resolution dataset (https://data.humdata.org/organization/facebook), which provides population, gender and age information at approximately 20 m in Central Asia. The Facebook population data, retrieved for 2020, was distinguished into three age classes: younger than 5 years old, older than 60 years old or the intermediate age class. The population layers were assembled as follows:

First, the total population in the Facebook dataset was compared with the WorldPop dataset (https://www.worldpop.org/), that provides total population (but no information on age and gender fractions) for 2020. The comparison was performed after aggregating the Facebook data at the resolution of the WorldPop layer (100 m) and showed a good agreement. This operation was performed directly on the spatial layers using the QGIS open-source program.

Second, population, age and gender data in the Facebook dataset was compared with national census data collected by local partners. Local partners retrieved the available population data from national sources, including population data by age and gender in each country and sub- national administrative units (Oblasts). The collected data were extracted from the latest available population census or equivalent data source (2021 for Uzbekistan, 2020 for Kazakhstan and Kyrgyz Republic, 2019 for Turkmenistan, and 2018 for Tajikistan).

Finally, for each Oblast, the Facebook base layer was corrected according to the recent national-scale data. This is done under the assumption that recent national census data is more reliable than global datasets. The difference was greater than 20% in 7 Oblasts of the 4 considered countries. In all regions, the 100-m population grid was corrected proportionally to the estimated difference with the national census data. The correction was performed also for a number of cities in Kyrgyz Republic, Kazakhstan and Turkmenistan, for which data were available. Gender and age percentages were also corrected based on the national data collected after 2019, when available from country-based data (table 1 only for Kazakhstan). The exception of the elder fraction (greater than 60 years old) was maintained from the Facebook population dataset because the data at national scale was only available for different age thresholds (e.g., 70 for Kyrgyz Republic and Uzbekistan, 63 for Kazakhstan).

Figure 1 shows a detail of the population exposure dataset provided by the high-resolution Facebook dataset and the grid developed at 100m resolution in this project (bottom) showing that it matches successfully the building's distribution in the aerial image (top).

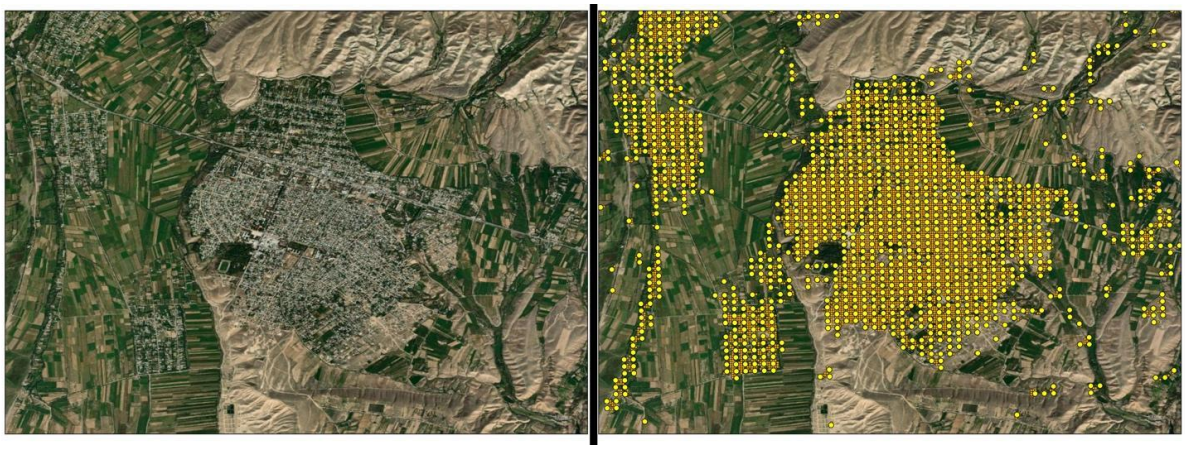

Fig. 1. Distribution of the buildings based on an aerial image in a village in Jalal-Abad Oblast, Kyrgyz Republic (top), (bottom) population grid at 20m (Facebook) and 100m resolution (orange and yellow dots respectively).

Country	Oblast	Total	Men	Women	>60 years old	<5 years old
Kazakhstan	Akmola	1.732.686	831.689	900.996	190.595	138.614

	Aktobe	915.196	439.294	475.902	100.671	73.215
	Almaty	2.440.375	1.171.380	1.268.995	268.441	195.230
	Almaty (city)	1.437.016	689.767	747.248	158.071	112.961
	Atyrau	653.678	318.765	339.912	71.904	52.294
	East Kazakhstan	1.431.196	686.974	744.222	157.431	114.495
	Jambyl	1.166.798	560.063	606.735	128.347	93.343
	Karagandy	1.439.313	690.870	748.443	158.324	115.145
	Kostanay	907.530	435.614	471.915	99.828	72.602
	Kyzylorda	832.005	399.362	432.642	91.520	66.560
	Mangystau	711.729	341.630	370.099	78.290	56.938
	North Kazakhstan	786.807	377.667	409.140	86.548	62.944
	Pavlodar	784.726	376.668	408.057	86.319	62.778
	Shymkent (city)	1.038.152	500.439	537.713	78928	n.a.
	Turkestan	3.084.568	1.480.593	1.603.975	339.302	246.765
	West Kazakhstan	682.746	327.718	355.028	75.102	54.619
	Total	19.006.369	9.123.054	9.883.309	2.090.693	1.520.503

Table 1. Population in each Oblast of Kazakhstan according to the Facebook layer and the national census. Total population and gender and age fractions in Kazakhstan country and for the whole region.

Residential buildings

The method adopted here for developing exposure maps of residential buildings consists of refining the exposure model of Pittore et al. (2020) by increasing its spatial resolution and by better characterizing the residential building typologies. The building typologies used in the exposure model of Pittore et al. (2020) were defined during the Earthquake Model Central Asia project (EMCA, http://www.emca-gem.org/) and will be referred to here as 'EMCA' typologies. Each typology and sub-typology is associated to a description and a taxonomy, which can also specify if the structure is designed to be Earthquake Resistant (ERD). The taxonomies are expressed based on the GEM building taxonomy (https://taxonomy.openquake.org/).

The spatial layer produced by Pittore et al. (2020) has a variable resolution ranging from a few hundred meters in urban areas to several km in rural areas. This layer was developed specifically for earthquake damage and risk assessment purposes, for which the spatial resolution was appropriate. However, in order to perform a risk assessment for fluvial and pluvial hazard, spatial resolution needs to be increased considerably. During this project, we increased the layer spatial resolution in order to produce a residential buildings exposure layer on a constant-resolution grid. Local partners collected and provided information on the number of buildings or households by Oblast or city and, when available, the number of buildings for each structural typology. For two countries, Kazakhstan and Uzbekistan, local partners provided the information about the number of households by Oblast and load-bearing material (which were associated to EMCA structural typologies). This information was used to update the spatial distribution of building typologies in each country of Central Asia based on national-scale data. The method for deriving the final residential buildings exposure layer has 4 main phases:

The original polygons from Pittore et al. (2020) were classified into urban and rural areas based on the urbanized areas mask provided by the GRUMP dataset (Center for International Earth Science Information Network - CIESIN, 2021, Figure 2a)

For each country and Oblast, the number of buildings in each typology (provided by local partners) was distributed into the urban and rural polygons identified in the previous step (Figure 2b). This method was applied to the countries where local data were available. Buildings were distributed based on the population in the buildings in each polygon (provided by Pittore et al., 2020). The fraction of different typologies in urban and rural areas of each Central Asia country was extracted from Wieland et al. (2015).

For each building type, the total number of buildings was distributed among the sub-typologies (EMCA) based on the relative fraction of each sub-typology in the Pittore et al. (2020) dataset. This operation was carried out for each polygon.

Finally, residential buildings in each polygon were distributed spatially based on the population layer developed for Central Asia at 100m resolution. This allowed increasing the resolution and obtaining an equally spaced grid of 100-m resolution (Figure 2c).

Figure 2 shows examples of the exposure development main steps for Eastern Uzbekistan. Figure 2a shows the urban and rural mask provided by the GRUMP dataset. Figure 2b shows an example of how data provided by locals for each country's Oblast (e.g., Navoi province, Tajikistan) are distributed on the existing variable-resolution grid. Figure 2c shows how the data are distributed on the population grid in order to reach higher resolution. The result of this procedure is an equally-spaced grid of 100m resolution with the number and type of buildings in each sub-typology (EMCA). Finally, the information was aggregated on a regular 500 m grid to better manage the spatial data. Information on exposed residential buildings is

therefore provided in aggregated format (i.e., a number of buildings are located on a point belonging to a constantly-spaced grid).

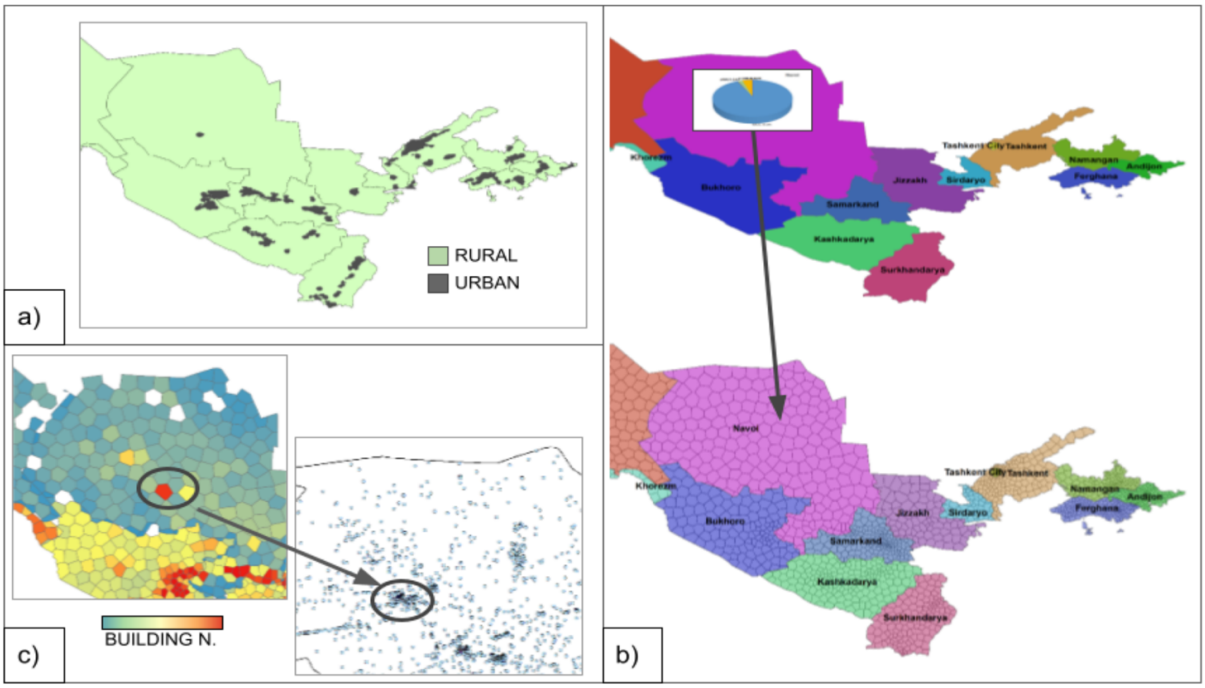

Fig. 2. a) Urban and rural mask provided by the GRUMP dataset, b) example of distribution of national and sub-national scale buildings data on the variable-resolution grid (Pittore et al., 2020), c) distribution of buildings data on the high-resolution Facebook population grid.

The building typologies were enriched with age information based on the characteristics extracted from past projects and from local partners' data. As for the storey number, similarly for the age of construction, a value was associated to each building typology based on the information provided with the EMCA macro typologies (see Wieland et al., 2015 for details) and on the data collected from past projects and/or provided by local partners.

Figure 3 (above) shows examples of images of residential buildings provided by local partners in the Kyrgyz Republic and Tajikistan (left and right columns) for typical precast panel buildings (a, b) and adobe buildings (d, e). These images contributed to the characterization of the building types and were used for the elaboration of the capacity building activities and especially for the training material. Figure 3 below shows the spatial distribution of one sub-typology of the EMCA1 typology, unreinforced masonry (URM). The map shows the spatial distribution of buildings in the entire Central Asia region (left) and for a selected study area (right) with a resolution of 500 metres. Similar maps can also be created for other building typologies.

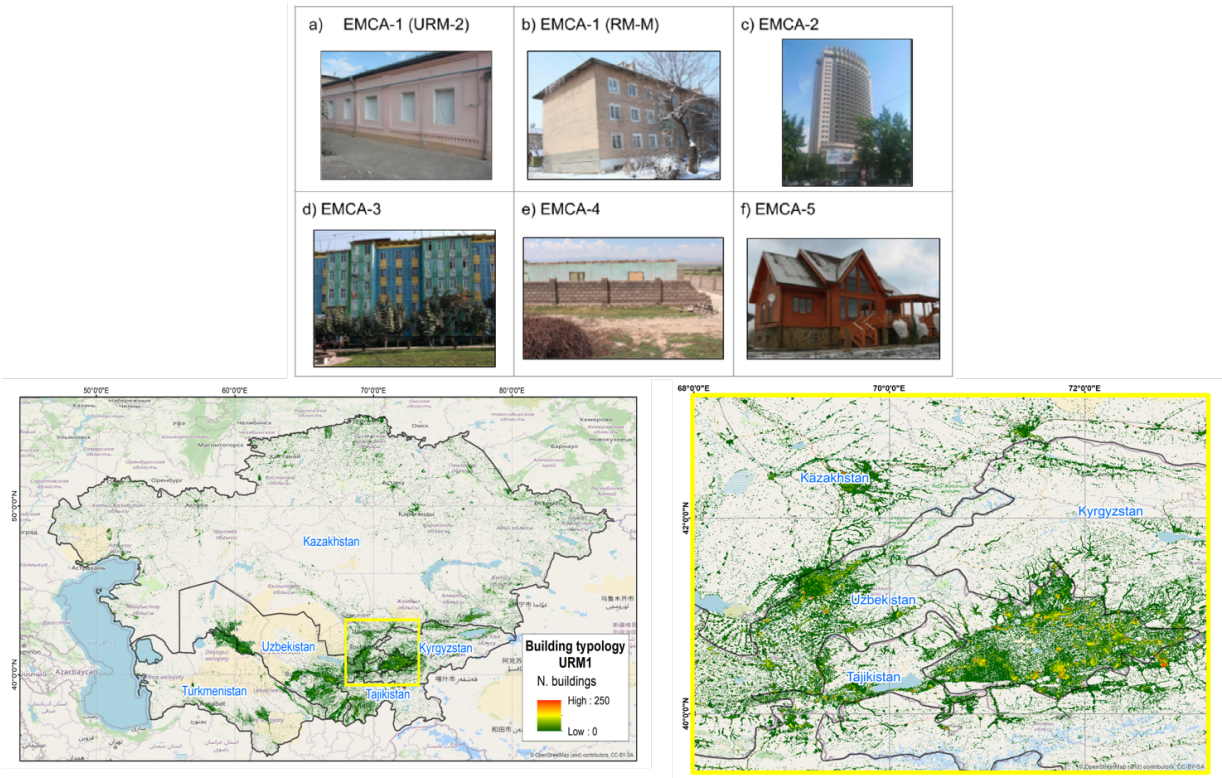

Fig. 3. Above examples of residential building images provided by local partners for selected EMCA typologies; in particular, two types of EMCA1 are shown (URM-2 and RM-M). typical precast panel buildings (a, b) and adobe buildings (d, e), which correspond to the EMCA3 and EMCA4 typologies, respectively. Below, examples of the number of buildings in each 500 m cell belonging to one sub-typology of EMCA1 (unreinforced masonry, URM1) in the entire Central Asian region (left) and in a selected area (right).

Reconstruction costs of residential buildings:

Past research projects provided an estimate of reconstruction costs for residential building typologies (Pittore et al., 2020) and other assets (Project 'Measuring Seismic Risk in Kyrgyz Republic', World Bank project P149630). Here, we updated the information with reconstruction costs retrieved by local partners for each country. Costs provided by local partners were compared with each country's GDP 2020 per capita, and across the different countries. In order to reduce discrepancies between country-specific costs, and to provide a regionally-consistent dataset of reconstruction costs. The final exposure layers contain, for each asset type, the average reconstruction cost for each country, converted from local currency to USD (Table 2). The residential buildings content cost can be estimated based on the procedure described in the HAZUS inventory technical manual (2021). The content cost is expressed as a percentage of the building structural cost, and is 50% for all residential building types.

Type EMCA	Material	Kazakhstan	Kyrgyz Republic	Tajikistan	Uzbekistan	Turkmenistan
EMCA 1	Unreinforced masonry (URM)	190	175	175	175	105
EMCA 2	Reinforced concrete frame (RC)	570	400	425	400	180
EMCA 3	Reinforced concrete precast (RCPC)	425	425	425	400	180
EMCA	Adobe	125	125	125	190	125
EMCA	Wood	330	330	177.5	300	648
EMCA	Steel	175	175	175	175	175

Table 2. Reconstruction unit costs (in 2021 USD/m²) defined in this project for each EMCA residential building typology in each Central Asia country.

Conclusion

This short note describes the exposure model (population and residential buildings) developed for Central Asia within the project "*Regionally consistent risk assessment for earthquakes and floods and selective landslide scenario analysis for strengthening financial resilience and accelerating risk reduction in Central Asia*".

The regional exposure database relies on the previous exposure assessments carried out in Central Asia. However, it introduces substantial improvements by including up-to-date local-scale data for each Central Asia country and by homogenizing these data into a single, regionally-consistent database. In particular, the exposure assessment allows to increase the spatial resolution of the previously existing exposure layers, comprise a large number of assets into a single and consistent regional dataset, and include exposure attributes that were not characterized prior to this project (e.g., country-based reconstruction costs).

Results of the exposure assessment show that the exposed assets in central Asia are distributed heterogeneously, with large differences between urban and rural areas. In particular, a large fraction of residential reconstruction costs is located in the main cities and urbanized areas. One of the challenges when developing such a comprehensive database is the difficulty of gathering data and combining different data sources together. The work presented here relies on the available global and regional-scale datasets, mostly provided by third-parties, which are paramount in order to collect exposure layers in a timely manner. To the extent possible, such data underwent specific validation procedures, made possible by

the use of national and sub-national data and remote sensing images. The global and regional-scale datasets were substantially improved also thanks to the large amount of country-based data provided by local partners. Such data were collected for each country in Central Asia as a result of an extensive effort, carried out in cooperation with the consortium partners in the region (See Peresan et al., 2023 for details). We are therefore thankful to all the working team for their contributions to the development of the exposure layers.

References

Peresan A., Scaini C., Tyagunov S., Ceresa P.; 2023: Capacity Building Experience for Disaster Risk Reduction in Central Asia. Natural hazard and Eart System Sciences. https://doi.org/10.5194/nhess-2023-156. Preprint. Discussion started: 6 September 2023.

Pittore M., Haas M. and Silva V.; 2020: Variable resolution probabilistic modeling of residential exposure and vulnerability for risk applications. Earthquake Spectra, 36(1_suppl), pp. 321–344. doi: 10.1177/8755293020951582.

Wieland M., Pittore M., Parolai S., Begaliev U., Yasunov P., Niyazov J., Tyagunov S., Moldobekov B., Saidiy S., Ilyasov I., Abakanov T.; 2015: Towards a cross-border exposure model for the Earthquake Model Central Asia. Ann. Geophys58.

Scaini C., Tamaro A., Adilkhan B., Sarzhanov S., Ismailov V., Umaraliev R., Safarov M., Belikov V., Karayev J., Faga E.; 2023a: A new regionally consistent exposure database for Central Asia: population and residential buildings. Natural hazard and Eart System Sciences.https://doi.org/10.5194/nhess-2023-94. Preprint. Discussion started: 19 June 2023.

Scaini C., Tamaro A., Adilkhan B., Sarzhanov S., Ismailov V., Umaraliev R., Safarov M., Belikov V., Karayev J., Faga E.; 2023b: A regional scale approach to assess non-residential buildings, transportation and croplands exposure in Central Asia. Natural hazard and Eart System Sciences. https://doi.org/10.5194/nhess-2023-95. Preprint. Discussion started: 21 June 2023.

Corresponding author: atamaro@ogs.it

A new service for the exchange of national and transboundary station information: *STATION* (*Seismic sTATion and amplificatION service*)

G. Tarchini[1], D. Spallarossa[1], D. Scafidi[1], S. Parolai[2], M. Picozzi[3], D. Bindi[4]

[1] *DISTAV, University of Genoa, Genoa, Italy*
[2] *Department of Mathematics, Informatics and Geosciences, University of Trieste, Trieste, Italy*
[3] *National Institute of Oceanography and Applied Geophysics – OGS, Udine, Italy*
[4] *Helmholtz Centre Potsdam, GFZ German Research Centre for Geosciences, Potsdam, Germany*

STATION (*Seismic sTATion and sIte amplificatiON* – https://distav.unige.it/rsni/station.php) is the prototype of a web interface and service for the exchange and dissemination of 'seismological' data related to seismic stations installed since 2005 on Italian territory and in cross-border areas that have recorded seismic events with local magnitude values greater than 1.8. By 'seismological data' we mean products from the processing of seismic signals that are useful for a 'seismic' characterisation of the station: for example, horizontal-to-vertical spectral ratios from noise and S phases as well as residuals of magnitude.
Processing is quasi-automatic based on *INGV* reference data. It consists of:

- the selection of data records within a radius of 120 km from the event;
- the automatic picking of P and S phases;
- the calculation of horizontal-to-vertical spectral ratios, average and NS and EW components separately, both for the S-wave phase and noise windows; and
- the calculation of station magnitude, and subsequently of the residual of magnitude.

Currently, the STATION database includes more than 2,200 seismic stations throughout the entire national territory and neighbouring states (Fig. 1) and was created by processing data of more than 15,000 seismic events and two million of waveforms. In this way, about four million values for magnitude residuals and horizontal-to-vertical curves were obtained.
For each station a dedicated webpage is available (Fig. 2), developed according to *FAIR* principles, through which it is possible to access general station information and seismological data. Each station webpage contains:

- an interactive map showing the station location;
- a table containing site name, station code, network, location, channel, link to station metadata, link to station data in the *Earthquake Strong Motion* (*ESM*) database, and the link to download a PDF summary document of the station;
- another table containing the number of S phases and noise time-windows analysed, magnitude and hypocentral distance ranges, start time and end time; and
- plots of noise spectra (mean) and horizontal-to-vertical spectral ratios – average and NS and EW components separately – for both the S-wave phase and noise windows.

There are many possible applications for this service. For example:

- STATION is the only seismological service that allows to view the map of all the stations installed on Italian territory and in the neighbouring regions (whether they are still operating or have been decommissioned, but whose data are in any case 'open');
- the database contains information on 559 seismic stations of the INGV national monitoring network (network code IV) and information on 753 stations of the monitoring network of the Italian Civil Protection Department (network code IT);
- the stations of many temporary networks are also included (*e.g.*, *'AlpArray'* (network code Z3) and '*Centro di microzonazione sismica Network, 2016 Central Italy seismic sequence*' (network code 3A));
- in the event of a seismic 'crisis', the available services could be effectively used both to define the characteristics of a temporary monitoring network and to support microzonation activities.
-

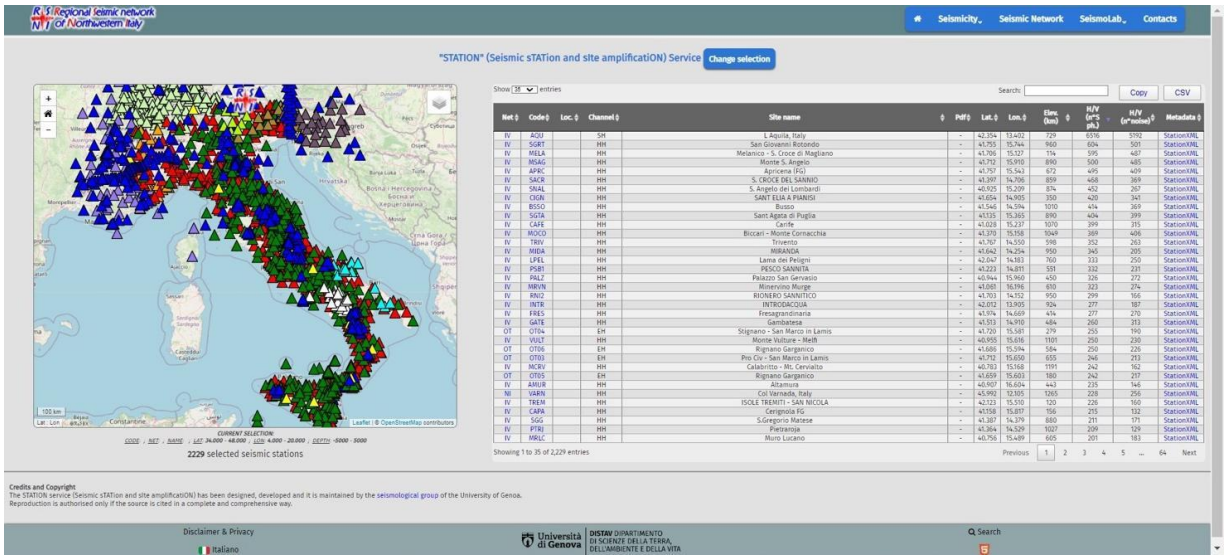

Fig. 1 – STATION main webpage.

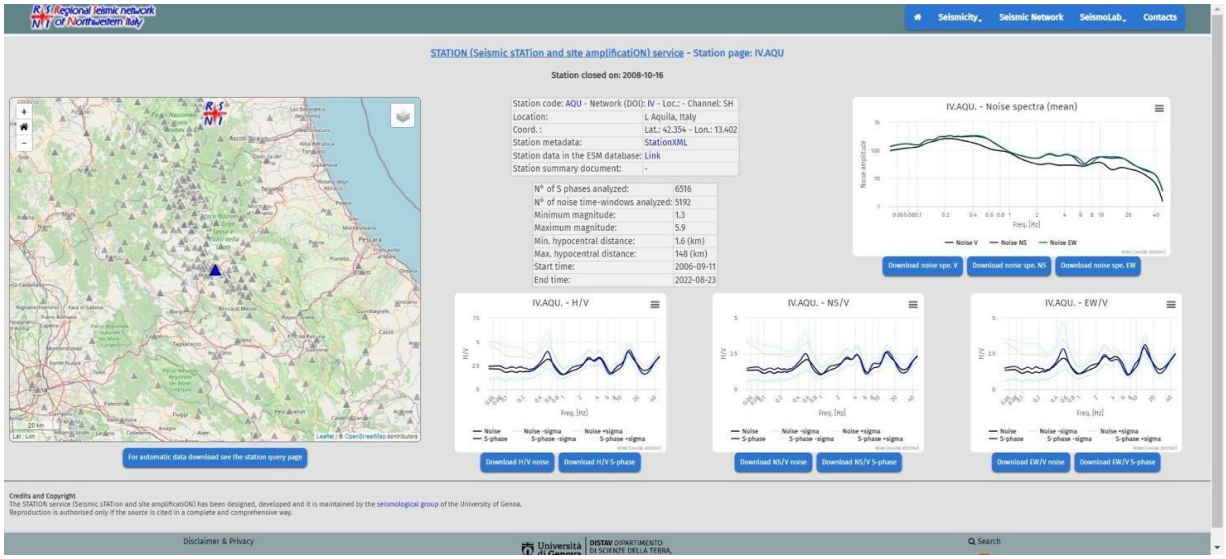

Fig. 2 – Example of specific webpage for the station IV.AQU.

Corresponding author: Gabriele Tarchini – gabriele.tarchini@edu.unige.it

SDQ: a new tool for the evaluation of seismic-accelerometric data quality

F. Varchetta[1], M. Massa[1], R. Puglia[1], P. Danececk[2], S. Rao[2], A. Mandiello[2], D. Piccinini[3]

[1] INGV, sezione di Milano, Italia

[2] INGV, ONT, Osservatorio Nazionale Terremoti, Roma, Italia

[3] INGV, sezione di PISA, Italia

Abstract

In recent years, many works have focused their attention on the issue of data processing and verification procedures, in particular of strong-motion data because of their fundamental role in the case of strong earthquakes At the national level in Italy, there are currently two web portals available for checking seismic data quality: EIDA Italia (https://eida.ingv.it/it/getdata) and ISMDq (http://ismd.mi.ingv.it/quality.php). The EIDA Italia (Danecek et al., 2021) employs the data quality tools directly from the ORFEUS website (http://www.orfeus-eu.org/data/eida/quality/), while ISMDq (Massa et al., 2022) is a recent system for dynamic quality check both of continuous data stream and earthquake data.

In this work, we introduce the SDQ (Seismic Data Quality) project, a new open-source Python tool freely available and downloadable. It is designed for the automatic monitoring of sismo-accelerometric stations by analyzing both events - selected based on magnitude and distance - and continuous data streams.

Regarding earthquake data, the quality of individual waveforms is assessed by comparing the ground motion parameters derived from co-located accelerometers and velocimeters. SDQ operates by utilizing a simple external input file containing the INGV event identifier, station, and network codes. SDQ is organized into three main phases: acquisition, pre-processing, and processing. In the acquisition phase, event information, station metadata, and waveforms are downloaded from FDSN (https://www.fdsn.org/) web services (https://www.fdsn.org/webservices/). Initially, the waveforms are analyzed to identify event and pre-event noise windows. Then, the data are converted into physical units, accounting for pre-filter parameters and exclusion conditions. Finally, each single waveform is assigned to a quality class ranging from A (excellent) to D (data to be rejected) based on time- and frequency-dependent algorithms. Thresholds for classification were empirically obtained by combining visual signal inspection and statistical analysis. Tests were performed considering about 15,000 waveforms in the time interval from January 2012 to June 2023, encompassing all 6-channel stations of the IV (National Seismic Networks (https://www.fdsn.org/networks/detail/IV/)) and MN (MedNet network, https://www.fdsn.org/networks/detail/MN/), both managed by the Italian National Institute for Geophysics and Volcanology (INGV, https://www.ingv.it/).

Concerning continuous ambient noise data streams, 24-hour mini-seed recording signals are analyzed at each selected station to set empirical thresholds considering data metrics and data availability. The goal is to build a station-quality archive.
Users can select and build the time history for each network, station, stream data type, and single ground motion component related to selected input data included in a local mini-seed data archive representing the starting point of the procedure.
Data metrics are evaluated considering RMS (Root Mean Square, Bormann, 2012) and PSD (Power Spectral Density, Bormann, 2012) in several frequency intervals (i.e., 0.01-0.1; 0.1-1; 1-5; 5-10; 10-20; 20:50 Hz).
For availability, the graphs show the results in terms of daily %gap, maximum daily availability, sum of the time gaps, and maximum duration of the maximum daily gap. Daily results are represented by static images related to the 24 hours of the data selected at each target station. Daily results include the PDF (Probability Density Function, McNamara and Buland, 2004), the frequency-dependent PSD, the comparison between RMS and PSD variations, time histories, and spectrograms. SDQ provides final summary tables for both earthquake and continuous data, collecting all relevant parameters for each processed waveform and data stream, along with explanatory text files (log and warning files), allowing the user to better evaluate the results.
Although SDQ is currently under development, the release presented and discussed in this work is uploaded to the INGV GitLab platform and is available at: https://gitlab.rm.ingv.it/EIDA/quality/sdq.

References

Bormann P.; 2012: New manual of seismological observatory practice (NMSOP-2). IASPEI, GFZ Ger. Research Centre for Geosciences.

Danecek P., Pintore S., Mazza S., Mandiello A., Fares M., Carluccio I., ... & Michelini A.; 2021. The Italian node of the European integrated data archive. *Seismological Research Letters*, *92*(3), 1726-1737.

Massa M., Scafidi D., Mascandola C., & Lorenzetti A.; 2022: Introducing ISMDq - A web portal for real-time quality monitoring of italian strong-motion data. *Seismological Research Letters*, *93*(1), 241-256.

McNamara D. E., and R. P. Buland; 2004: Ambient noise levels in the continental United States, Bull. Seismol. Soc. Am. 94, no. 4, 1517–1527.

Varchetta F., Massa M., Puglia R., Danecek P., Rao S., Mandiello A., Piccinini D.; 2023: SDQ: a python-based open-source to improving data quality check of the INGV Italian Seismic Network, *Rapporti Tecnici INGV* (in revisione).

Corresponding author: fabio.varchetta@ingv.it

Machine Learning-based modelling for Near Real-Time prediction of liquefaction

C. Varone[1], F. Mori[1], A. Mendicelli[1], G. Ciotoli[1], G. Acunzo[2], G. Naso[3], M. Moscatelli[1]

[1] *CNR Italian National Research Council, Institute of Environmental Geology and Geoengineering (IGAG), Montelibretti, Italy*
[2] *Theta Group Srls, Rome, Italy*
[3] *Presidenza del Consiglio dei Ministri, Dipartimento della Protezione Civile (DPC), Rome, Italy*

The occurrence of an earthquake may involve extensive consequences, highlighting the critical requirement from prompt and reliable information to minimize the effects of the disaster. The rapid execution of emergency response strategies also depends on the accurate prediction of seismically induced effects. This study aims to develop an approach based on machine learning to predict seismically induced liquefaction phenomena in near real-time. This method combines factors such as ground shaking scenarios (Magnitude and Peak Ground Acceleration PGA), shear-waves velocity to a depth of 30 meters (Vs30), and groundwater table depth to predict the likelihood of liquefaction phenomena. The implementation is planned within the SEARCH (Seismic Emergency Assessment and Response Computing Hub) software, which is an innovative solution able to generate impedance maps for landslides, liquefaction, and building collapses. These maps provide valuable assistance for emergency management.

Corresponding author: chiara.varone@cnr.it